PNAS
www.pnas.org

Supplementary Information for

Multiple origins of green coloration in frogs mediated by a novel biliverdin-binding serpin

Carlos Taboada[1, 2, 3, 4*], Andres E. Brunetti[4,5], Mariana L. Lyra[6], Robert R. Fitak[1,7], Ana Faigon[2], Santiago R. Ron[8], Maria G. Lagorio[3,9], Célio F. B. Haddad[6], Norberto P. Lopes[4], Sönke Johnsen[1], Julian Faivovich[2,10#], Lucia B. Chemes[11,12*#], Sara E. Bari[3*#]

* Carlos Taboada, Lucía B. Chemes, Sara E. Bari
Email: carlostaboada84@gmail.com, lchemes@iib.unsam.edu.ar, bari@qi.fcen.uba.ar

This PDF file includes:

Supplementary text
Figures S1 to S15
Tables S1 to S15
SI References

Supplementary Information Text

Materials and Methods

Taxonomic distribution of chlorosis

We surveyed the taxonomic distribution of chlorosis in anurans to gain an idea of its prevalence and infer the minimum number of times that it evolved during the evolutionary history of the group. We identified those species that show clear accumulations of green lymph and or green tissues (many times evident in the oral mucosa and inguinal region) or green bones (usually evident by skin transparency in phalanges of fingers and toes, humerus, femur, tibiofibula, maxilla, and premaxilla). We surveyed the taxonomic literature of all extant anurans and, when in doubt, asked colleagues with expertise on the relevant groups.

To infer the number of independent origins of chlorosis during the evolutionary history of anurans we made ancestral character reconstruction. For this, we used both the phylogenetic results of Jetz & Pyron (26) (see Fig. 1, main text) to have a general perspective and more recent and densely sampled phylogenetic hypotheses for several families for a more thorough approach. The ancestral character reconstruction was done using Fitch optimization (48) as implemented in T.N.T. (49, 50). Phylogenetic tree was generated using the iTOL webserver (51).

Specimen collecting and handling

We selected different species for performing experiments. We purified BBSs and performed RNAseq from nine species: Family Hylidae: *Aplastodiscus leucopygius, Boana puncata*, *B. cinerascens*, *Hyloscirtus phyllognathus*, *Pseudis minuta* and *Sphaenorhynchus lacteus*; Family Centrolenidae: *Chimerella mariaelenae, Espadarana prosoblepon* and *Nymphargus posadae*. Additionally, we purified BBSs from *Aplastodiscus flumineus* and *Boana atlantica*.

For lymph and tissue extractions, specimens were euthanized with a lethal dose of 20% lidocaine applied in the pelvic and interocular region. Some adult specimens of *B. punctata* were also kept in terraria, with dechlorinated tap water and provided with different aquatic and terrestrial plant species. Frogs were kept at 20–28°C, with a 12:12 light:dark cycle, and fed with small crickets, mealworms and cockroaches.

All procedures involving animals were carried out according to the regulations specified by the Institutional Animal Care and Use Committee of the Facultad de Ciencias Exactas y Naturales, Universidad de Buenos Aires (Res C/D 140/00), and by Conselho Nacional de Controle de Experimentação Animal, Ministério da Ciência, Tecnologia e Inovação, Brazil.

Lymph extraction and BBS purification

Lymph was extracted by performing small incisions in the tegument exposing different lymph sacs. Lymph was collected with capillary tubes or hypodermic syringes. Given that blue-green lymph is clearly observed covering the whole musculature as well as the skin ventral surface, we sampled pieces of both tissues to obtain a larger sample amount. Basically, fragments of 5x5 mm were suspended in 150 µl amphibian phosphate buffer (52), vortexed and centrifuged (10 min, 2000 rpm). The limpid blue-green supernatant was collected for further protein purification steps.

Lymph supernatant was diluted 20-fold with phosphate buffer 100 mM pH 7.2, submitted to organic extraction with dichloromethane to remove lipids (150 µl lymph:50 µl dichloromethane), vortexed and centrifuged (5 min, 500 rpm). The blue-green coloration remained completely in the aqueous phase. Proteins were sequentially precipitated by gradual increase in ammonium sulphate concentration. Initial saturation was set at 40%, and samples were stored at 4°C for one

hour, followed by centrifugation (13 min, 14000 rpm) and the blue supernatant collection. Ammonium sulphate saturation was increased in four sequential steps (55%, 70%, 80%, 90%), followed by centrifugation. At 80–90% saturation, blue proteins precipitate and the pellet was washed three times with milli-Q water, resuspended in 10 mM Tris-HCl Buffer pH 7, and passed through a previously equilibrated Sephadex G25 column. Blue fractions were collected and concentrated by lyophilization. Samples were then subjected to 1D 14% native PAGE. Blue bands corresponding to BBSs were excised from the gel and washed five times with milli-Q water. Then they were cut into smaller pieces (~1 mm^3), transferred to 1.5 ml tubes and covered with Tris-HCl 20 mM pH 7 buffer. The samples were incubated for 2–5 hours in the dark at 4°C, followed by a 5–10 min sonication. The extracted blue bands from the polyacrylamide matrix were re-filtered through Sephadex G25 equilibrated in Tris-HCl 10mM pH 7 buffer and the blue eluate was stored lyophilized for further experiments. The purification quality was evaluated by UV-VIS spectrophotometry, circular dichroism (CD), and fluorescence spectroscopy.

Apoprotein-biliverdin dissociation

To separate the pigment from the apoprotein, 50 μl of ethanol were added to 1 ml of protein solution in Tris-HCl 20 mM buffer (pH 7.2), followed by acidification with HCl (pH 4). Dichloromethane (250 μl) was added to the sample followed by centrifugation (3 min 2000 rpm). The green organic phase was collected, washed 5 times with milli-Q water, re-centrifuged and dried with sodium sulphate. The organic phase was filtered, and the organic solvent was evaporated to dryness.

The extracted pigment was esterified by addition of 4% sulfuric acid in anhydrous methanol (4 hours in the dark). The pigment was then extracted with organic solvent (chloroform), washed three times with milli-Q water and the organic phase was concentrated to dryness. Esterified biliverdin was then subjected to thin layer chromatography (TLC) using dichlorometane:methanol (1.1%) as mobile phase. The green band was excised from the silica plate and the biliverdin was eluted using dichloromethane:methanol (1.5%). Samples were centrifuged (3 min 2000 rpm) to remove silica remnants. The green supernatant solution was dried and stored at -20°C in the dark until further analysis.

NMR

The esterified and purified BV was washed with hexane. Then, it was exhaustively dried under vacuum and resuspended in deuterated chloroform ($CDCl_3$). The 1D ^1H and 2D NOESY spectra were recorded at 25°C on a 11.2 Tesla Bruker Avance DRX 500 spectrometer operating at a proton frequency of 500.13 MHz (Bruker, Karlsruhe, Germany). For the NOESY, the pulse sequence *noesygpph* was used. Spectra were analyzed with Topsin Software (Bruker).

HPLC-DAD ESI MS and MS/MS

LC-DAD-IT and LC-DAD- TOF analyses were performed with an UFLC instrument (Shimadzu, Japan) consisting of two LC20AD solvent pumps, a SIL20AHT auto sampler, a CBM20A system controller, a CTO20A column oven and a diode array detector (SPD- M20AV, Shimadzu). LC-DAD-MS/MS was acquired using the UFLC apparatus hyphened to an Ion Trap (IT) mass spectrometer (Bruker, amaZon SL, Billerica – USA), while LC-DAD-TOF was conducted by UFLC equipped with an UltrOTOF (Bruker Daltonics, Billerica– USA) mass

spectrometer. The qTOF-MS experiments were conducted as follows: capillary voltage 3.5 kV, end plate offset 500 V, capillary temperature at 200°C; nitrogen was used as the sheath gas; drying gas flow at 9.0 L/min; drying gas temperature at 300°C; nebulizer gas pressure of 4 bar; positive ESI modes. Spectra (*m/z* 100–1000) were recorded every 2 s. Accurate masses were obtained by using TFA-Na^+ (sodiated trifluoroacetic acid) as the internal standard. IT acquisition parameters were as follows: capillary 3.5 kV, end plate offset 500 V, nebulizer 40 psi, dry gas (N_2) with flow of 9 L/min and temperature of 300°C. CID fragmentation experiments were performed in autoMS^n mode using enhanced resolution mode for MS and UltraScan mode for MS/MS acquisition. ESI-MS/MS analyses were performed by collision-induced dissociation (CID) using nitrogen as the collision gas with the collision energy varied in the range from 5 to 50 eV for each precursor ion. Lyophilized BBS samples were dissolved in water:acetonitrile (9:1) with 0.1% T(v/v) trifluoroacetic acid (TFA) and filtered (Millex 0.22 μm). Samples were injected into a C_{18}-Kinetex Phenomenex® (100 mm X 2.1 mm x 2.6 μm) column with temperature adjusted to 35°C. Two gradients were tried, using a flow of 0.3 ml/min and a mobile phase that consisted of water+0.01%TFA (A) and acetonitrile+0.01%TFA (B). The two gradients were: (i) 0.0–34.0 min (15% B), 34–36.0 min (15–70% B), 36.0–42.0 min (70–100% B), 42.0– 45.0 min (100-15% B) and 45.0–49.0 min (15% B), (ii) 0.0–2.0 min (10% B), 2-26.0 min (10–60% B), 26.0–30.0 min (60–100% B), 30.0– 34.0 min (100% B), 34.0–36.0 min (100-10% B) and 36.0-40 min (10% B). For spectra acquisition and analysis, the software DataAnalysis (Bruker) was used.

MALDI TOF OF BBS

Molecular weight of purified native BBSs and the isolated apoprotein were determined by MALDI-TOF. Samples were prepared mixing 2 µl of protein in 0.1%TFA solution with 2 µl of aqueous sinapinic acid (SA) + 0.1% TFA. Sample and matrix were co-crystalized at ambient temperature. For external calibration, a mixture of proteins containing Trypsinogen, Protein A and albumin-bovine was used (Protein Calibration Standard II; Bruker), ranging from 24 to 67 KDa. Measurements were performed with a Microflex mass spectrometer (Bruker) from the Protein Structure-Function and Engineering Laboratory, Fundación Instituto Leloir, an Ultraflex II (Bruker) from the Mass Spectrometry Facility (CEQUIBIEM) at the Facultad de Ciencias Exactas y Naturales, University of Buenos Aires, Argentina or an ultrafleXtreme (BrukerDaltonics) from the Núcleo de Pesquisa Produtos Naturais e Sintéticos (NPPNS), Faculdade de Ciências Farmacêuticas de Ribeirão Preto, Universidade de São Paulo, Brazil. For spectra acquisition, the FlexControl software was used.

BBS quantification strategies

BV absorbs in the UV as well as in the visible regions, and a direct determination of native BBS concentration based on colorimetric assays is ruled out. To overcome this, a two-step methodology was developed:

Quantification using molar extinction coefficient at 280 nm for the unfolded apoprotein

To estimate the concentration of the free unfolded apoprotein, the latter was obtained from the dichloromethane/water interphase during apoprotein/biliverdin separation step (see section: Apoprotein-biliverdin dissociation), dried and resuspended in 6M guanidinium chloride. Molar extinction coefficient for the apoprotein was estimated based on Tyrosine (Y) and Tryptophan

(W) molar absorptivities at 280 nm following the equation described by Pace (53). For this method, it is necessary to know the protein sequence (see below, "Sequencing methodology"). The determined molar extinction coefficient for the apoprotein was ε_{280nm}=27390 $cm^{-1}M^{-1}$.

Quantification using biliverdin molar absorptivity wavelengths

To quantify the holoprotein of *Boana punctata*, a method was developed to use either the Soret or Q bands from biliverdin inside the protein moiety. This method relies on the stoichiometry apoprotein/biliverdin (see below Stoichiometry apoprotein-biliverdin), and on the native BBS UV-VIS spectra. For the Soret band we used absorbance at 390 nm (red-shifted relative to free biliverdin) and for the Q band at 667 nm.

Stoichiometry apoprotein-biliverdin

Apoprotein and biliverdin were separated as previously described (Apoprotein-biliverdin dissociation). Apoprotein in the dichloromethane/water interphase was dried and resuspended in guanidinium chloride 6M. Protein concentration was determined following the methodology described before. The biliverdin in the organic phase was dried under nitrogen flux and then resuspended in ethanol for spectrophotometric analysis. Both apoprotein and biliverdin were resuspended in identical volumes. Biliverdin was quantified by UV-VIS spectrophotometry using the published molar extinction coefficient for biliverdin IX α in ethanol at neutral pH (35): ε_{379nm}=50600 $M^{-1}cm^{-1}$. The quotients apoprotein/biliverdin were determined using three independent trials with three different protein stocks.

***Boana punctata* BBS Identification**

The general methodology followed this general pipeline: (1) BBS purification (2) partial or total in gel or in solution tryptic digestion (3) MALDI TOF of the peptides (4) peptide mass fingerprint (PMF) using different databases with heterospecific data. Given that BBSs belong to the highly diversified clade A of the serpins superfamily with low interspecific identities, no matches were found using PMF and available databases. Hence, we continued with (4) *de novo* sequencing of the MALDI TOF-TOF spectra of peptides, (5) N-terminal Edman sequencing, and (6) Msblast using the list of *de novo* sequenced peptides as a query (27).

N-terminal sequencing by Edman degradation

N-terminal Edman sequencing was performed by Alphalyse (Denmark) and covered the first 20 amino acid residues.

Peptide mass fingerprint (PMF). Sample preparation

SDS-PAGE and in-gel digestion: Proteins were separated in 12.5% polyacrylamide gel in denaturing and reducing conditions. In-gel digestion and mass spectrometry procedures for the BBS of *Boana punctata* were performed in the Mass Spectrometry Facility (CEQUIBIEM) at the Facultad de Ciencias Exactas y Naturales, University of Buenos Aires.

In-solution protein digestion: Purified proteins (10.5 µl, 2 µg of BBS) were mixed with of HCO_3NH_4 (15 µl, 2 mg/ml), DTT (1.5 µl, 15 mg/ml). The mixture was incubated 5 min at 100°C. Then iodoacetamide was added (3 µl, 15 mg/ml) and the sample was incubated at room temperature for 20 minutes in the dark. Afterwards, 1 µl trypsin (Sigma) in 0.1 mM HCl was added and the sample was incubated overnight at 37°C.

Maldi-TOF

2 µl of peptides were co-crystallized onto the MALDI target (MTP Anchor Chip, BrukerDaltonics) with 2 µl of matrix solution (3 mg/ml of α-cyano-4-hydroxycinnamic acid, HCCA) in 50% acetonitrile 0.1% TFA. External calibration was performed using molecular weight standards (Peptide calibration standard I, Bruker), covering the range 1050–3120 Da. Positive ion spectra were acquired in reflectron mode. Flex Analysis (version 3.3; Bruker Daltonics, Inc.) was used to detect peptide peaks for both MS and tandem MS (MS/MS).

Mass search

The list of peaks obtained by MALDI-TOF MS was used to perform searches using MASCOT against NCBI database, restricting taxonomically the results to vertebrate proteomes. Additionally, a second search was performed using MsFit from Protein Prospector against the Uniprot database. Enzyme: Trypsin; Constant modifications: Carbamidomethylation (Cys); Variable Modifications: oxidation (Met); Peptide Mass/Charge Tolerance: 150 ppm; Peptides charge: +1.

In both cases the identification of the BBS was negative due to the scarcity of amphibian genomic data, or to large sequence divergence from the available genomes.

De novo sequencing

Mass spectrometry data was converted to mzML extension using ProteoWizard (54), and analyzed with Mass++ (55). Data were processed by baseline suppression using ABC algorithm, according to the following parameters: Windows width: 0.1, Noise factor: 2.0, Smoothing width: 10. MSMS spectra were manually interpreted, either for *de novo* sequencing, as well as to verify the sequences predicted by PMF. For *de novo* sequencing, we followed the recommendations published elsewhere (27).

BBS complete sequence

We selected *Boana punctata* as the reference species to get the complete BBS sequence. We designed degenerate primers using the peptide sequences obtained by Edman and MSMS and results of MSBLAST and alignments. The criterion to select a *de novo* peptide sequence was to maximize the number of present amino acids that are codified by one or only a few codons (e.g. W). The two sequences that were selected were HHEEGHHDD (Edman, N-terminus of mature protein), and WQHPFDEK (*de novo* MSMS). To determine the 5' end of BBS transcripts (sequence that encodes the signal peptide + 5' UTR) we first reverse transcribed the *B. punctata* RNA extraction into a cDNA library using Superscript IV Reverse Transcriptase (ThermoFisher Scientific). Then we amplified the BBS transcripts using 3'RACE (56) and thermal asymmetric interlaced PCR (57, 58). List of primers used is found below: Degenerated primer designed form peptide sequence HHEEGHHDD: (5′CAYCAYGARGARGGNCAYCAYGAYGA). Nested primer designed from sequence WQHPFDEK: (5′ TGGCARCAYCCNTTYGAYGARAA).

Sequence validation

To verify that the PCR product corresponded to BBS, the following methodology was considered: (a) The complete protein sequence was predicted using GetORF. For *in silico* digestion of the BBS we used the software MassSorter (59), using trypsin, and allowing for different modifications: carbamidomethylation (C), oxidation (M). (b) *De novo* sequenced peptides were aligned to the predicted protein sequence. (c) For those peptides with available MSMS spectra that could not be interpreted due to their complexity or low quality, the sequence was obtained *a posteriori* to verify that it was compatible with the predicted sequence. (d) The few peaks used for the PMF that could not be explained by the predicted protein sequence were

thoroughly studied to look for putative posttranslational modifications, a larger number of omitted cleavage sites, or the differential cleavage of different amino acids (No K or R).

Multiple alignments

For the multiple alignments we used M-Coffee, which uses consistency to estimate a consensus alignment combining the output of several individual methods (60, 61). Additionally, we performed multiple sequence alignment using the structure based method implemented in Expresso (62). The resulting multiple sequence alignment was manually refined using UGENE (63), particularly at the Reactive Center Loop (RCL) region. The N-terminal region of the serpins as well as the signal peptide (not part of the protein fold) were considered un-alignable (22) and hence not considered for the reported identity percentages, except when explicitly indicated. Alignments are considered from the N-terminus of the α helix A in α1-AT. Figures with alignments and secondary structure information were created with ESPRIPT3.0 (64) and edited to highlight the serpins nomenclature for elements of secondary structure.

Post-translational modifications analysis

Enzymatic deglycosilation of *Boana punctata* BBS

Digestion under denaturing conditions: 10 µl of BBS solution (500 µg/ml) in 50 mM phosphate buffer pH 7.5, 0.5% SDS, 0.1 M 2-mercaptoethanol were incubated 10 min at 100°C followed by fast cooling on ice. Then, 50 mM phosphate buffer pH 7.5, 0.2% NP-40 was added to reach the final volume of 25 µl. Finally, 1 µl PNGaseF (NEB, P0704) was added and the sample was incubated 4 hr at 37°C.

Digestion under native conditions: 1 µl of PNGaseF was added to 40 µl of BBS solution (125 µg/ml) in 50 mM phosphate buffer pH 7.5. The sample was incubated for 24 hr at 37°C. As a control, a PNGaseF-free BBS solution was incubated in the same temperature conditions to rule out temperature degradation effects.

Mass spectrometry with LTQ-ORBITRAP analyzer

For the analysis of post-translational modifications, purified native BBS was trypsinized and the peptides were analyzed by ultra-performance liquid chromatography hyphenated with quadrupole Orbitrap mass spectrometry in the Centro de Estudios Químicos y Biológicos por Espectrometría de Masa (CEQUIBIEM, Universidad de Buenos Aires and CONICET). Liquid chromatography was performed in an Easy-nLC 1000 (Thermo Scientific). Mobile phase consisted of water + 0.1% formic acid (A) and acetonitrile + 0.1% formic acid (B) in the following gradient: 0.0–60.0 min (3–30% B). Ionization was performed by ESI operated at 3kV. For mass spectrometry, a Q-Exactive (Thermo Fischer) Orbitrap Spectrometer was used. The instrument was configured to operate at high resolution (70000 at 200 m/z) in data-dependent acquisition mode (DDA). The 12 most intense precursor ions in a full MS scan were consecutively isolated and fragmented to acquire their corresponding MSMS scans. Auto gain control (AGC) was set to 3e6 and dynamic exclusion duration set to 20 s. Maximum injection time was set at 100 ms. Fragment ion spectra were produced via high-energy collision dissociation (HCD). Resolution was set at 17500. AGC was set to 1e5, and maximum injection time for MSMS was set at 120 ms. All the data were exported to mgf extension. With the LC-MS Orbitrap data we used GlycoPeptideSearch (65) using as query the BBS sequence and the database GlycomDB (http://www.glycome-db.org/). The parameters used were

as follows: Enzyme: Trypsin; Minimum Peptide Molecular Weight: 400 m/z; Maximum Peptide Molecular Weight: 5000 m/z; Min. Oxonium ions: 2; Min. Oxonium ions Relative Intensity: 8%; Min. Peptide Fragments: 5; Min. Peptide Fragments Relative Intensity: 5 %. Results were analyzed manually to confirm the sequences and for the partial analysis of the glycosidic structure from the oxonium ions data. This approach did not result in all the glycosylated peptides and found some false positives that were manually depurated. To look for more peptides compatible with glycosylation, raw data was interpreted by a custom Python script that allowed us to find the glycosylated peptides. Once isolated, raw data were manually interpreted to verify the sequence (*SI Appendix*, Fig. S3)

Fluorescence spectroscopy of BBSs

Fluorescence spectra were obtained using an Aminco-Bowman Series 2 spectrofluorimeter (Specetronic Co. Rochester, NY, USA) with excitation and emission monochromators. Spectra were acquired at constant temperature (25 ± 0.1°C) starting at an emission wavelength equal to excitation wavelength + 15 nm. Scanning speed was set at 200 nm/min using 5 and 10 nm excitation and emission slits respectively. For tryptophan fluorescence spectroscopy the excitation wavelength was set at λ_{ex}=295 nm. Emission spectra were smoothed using Savitzky-Golay algorithm (66), using 11 points in the smoothing window. Second derivative of the spectra were calculated and smoothed accordingly. The fluorescence emission peaks inferred from the second derivatives were used to fit the original data with Gaussian curves using the iterative Levenberg Marquardt algorithm.

Circular dichroism (CD)

Far UV CD spectra (185nm-260nm) of the purified BBS protein were measured using a spectropolarimeter Jasco J-810 (Nikota, Japan). Five to eight spectra obtained at a scanning speed of 100 nm/min, data pitch 0.2 nm and integration time of 2 s were averaged per sample, were averaged per sample, and buffer signal was suppressed. Temperature was kept constant with a Peltier device at 25 ± 0.1°C. Spectra were measured using 0.1 cm path length spectrasyl Quartz cuvettes (Hellma, Germany)

For far UV spectra, mean residue molar ellipticity was calculated using the following equation:

$$MRW(deg.cm^2.dmol^{-1}) = mdeg/10*L*[M]*(\#p)$$

Where mdeg is the raw ellipticity signal (milidegrees), L is the optical path of the cuvette (in cm), [M] is the sample concentration (mol/l), #p the number of peptide bonds in the BBS protein. BBS percent secondary structure composition in solution was estimated using CDpro (67) which incorporates SELCON3, CONTIN, and CDsstr that estimate secondary structure composition based on different methodologies that use protein standards with crystallographic and CD data. For this study, we incorporated 37 globular protein standards. Experiments were performed at the Protein Structure-Function and Engineering Laboratory, Fundación Instituto Leloir, Buenos Aires, Argentina.

Size exclusion chromatography

500 µl of protein solution (5 µM) in phosphate-buffered saline 20 mM pH 7 were applied to a Superdex 200 column previously equilibrated with phosphate-buffered saline 20 mM, NaCl 20 mM pH 7, and run at 0.5 ml/min. Detection was performed at 215, 280 and 667 nm, to detect both proteins and biliverdin.

Transcriptomes RNAseq

A male specimen of each species was euthanized and the liver was immediately excised and preserved in 1.5 mL RNAlater (Thermo Fisher Scientific). Total RNA was extracted under liquid nitrogen, using TRIzol™ (Life Technologies, Ltd.) following the manufacturer's instructions. The extractions were precipitated in 99% ethanol and sent to Macrogen Korea Inc for sequencing. The cDNA libraries were prepared using TruSeq RNA Sample Prep Kit v2 (Illumina) or TruSeq Stranded mRNA LT Sample Prep Kit and sequenced on an Illumina HiSeq 2000 or Illumina HiSeq 4000, with 100-bp paired-end reads.

The raw sequences were cleaned using Trimmomatic v0.39 (68), run in pair-end mode and using the following settings: 3'end quality = 20; sliding window mean quality = 20, and minimum length = 45. Cleaned sequences were assembled using SOAPdenovo-Trans v1.03 (69) with multiple *k*-mer values (*k* = 35, 45, 55 and 65). The assemblies for each individual were combined with cd-hit v4.8.1 (70) using a 99% identity threshold and a word size of 10. Contigs were extended using cap3 (71) with at least 95% identity and minimum overlapping length of 40 bp. For a preliminary assessment of potential protein-coding regions, the final contigs were translated using ORFpredictor v3.0 (72).

BBSs identification in other frog species

Purified BBSs were processed to study by Peptide mass fingerprint (See "Peptide mass fingerprint"). Lists of peaks from each species were searched against their translated transcriptomes using Protein Prospector. BBSs were also subjected to MALDI-TOF to estimate their molecular weight, and to LC-MS/MS to determine the identity of the biliverdin, by comparison with *Boana punctata* biliverdin. BBSs were identified as serpins, but some of them were incomplete or inaccurate due to the mis-assembly of paralogs (i.e., chimeric sequences). To

overcome this issue, we implemented a different approach (*SI Appendix*, Fig. S12 and Discussion):

1) For each transcriptome we performed a tblastn search, using a custom query that implemented all the human Clade A serpins, *Xenopus tropicalis* serpins (36), and the BBSs that had already been identified with high accuracy in the first search. Only matches with an E-value <1e-5 were retained.
2) The cleaned sequencing reads used to generate the transcriptome were aligned to the serpins matched in step #1 above using blastn. Read pairs were aligned independently (treated as single-end reads). Only reads with at least one match and an aligned length of i) ≥20 bp or ii) ≥40 bp were kept. These aligned reads were retrieved, synchronized back into pairs when possible using fastq-pair (73), and duplicates removed using cdhit. Clusters generated in cdhit were examined at different cutoff levels of reads (an approximation of cluster expression) (cutoff values: 1, 5, 10, 20, 30, 40, 50, 75, 100, 150, 200, 250, 300, 350, 400, 450, 500, 600, or 700 reads). At each cutoff level, the included reads were assembled using SPADES v3.13.0 (74).
3) The newly assembled contigs for different cutoff values were merged and clustered with strict criteria (100% identity) using cd-hit. The final, merged assembly at each cutoff value was translated to ORFs using GetORF and the sequences were submitted to Protein Prospector for PMF analyses.

The new contigs were used as a query for a new blastn search and the whole filtering and assembly process was repeated once. At the end, the final merged assembly for different cutoff values was translated to ORFs using GetORF and the sequences were submitted to Protein Prospector to do PMF analyses (see Peptide mass fingerprint (PMF), above).

Using the same RNA extraction and amplification protocols described above (BBS complete sequence), we also tried to obtain BBSs orthologous serpin sequences from non-chlorotic amphibian species. However, the existence of a large number of paralogs with approximately the same length (See *SI Appendix, Orthology and Paralogy of Clade A Serpins)*, produced mixed chromatograms when we extracted DNA from single bands, and thus impeded accurate sequencing. In any case, the isolation of any specific paralog from non-chlorotic animals cannot guarantee that it is the BBSs ortholog of any of the chlorotic species *(SI Appendix, Orthology and Paralogy of Clade A Serpins)*.

BBS transcripts quantification

Once the complete BBS sequences were validated, we aligned the cleaned RNAseq reads to them using blastn. To estimate expression level, we only counted aligned reads that resulted in alignments with 100% identity to minimize the potential of false positive alignments resulting from paralogous sequences, and restricted the alignments to only the coding region of the transcripts. Furthermore, we only considered reads whose alignment overlapped ≥60 or ≥80 bp with a reference contig and if matching with an edge, we only considered reads whose alignment overlapped ≥20. Both properly paired and discordant (one read in a pair was unaligned, weighted 0.5 the expression of a mapped read pair) reads were counted in the quantification. Expression values were reported as the number of mapped reads per kilobase of coding transcript per million cleaned reads (FPKM). Although it is still possible that a portion of the aligned reads originated from one or more paralogs, the sequence identity between paralogous serpins of the same clade is quite low (~50%) thus the effect on FPKM estimates is minimal and relatively similar across

species. Heme oxygnase (HMOX1), responsible heme oxidation that yields biliverdin was also quantified following the same criteria used for BBS (*SI Appendix*, Table S15).

Spectrophotometry measurements and simulation of BBSs influence on coloration

Diffuse reflectance measurements were performed with a spectrophotometer (UV3101PC; Shimadzu, Tokyo, Japan) equipped with an integrating sphere (ISR-3100; Shimadzu). Barium sulphate was employed as a white reference standard to adjust 100% reflectance level. We selected three common floating plant species naturally co-occurring in the habitat of *Boana punctata*: the common water hyacinth (*Eichhornia crassipes,* adaxial and abaxial surfaces), the water lettuce (*Pistia stratiotes*) and the water fern (*Salvinia biloba*).

Frogs diffuse transmittance and reflectance spectra were obtained from the material published elsewhere (2). We considered full animals' dorsal reflectance, transmittance and reflectance of skins (T_S and R_S) sequentially washed with amphibian PBS (52) to partially remove pigments (hyloins, BBSs adsorbed to the skin), transmittance and reflectance of muscles (T_M and R_M), reflectance of the guanine crystals containing layer (R_{CCL}) underneath the musculature (Fig. 3C) (see Taboada et al. (2)). We did not consider reflectance at the skin/lymph interphase specially because in physiological conditions lymph impregnates the dermis of amphibians.

To calculate the red edge in the frogs the first derivative of the reflectance spectra were obtained using Matlab isignal totolbox version 6.1.

To evaluate the influence of BBSs in the animals' coloration, we followed a methodology similar to the one used by Taboada et al. (2). Briefly, we considered the light emerging from the frogs as:

$$I^{out}(\lambda)/I^{in}(\lambda)=R_S(\lambda) + T^2{}_S(\lambda)T^2{}_L(\lambda)T^2{}_M(\lambda)\ R_{CCL}(\lambda) + T^2(\lambda)_S\, T^2(\lambda)_L\, R_M(\lambda)$$

Where I^{in} is the incident photon flux (from the lamp), I^{out} is the emerging photon flux from the animal, T is transmittance and R is reflectance. To assess the influence of BBSs, we simulated three simplified conditions for lymph composition: (1) 46 μM BBSs (2) 46 μM free helical IXα biliverdin at neutral pH and (3) no pigments. To calculate transmittance from absorbance (A) we assumed that lymph is a solution that follows Lambert Beer law ($T=10^{-A}$). For the thickness we considered 700 μm, which can account for skin thickness (~300–400 μm (75)) plus the thickness of lymphatic sac. We did not consider hyloins fluorescence for the modeling (2) and we assumed that their concentration would be equal in the three simulated conditions. Additionally, it has been shown that their emission spectra do not overlap with lymph absorbance spectrum (2).

Supplementary Information Text

Taxonomic distribution and evolution of chlorosis in anurans

Chlorotic species show clear accumulations of blue-green lymph and tissues and/or blue-green bones. In some cases, this information was obtained from the literature, but the occurrence of these characteristics associated with chlorosis is frequently not mentioned explicitly in taxonomic descriptions. However, in most cases, they are easily identifiable from good quality photographs. The limitations of this approach are that (1) the taxonomic descriptions are insufficient for several species, (2) the available photographs may not be informative, and (3) in some instances, when chlorosis is associated only with one phase of coloration or is only evident in recently metamorphosed juveniles, this may not be reported, or the latter may be unknown. In the groups that have chlorosis, but the bones are not chlorotic, the latter is mentioned usually in

the literature, but the green tissues are not. For these reasons, the resulting list of chlorotic species in the current study is necessarily a minimum estimation.

In Supplementary Table 1, we list the chlorotic species, and we note when the datum is based on the explicit mention in the literature or from the interpretation of pictures. From the Table, it is noteworthy that the amount of chlorotic frog species that are not arboreal (nor closely related phylogenetically to arboreal species) is minimal (~1% of the known chlorotic species). We discuss for each family the limitations that we found in terms of phylogenetic knowledge and their influence on the minimum estimation of 40 independent origins of chlorosis.

Arthroleptidae

Our survey indicates that there are at least three chlorotic species of *Leptopelis*. This genus has 56 recognized species (76), of which 28 were included in the phylogenetic analysis of Portik et al. (77). Of these, only *L. karissimbensis* is chlorotic. We are not aware of any suggestion regarding the phylogenetic relationships of the two other chlorotic species, *L. grandiceps,* and *L. uluguruensis*. We tentatively consider a single origin of chlorosis in *Leptopelis* (*SI Appendix*, Fig. S1)

Centrolenidae

The occurrence of chlorosis, while never using that name nor referring to biliverdin, but only to green bones, has almost turn into an instant reference to “glassfrogs”, the family Centrolenidae. This family includes 157 species (76) of which all but 30 of the 32 species of *Hyalinobatrachium* have been characterized for having green bones (78, 79). In centrolenids there is large variation regarding other characters commonly associated with chlorosis, such as

skin transparency and white membranes. Frequently there are no references to lymph or non-osseous tissue coloration, but photographs of most species commonly show that besides the bones, there are high concentrations of biliverdin in other tissues. Regarding the species of *Hyalinobatrachium*, although most of them do not show green bones, photographs of live specimens suggest that biliverdin is present in other tissues in several species, indicating that they have chlorosis as well. Further studies should determine the nature and extent of its occurrence in non-osseous tissues. Chlorosis optimizes in the most recent common ancestor of this family, indicating that it evolved only once (Fig. 1).

Craugastoridae

In this family of 835 species(76), only one described species so far is known to be chlorotic, *Pristimantis galdi.*

Dendrobatidae

Silverstone (80) described the occurrence of green bones in one of the 199 species included in the family (76), *Epipedobates tricolor*. Despite having extensive experience with this species in the field and in the lab, one of the coauthors (Santiago Ron) has never noticed green bones in this species, something corroborated by Taran Grant and Karl-Heinz Jungfer (pers. com.). We do not consider this record, pending its corroboration.

Hemiphractidae

In this family, chlorosis occurs only in the genus *Gastrotheca*, for which there is evidence of chlorosis for 11 of its 74 species. These include six of the eight species of the *G. longipes*

group, all species of the *G. microdiscus* group, and one species of the *G. masupiata* group (*G. argenteovirens*). Of these 11 species, 10 were included in phylogenetic analyses (single exception *G. andaquiensis*). The analysis of Jetz & Pyron (26) includes the most recent, relevant phylogenetic results for Hemiphractidae (81). The ancestral character reconstruction of chlorosis in the hypothesis of Jetz & Pyron (26) indicates that chlorosis evolved at least two times during the evolutionary history of *Gastrotheca*, being equally parsimonious two origins and two reversals, or three origins and one reversal.

Hylidae

In this family, there are at least 177 of its 1000 species that are chlorotic (we follow the taxonomy of hylids as discussed by Faivovich et al. (82, 83), but take the species numbers from [3]). Of those, 170 are in the subfamily Hylinae (720 species), and mostly in the tribes Cophomantini, Lophiohylini, Pseudini, and Sphaenorhynchini. The phylogenetic hypothesis of Jetz & Pyron (26) does not fully incorporate most terminals and sequences employed by Duellman et al.(84), the largest reanalysis of hylid GenBank sequences made up to that time. Furthermore, recently, Rojas-Runjaic et al. (85) and Pinheiro et al. (86) published analyses of Cophomantini that increased our knowledge on the relationships and diversity of the basal Cophomantini (*Hyloscirtus*, *Myersiohyla*, and *Nesorohyla*). These discrepancies in taxonomic and character sampling, however, do not seem to be relevant for our understanding of the evolution of chlorosis in the family, as the topology for Hylinae overall is congruent among the different analyses, while the level of understanding of relationships of Pelodryadinae is still weak.

There is evidence of chlorosis for seven of the 215 species in the subfamily Pelodryadinae. From those, only two have been included in phylogenetic analyses (*Litoria thesaurensis* and *Ranoidea dayi*), and are recovered very distantly related. Kraus (87) hypothesized that two chlorotic species are related with *L. thesaurensis* (*L. flavescens* and *L. lutea*), two other (*L. nullicedens* and *L. pallidifemora*) belong to the *L. graminea* group, and *R. aruensis* is included in the *R. gracilenta* group. These hypotheses require corroboration through a thorough phylogenetic analysis of Pelodryadinae. In the meantime, and lacking other sources of evidence, we consider that chlorosis evolved four times in Pelodryadinae.

In Hylinae, the optimization indicates (Fig. 1), that chlorosis evolved independently in all the tribes where it occurs (Cophomantini, Dendropsophini, Lophiohylini, Pseudini, Scinaxini, and Sphaenorhynchini). It evolved one time each in Pseudini and Sphaenorhynchini, while in Lophyohylini it evolved two times. In Cophomantini, it is equally parsimonious to infer a single origin and three subsequent losses, or four independent origins. In Dendropsophini and Scinaxini chlorosis evolved at least six times.

Summing up, chlorosis evolved at least 15 times during the evolutionary history of hylids. The relationships among the tribes of Hylinae are poorly supported (82). Also, relationships inside Cophomantini (particularly *Myersiohyla*, *Nesorohyla*, and the clade, including all other genera) are unstable (86), as are inside Lophyohylini (247). These uncertainties should be kept in mind, and are the reason why the minimum number of inferred origins of chlorosis in hylids is strictly tentative.

Hyperoliidae

Our survey indicated that at least 48 of the 145 recognized species of *Hyperolius* are chlorotic, at least in one of their color phases (*SI Appendix*, Fig. S1). Furthermore, two species of *Alexteroon* are chlorotic. The most thorough phylogenetic analysis of afrobatrachians is that of Portik et al. (77); they included 83 currently recognized species of *Hyperolius*, 41 of which are chlorotic; they did not include any species of *Alexteroon*. The optimization of chlorosis in the hypothesis of Portik et al. (77), indicates that it evolved in the common ancestor of most species of *Hyperolius* (with the exception of *H. semidiscus*), and it was apparently lost several times during the evolutionary history of *Hyperolius*, having re-evolved at least three times (in *H. chlorosteus*, *H. dintelmanni*, and *H. picturatus*). The hypothesis of Portik et al. (77) did not include *H. drewesi*, a chlorotic species shown to be very closely related to *H. molleri* by Bell et al. (88) . As the latter is included in the hypothesis of Portik et al. (77) and is distantly related to other chlorotic species, *H. drewesi* should count as a fifth independent origin of chlorosis in *Hyperolius*. Considering that more than 60 recognized species of *Hyperolius* have still not been included in phylogenetic analyses and that several species of this genus have several color phases, some of which involve chlorosis, our inferences should be considered strictly tentative. So far, it is unclear if *Alexteroon* is nested in *Hyperolius* (as obtained by Frost et al. (89) and Jetz & Pyron (26)) or not. Tentatively we count the chlorosis in *A. obstetricans* and *A. jynx* as another independent origin in Hyperoliidae, for at least six instances of evolution of chlorosis in the family (*SI Appendix*, Fig. S1)

Limnodynastidae

In this family chlorosis has been reported as green bones occurring in two of the six species of *Philoria* (90), one of which (*P. frosti*) has never been included in phylogenetic

analyses (89, 91, 92). Pending a thorough phylogenetic study of *Philoria*, we tentatively consider that chlorosis evolved only once in limnodynastids.

Mantellidae

Our survey indicated at least 39 of the 227 species of Mantellidae (77) are chlorotic. These include species from five species groups of *Boophis* (32 of the 79 species, plus a number of undescribed species identified by Hutter et al. (93)), three of the 18 species of *Guibemantis*, and one of the 33 species of *Mantidactylus*, and three of the 14 species of *Spinomantis*. While the mantellid sampling of the hypothesis of Jetz & Pyron (26) allows to infer that chlorosis arose independently in *Boophis*, *Guibemantis*, *Mantidactylus* and *Spinomatis*, we will base our inferences for the first two genera in the most densely sampled phylogenetic studies for *Boophis* (93), *Guibemantis* (94) and Spinomantis (95).

The optimization of chlorosis in *Boophis* (*SI Appendix*, Fig. S2) indicates that there are several alternative reconstructions, all of which imply between two and five origins during the evolutionary history of the group and some reversals. In all reconstructions, chlorosis evolved in *B. pauliani* independently from its occurrence in other species of *Boophis*, where it is equally parsimonious to infer one single origin and four reversals or five independent origins. In the case of *Guibemantis*, the phylogenetic hypothesis of Bletz et al. (94) implies that chlorosis evolved independently in *G. pulcher*, and the clade including *G. liber* and *G. tasifotsy*.

In the case of *Spinomantis* the results of Wollenberg et al. (95) imply that chlorosis evolved once and then was lost in the most recent common ancestor of *S. aglavei* + *S. fimbriatus*, or it evolved independently in *S. peraccae* and in the common ancestor of *S. massi* + *S. phantasticus*.

Summing up, chlorosis in Mantellidae evolved at least five times (once in *Mantidactylus argenteus*, once in *Spinomantis*, at least twice in *Boophis*, and twice in *Guibemantis*, and at least twice in *Boophis*).

Myobatrachidae

Chlorosis was reported in this family as the occurrence of green bones in one of the five species of *Taudactylus* (*T. acutirostris* (90)) and the monotypic *Paracrinia haswelli* (90). Most recent phylogenetic hypotheses of Myobatrachidae (26, 89, 92, 96) allow inferring that chlorosis evolved independently in both species.

Ranidae

Chlorosis so far is known to occur in only two of the 399 species of Ranidae (76), *Staurois guttatus* (97) and *S. natator* (98). The phylogenetic relationships of *Staurois* (26, 98) indicate that chlorosis evolved once and was subsequently lost, or that it evolved two times.

Rhacophoridae

In this family, chlorosis occurs in a few species of the genera *Beddomixalus*, *Chiromantis*, *Gracixalus*, *Rhacophorus*, and *Zhangixalus*. The relevant phylogenetic analyses for the study of chlorosis in this family are those of Onn et al. (99) and of Jiang et al. (100), both of which have a more thorough sampling than the analysis of Jetz & Pyron (26). For the evolution of chlorosis in *Beddomixalus* and *Gracixalus*, the hypotheses of Onn et al. (99) and Jetz & Pyron (26) allow inferring similar results (at least one origin in *Beddomixalus bijui*, and other in an internal clade of *Gracixalus*). Jiang et al. (100) recover *Z. achantharrhena, Z. dulitensis,* and *Z. prominanus* monophyletic, indicating a single origin of chlorosis in this clade.

Rhacophorus calcadensis was included only by Jetz & Pyron (26), who recover it as the sister taxon of a clade including *Feihyla*, *Ghatixalus*, *Taruga* and *Polypedates*. It is unclear why it was not included by Onn et al. (99) and Jiang et al. (100). Pending its inclusion, tentatively we consider that chlorosis evolved only once in *Rhacophorus*.

The only chlorotic species of *Chiromantis*, *C. samkosensis* has not been included in phylogenetic analyses. As long as the monophyly of *Chiromantis* is corroborated in future analyses, chlorosis in *C. samkosensis* would count as a fifth independent instance of evolution.

The results of Onn et al. (99) recovered the non-chlorotic *Gracixalus quyeti* nested among the chlorotic species of this genus, unlike Rowley et al. (101) that recovered them monophyletic. This difference does not affect the minimum number of five origins of chlorosis inferred for Rhacophoridae.

Biliverdin isomer identification

Previous reports on MS/MS analysis of biliverdin of the IX series suggested the expected fragments values for α, β, δ and γ, but there is no chemical evidence of the ions formation (125). In the present investigation we observed the pattern of fragmentation corresponding to the IXα BV isomer. Detailed analyses of the gas phase chemistry (102) allowed us to describe the ions formation (*SI Appendix*, Fig. S8) and confirm the proposal as biliverdin IXα.

Serpins in bones and lymph

In addition to lymphatic BBSs, we extracted and purified the blue pigments from the bones of most of the studied species. Two clear patterns are seen in the bones. Lightly stained ones - especially in the epiphysis- are easily extracted, and mass spectrometry data is identical to the

BBSs extracted from lymph (*SI Appendix*, Fig. S11). In some species with strongly pigmented blue bones (*Hyloscirtus phyllognathus* and *Pseudis minuta*), blue pigment extraction required longer incubation periods and stronger ionic forces in the buffers during grinding. In these species, the blue proteins were purified and processed by mass spectrometry, LC-MS. They are in the range of 46-48 KDa. MSMS data from purified peptides identified them unambiguously as clade A serpins (*SI Appendix*, Fig. S15). However, because the sequenced fragments could not be detected from RNAseq reads it is likely that BBSs in those two species are serpins that are expressed in a different organ, perhaps in the bone marrow which is a known erythropoietic center (103, 104) .

BBS quantification

Although we analyzed RNAseq data from a single specimen of each species, BBS transcript quantification showed large FPKM values (10400-104000 FPKM). Given that there are many paralogs in the clade A serpin family, accurate quantifications are particularly difficult because the assemblies are prone to numerous chimeric contigs. As a result, mapping the raw reads to the reference contigs can result in spurious alignments. To overcome this, we restricted the quantification to reference transcripts from *Xenopus tropicalis* paralogs and from the BBSs, whose sequences are more thoroughly curated. We did not quantify clade A serpins from *de novo* assemblies from other amphibians. To adopt the most conservative approach we included mapped reads that had 100% identity to the different paralog sequences and that aligned at least 80 bp for reads fully contained within the query sequence and 30 bp for reads aligning to the ends. For *Xenopus tropicalis* (SRR579561) we used shorter alignments requirements (60 bp), given that reads lengths for the experiment were 75 bp instead of 100 bp like in the current work.

Quantifications considering a minimum alignment of 60 and 80 bp are shown in Supplementary Table 15. In *Xenopus tropicalis*, Serpin7 (following the nomenclature in (36) and implemented in the current paper) is likely to be homologous to alpha-antitrypsin (36), and has the largest expression values from the clade (~8800 FPKM) (105). Using our quantification approach (only using the coding region of the transcripts, applying a 100% identity filter for the read-to-transcript alignments, and requiring a minimum overlap of 20 bp for the ends of each transcript), we obtained smaller values (~4200 FPKM). The values we reported for BBS expression are high and are consistent with the large lymphatic concentrations of the protein in *B. punctata*.

Physiological vs. pathological chlorosis

In this report we avoided the use of the term hyperbiliverdinaemia, which can be potentially misleading due to its use in medical literature to denote pathological accumulations of biliverdin. In skinks, other term has been coined to denote the high concentration biliverdin: hyperbiliverdinism (20). In the current work, we decided to use the term physiological chlorosis to follow the first thorough description of the phenomenon (4).

Chlorotic animals do not show any pathological indications of enhanced haemolytic rates.

Pathological chlorosis induction: anatomical considerations

Experiments in non-chlorotic animals could not induce hyperbiliverdinemia either by direct injection of biliverdin (5) or of hemolytic agents such as phenylhydrazin (5, 15). Frogs and toads can excrete biliverdin through their urine (5, 15). In a different approach, Cabello Ruz (15) working with the non-chlorotic toad *Rhinella arenarum* could see biliverdin impregnation in a few (7 out of 52) experimental specimens after the injection of a hemolytic agent and simultaneous bile duct ligation. This meant that bile pigments could not be normally excreted

from the gallbladder to the duodenum and it was hence reabsorbed by the blood. Several anatomical alterations were observed in these toads, consistent with the pathologic high hemolytic rate: splenomegaly, gall bladder hypertrophy, muscles discoloration, green urine, and dark purple kidneys, spleen and liver. Diverse mucosae were stained with green/yellow hues. In humans, pathological hyperbiliverdinemia was detected in patients in which there was a simultaneous non-function of biliverdin reductase (homozygous mutations) and bile duct obstruction (13).

In amphibian chlorotic species, the gallbladder has normal coloration and size, and no obstructions of bile ducts were perceived (*SI Appendix*, Fig. S14). Bile can be transported from the bladder to the duodenum. No alterations of other organs such as those described in the induced pathological condition in the toads could be detected in any of the species. Additionally, the stool had a normally dark coloration, as opposed to the expected pale coloration after bile duct obstruction.

Heme oxygenase and biliverdin reductase:

Biliverdin is the first product of heme catabolism. The enzyme heme oxygenase (HMOX) is responsible for the formation of the α biliverdin isomer. Expression of the HMOX-1 gene in chlorotic livers is normal compared to other non-chlorotic amphibians (*SI Appendix*, Table S16). Increased hemolytic rates are then unlikely to be responsible for biliverdin accumulation. Biliverdin and bilirubin are normal excretion products in amphibians (8, 106, 107). In humans and many other vertebrates (mainly mammals) biliverdin reductase is the enzyme responsible for the reduction of biliverdin to bilirubin. Biliverdin reductase A reduces α isomers, while

biliverdin reductase B reduces the rest (β, γ, δ). Biliverdin reductase A could not be detected in the chlorotic species liver transcriptomes studied in this work.

Other biliverdin binding proteins in amphibians and early biliverdin impregnation of oocytes and embryos

Two additional biliproteins have been described in amphibians, specifically associated with oocytes. Upon experimental chronic stimulation of *Xenopus laevis* with estrogens, Redshaw et al. (108) showed that green coloration of the oocytes is caused by biliverdin bound to the complex lipovitellin-phosphovitin with one BV bound to each protein. Falchuk et al. (33) showed that biliverdin is present in oocyte cytoplasmic yolk platelets under physiological conditions too, and demonstrated a role in the dorsal axis development in *X. laevis* embryos. In the Mexican leaf frog *Agalychnis dacnicolor*, Marinetti and Bagnara (32, 109) showed that oocytes have BV bound to lipovitellin but not to phosphovitin. Many other amphibians have blue-green oocytes and embryos (110, 111), but the coloration disappears early during tadpole development. In these species, neither the interaction of the biliverdin and the protein, nor the protein nature have been reported so far.

Evolution of chlorosis and BBSs

Phenotypic convergence of chlorosis: high biliverdin concentrations, green coloration and red edge reflectance

Chlorotic animals evolved similar phenotypes, involving green tissues such as skin, bones, muscles and mucosae. Here, we showed that chlorosis evolved multiple times along the evolutionary history of amphibians and we provided a biochemical explanation for BV

accumulation based on the expression of a clade A serpin, named BBS, that binds BV. All of the BBSs from different species that we studied have spectroscopic properties consistent with that of stretched BV inside of the protein core ((34), Fig. 2), which suggests similar protein-ligand interactions in the different BBSs. This interaction between BV and the protein is responsible for the increase in absorbance in the red portion of the spectrum, which has at least three phenotypic consequences for frog coloration:

(1) Green coloration: In many chlorotic frogs it can be explained as a combination of BBSs in lymph and interstitial fluid (cyan color) in combination with yellow xanthophores in the skin and a broad band reflector (either guanine crystals or collagen bundles in fasciae, peritonea, and dermis). This mechanism provides an alternative biochemical origin of green coloration in vertebrates, which is normally explained by the theoretical background of the dermal chromatophore unit (three-dimensional arrangement of chromatophore cells (1) (Figs. 3 and 4)

(2) Red-edge reflectance: It consists of a steep increase in near infrared reflectance and was originally described in plants. To date, red-edge and near infrared reflectance have no mechanistic explanation in frogs, even though its existence has been reported in several amphibian species (41, 112, this study). Using Kubelka-Munk simulations for light propagation we showed that, contrary to isolated BV, physiological concentrations of BBSs can explain the red-edge effect by increasing absorption of red wavelengths (BBSs max absorbance ~660-670 nm)

(3) Cyan-blue coloration in different regions of the body (e.g. mucosae in mouth, pelvic patches, etc.): In the absence of yellow pigments such as those in xanthophores, which is normal in different skin patches, BBSs can also explain how animals can

achieve a broader array of colors that span the blue-cyan to the green portion of the spectrum. Blue-cyan coloration in vertebrates is normally achieved via structural mechanisms with selective light reflectance (113). Our work demonstrates an alternative mechanism that can result in blue-green coloration, via absorption properties of BBSs.

Considering that there are BBSs with similar biochemical properties in all the chlorotic species that we studied from clades where chlorosis evolved independently, we optimized the chlorosis on the phylogenetic tree of amphibians and posit that this physiological mechanism of chlorosis has originated multiple times across anurans. This physiological mechanism can explain the convergent origin of green and cyan tissues in chlorotic amphibians as well as their infrared reflectance properties. Future work is required to elucidate the genetic mechanisms underlying these phenotypes, but our description of the novel BBSs open up many interesting avenues for research in the evolution and diversification of serpins and physiological chlorosis.

Genetic bases underlying chlorosis

Despite our current work demonstrating a clear, convergent mechanism of phenotypic chlorosis among anurans (Fig. 1), whether or not identical amino acid substitutions in orthologous serpins have subtended the chlorotic phenotype remains unknown. Indeed, it is not possible to assess if different BBSs are orthologs or if they evolved from different paralog genes. The identification of convergent amino acid substitutions has proven useful in certain phenotypic contexts (e.g. (114-116), and specifically (117) for a review on the current methods). Also, it has been demonstrated that single amino acid mutations contribute to adaptive color patterns (e.g (118)).

At the moment, multiple factors make the identification of convergent amino acid substitutions within the serpin superfamily challenging: 1) the scarcity of highly curated amphibian genomes, 2) the lack of accurate annotations of serpin sequences and 3) the existence of numerous paralogs within clade A serpins resulting from recent duplication events in vertebrates ((36); see "*Orthology and Paralogy of Clade A Serpins"* below).

Future work on BBS crystallography together with mutagenesis studies will reveal whether there are key residues that may contribute to BV binding pocket(s) in BBSs, and eventually will help to identify specific convergent substitutions (if any) between different chlorotic species. However, if we consider the multiple origins of physiological chlorosis and the low identity between the numerous serpin paralogs (46-54% between different BBSs) (see below *Orthology and Paralogy of Clade A Serpins*), it is unlikely that convergent amino acid substitutions explain the increased binding affinity of BBS for BV. Indeed, it is likely that different BBS copies evolved different sets of substitutions that create the binding sites (e.g., corticosteroid binding globulins in birds (119)). In any case, whether the existence of convergent substitutions or the evolution of independent substitutions in different regions of the proteins, these do not contradict our finding that chlorosis is a convergent, physiological phenomenon in anurans.

Orthology and Paralogy of Clade A Serpins

Among vertebrates, the knowledge of clade A serpins is primarily limited to a few mammals and birds. Within amphibians, only the model genus *Xenopus* has been examined to any extent. Thus, any analysis to determine the orthology/paralogy of BBSs from chlorotic species would necessarily depend on non-amphibian sequences, mainly human. All the BBSs described in this study belong to the Clade A of the serpin superfamily. This group comprises multiple paralogs of

α1-antitrypsin-like genes (e.g. 13 in humans (11 genes and two pseudogenes (120)), 22 in mice (120), 9 in *Xenopus tropicalis* (36), 8 in chickens (36)) clustered in their genomes (except for Serpin8, angiotensinogen) and apparently derived from recent duplication events (36). These duplications result in proteins with high sequence similarities that preclude accurate one-to-one orthology comparisons (36). Indeed, in phylogenetic analyses the clade A serpins frequently cluster by species rather than by ortholog sequences. In addition, the exact number of members of the cluster is not known with certainty in many of the species, even in those with available genomes.

In addition, studies linking serpins sequences with their functions are scarce in non-mammalian species. Within frogs, only few serpins of clade A have been sequenced or characterized at the transcript (EP45 in *Xenopus tropicalis,* (121)) or protein level (Hylaserpin in *Hyla simplex* (122)). The orthology of those sequences remains unknown. Indeed, considering the frog model *X. tropicalis*, broad phylogenetic analyses could not assign the orthologs of the well characterized alpha-1-antitrypsin or the corticosteroid binding globulin. In fact, only two out of nine sequences from *Xenopus* cluster with other species orthologs (protein Z dependent inhibitor (SerpinA10 in humans) and AGT (angiotensinogen, which is the only clade A serpin located in a different chromosome) (36). It is worth noting that the genus *Xenopus* is part of an early diverging clade of anurans, and thus evolutionary analyses of proteins such as BBSs in anurans will require much more taxon-sampling.

Considering the arguments developed above, it is difficult to assess whether different BBS are orthologs or paralogs, or to find the orthologs among other non-chlorotic species. However, sequence identities can provide some good indications. The optimization of chlorosis (Fig. 1 and Supplementary Information), support a single origin in glass frogs (Centrolenidae), but it has

multiple origins in most other families. Sequence comparisons show that among glass frogs of different genera, BBSs have 76-88% identity (*SI Appendix, Table S13*). Among hylids, the highest sequence identity that we found was between *B. punctata* and *B. cinerascens* sequences (76%). Ancestral reconstruction of chlorosis (Fig. 1) showed that it arose in the ancestor of *B. cinerascens* and *B. punctata* and thus it is likely that BBSs are orthologs in those species. In all the remaining hylids studied – where chlorosis ancestral reconstruction revealed multiple origins – sequence identities range from 45-54% (*Sphaenorhynchus lacteus*, *Aplastodiscus leucopygius*, *Hyloscirtus phyllognathus*, *Pseudis minuta*). While these values are not conclusive, it is likely that BBSs correspond to different paralogs of clade A serpins. For a broader perspective, ortholog sequences in other groups of vertebrates reveal that for example, human alpha-1-antitrypsin has 75%, 72%, 72% and 70% with dogs, cats, horse, and sheep orthologs (respectively). In addition to the sequences' identities, it is interesting that at least some of the species studied here have two different BBSs paralogs bound to BV. In those species we found that bones express a different serpin from that of the lymph. The existence of two paralogs within the same species also supports the convergence of the BV binding affinity in chlorotic amphibians.

BBSs expression, ontogeny and phases

The existence of different serpin paralogs with expected different expression levels may be one of the causes that explain why some species have different color phases, ontogenetic changes as well as different bones coloration (*SI Appendix, Table S1*). Blue-green coloration of bones is normally -although not always- indicated when present in taxonomic reports. As we showed in this study, some species have only one BBS that is expressed in the livers and normally

impregnates all the tissues with a blue-green coloration. When this is the case, bones are impregnated in blue-green and the BBSs can be easily extracted from bones. In these species, the coloration of the bones can change based on the animal activity and time of the day, and is normally visible in the epiphyses. In the species in which we found a second BBS in the bones, we could not find evidence of liver expression, and those BBS may be a different paralog expressed in a different tissue, likely the bone marrow. If this is the case, liver BBSs could bind the free biliverdin from senescent red blood cells produced in the liver, whereas bone serpins could bind biliverdin from erythropoietic cells. The existence of at least two paralogs that bind biliverdin may explain how some species are described with blue-green bones but apparently, they lack blue-green soft tissues. The opposite is true for those species that have a liver BBS that is highly concentrated in plasma and lymph. In this case, tissues are blue-green but bones may or may not be in different times of the day, and will depend additionally on the local blood and lymph circulation of bones.

In the species with ontogenetic changes, that have chlorotic juveniles but later on they do not show green tissues, a decreased expression of the BBS gene is expected.

Green coloration in Centrolenid frogs: chromatophore C and biliverdin

In the centrolenid frog *Hyalinobatrachium fleischmanni,* Schwalm and McNulty (123) described a novel chromatophore type in their dorsal skin, which they named Chromatophore C. More recently it has been speculated that chromatophore C may contain biliverdin (78), but no empirical data has been shown to support this. Further studies will be necessary to know if it is bound to a protein, putatively an intracellular serpin.

Fig. S1. Ancestral character reconstruction of physiological chlorosis in afrobatrachian families. Reconstruction is based on the phylogenetic hypothesis of Portik et al. (78) The informal names of the undescribed species are those employed by the authors.

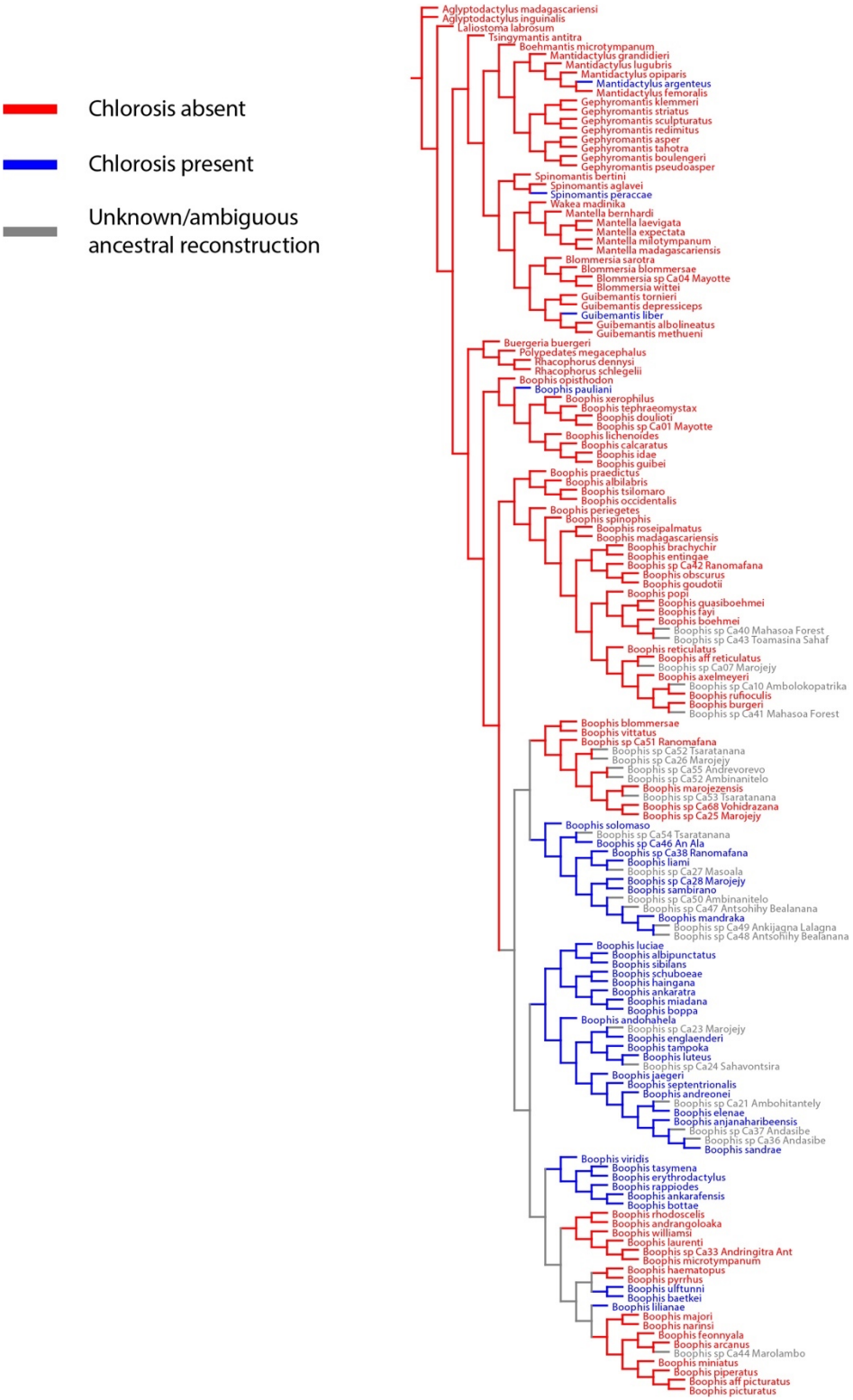

Fig S2. Ancestral character reconstruction of physiological chlorosis in Mantellidae. Reconstruction is based on the phylogenetic hypothesis of Hutter et al. (94). The informal names of the undescribed species are those employed by the authors.

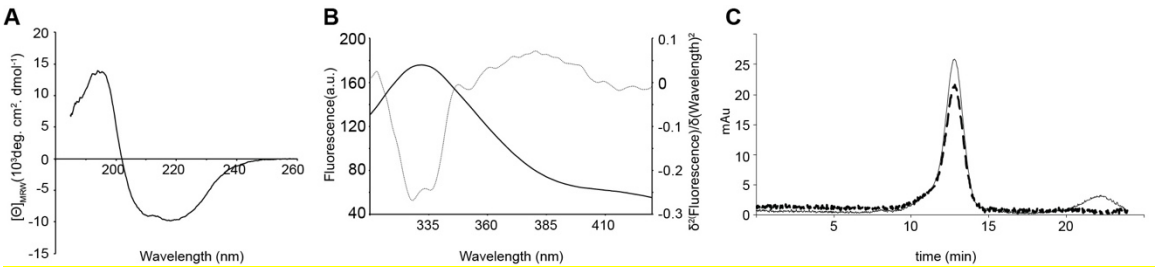

Fig. S3. Spectroscopic properties of *Boana punctata* BBS

(A) Far-UV circular dichroism (CD) spectrum of BBS at a concentration of 0.38 mg/ml. Assessment of secondary structure contribution using the CDSSTR algorithm implemented in CdPRO suggests that BBS is approximately 29% helical, which is consistent with the crystal structure of human α1AT (Protein Data Bank ID: 1QLP). [Θ]MRD, means residue ellipticity. **(B)** Intrinsic fluorescence emission spectrum of BBS. Maximum emission is in the 326 – 336 nm region. Second derivative spectrum (dotted line) revealed two minima at 327 and 337 nm, which agrees with the presence of two tryptophan residues in BBS that are protected from solvent. **(C)** Elution profile of BBS from *Boana punctata* on a Superdex 75 column, monitoring the absorption at 280 nm (–) and 667 nm (---). Information from **(A-C)** is compatible with the existence of secondary and tertiary compact structure in solution from BBS.

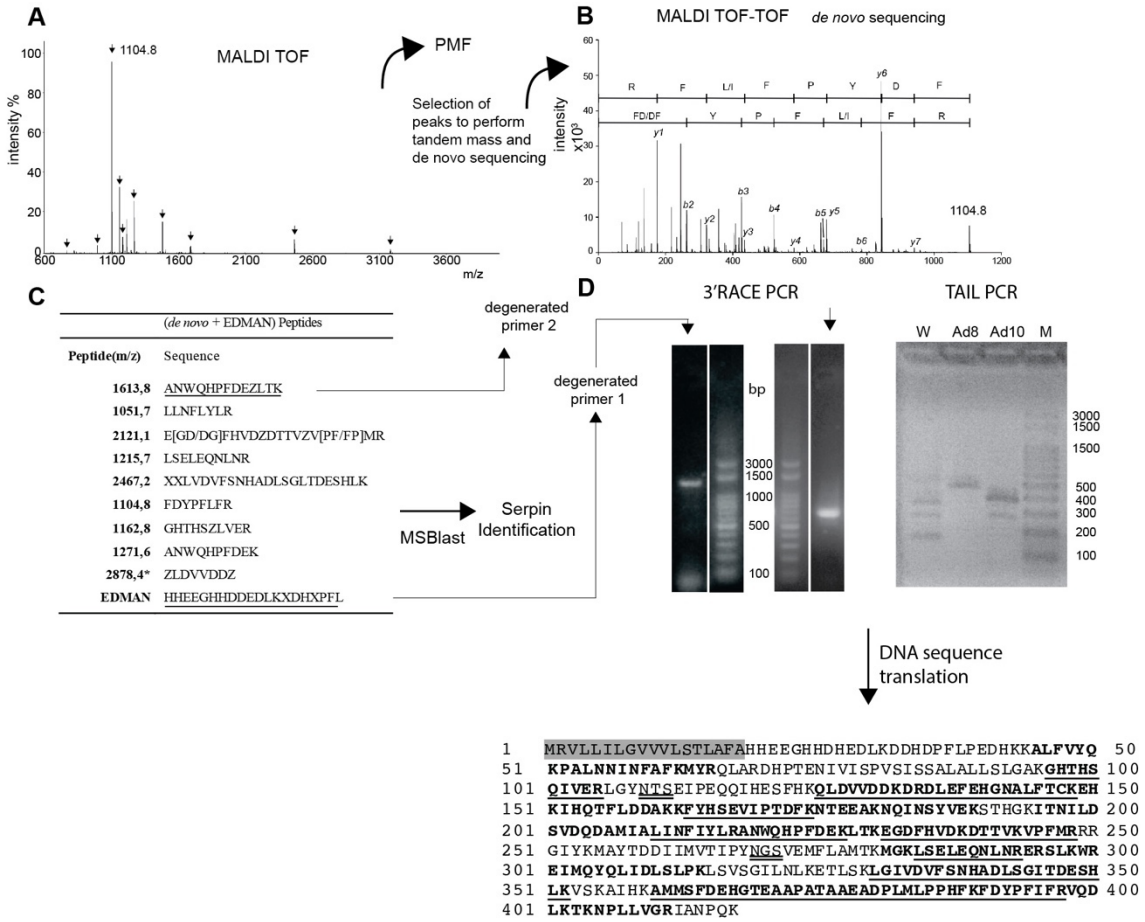


```
1   MRVLLILGVVVLSTLAFAHHEEGHHDHEDLKDDHDPFLPEDHKKALFVYQ  50
51  KPALNNINFAFKMYRQLARDHPTENIVISPVSISSALALLSLGAKGHTHS 100
101 QIVERLGYNTSEIPEQQIHESFHKQLDVVDDKDRDLEFEHGNALFTCKEH 150
151 KIHQTFLDDAKKFYHSEVIPTDFKNTEEAKNQINSYVEKSTHGKITNILD 200
201 SVDQDAMIALINFIYLRANWQHPFDEKLTKEGDFHVDKDTTVKVPFMRRR 250
251 GIYKMAYTDDIIMVTIPYNGSVEMFLAMTKMGKLSELEQNLNRERSLKWR 300
301 EIMQYQLIDLSLPKLSVSGILNLKETLSKLGIVDVFSNHADLSGITDESH 350
351 LKVSKAIHKAMMSFDEHGTEAAPATAAEADPLMLPPHFKFDYPFIFRVQD 400
401 LKTKNPLLVGRIANPQK
```

Fig. S4. Sequencing of *Boana punctata* BBS

(A) MALDI-TOF spectrum of peptides obtained from tryptic digestion of BBS. Peptide mass fingerprint (PMF) searches with available databases were unsuccessful and ions with good signal-to-noise ratio (arrows) were selected for MSMS analyses **(B)**. **(C)** *De-novo* sequenced peptides and Edman sequence of the N-terminus of BBS. For *de novo* sequences, L is one of the isobaric L or I and Z is either Q or K. X is any amino acid. The dataset was used for MSBlast searches and identified BBS as a serpin. **(D)** Degenerated primers were designed based on Edman and one *de novo* sequence (Nested primer). 3'RACE of liver cDNA showed only one band of ~1300 bp. TAIL PCR with random hexamers was used to obtain the 5' region coding sequence. W, Ad8, and Ad10 are different random primers, and Ad8 was selected for sequencing. The complete nucleotide sequence was translated and sequence accuracy verified by PMF (bold fonts) and MSMS (underlined, see *SI Appendix*, Table S3 for Orbitrap coverage, 100% of the sequence). Shaded in gray in the sequence is the signal peptide.

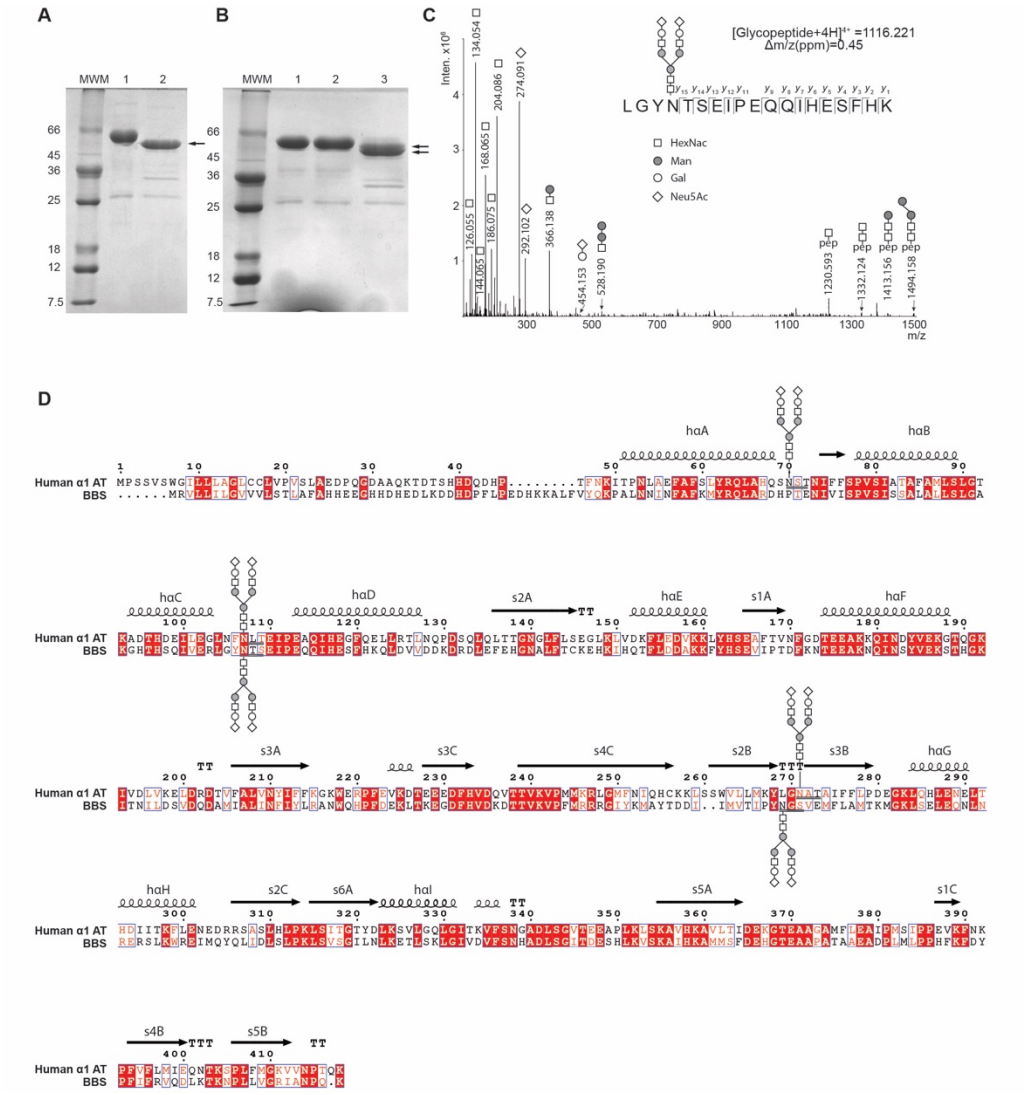

Fig. S5. BBS glycosylation

SDS-PAGE of enzymatic deglycosylation of **(A)** denatured and **(B)** native BBS. **(A)** *1*: 4 h, 37 37°C Bchr+PNGFaseF-. *2*: 4 h, 37 °C Bchr+PNGFaseF+. **(B)** *1*: Control, 24h, 4°C BBS PNGFaseF-. *2*: Control BBS 37°C PNGFaseF-. *3*: BBS 24 h 37°C PNGFaseF+. *MWM*: Molecular weight marker. *Arrows*: Mono and di-deglycosylated BBS. In the native conditions full deglycosylation cannot be accomplished in 24 h. The two glycans explain the difference between the theoretical molecular weight inferred from the sequence (average=45,852 Da) and the empirical molecular weight obtained by MALDI-TOF (average=50,260 Da). The difference is consistent with two complex biantennary glycans (BBS with 2glycans= 50,264Da). **(C)** HCD spectrum of one of the two glycopeptides. Oxonium ions and some peptide+glycan ions are shown in the graph. **(D)** Sequence alignment of BBS and human α1-AT. Secondary structure

was obtained from α1-AT crystallographic data (PDB=1QLP). The nomenclature is that of serpins (β-sheets A–C, α helixes A– I) (25). The most common glycans in humans α1-AT (biantennary complex structure) (113) are shown over the sequence. Two of the sequons for peptide glycosylation are structurally conserved (loop between helixes C–D, and turn between s2B-s3B).

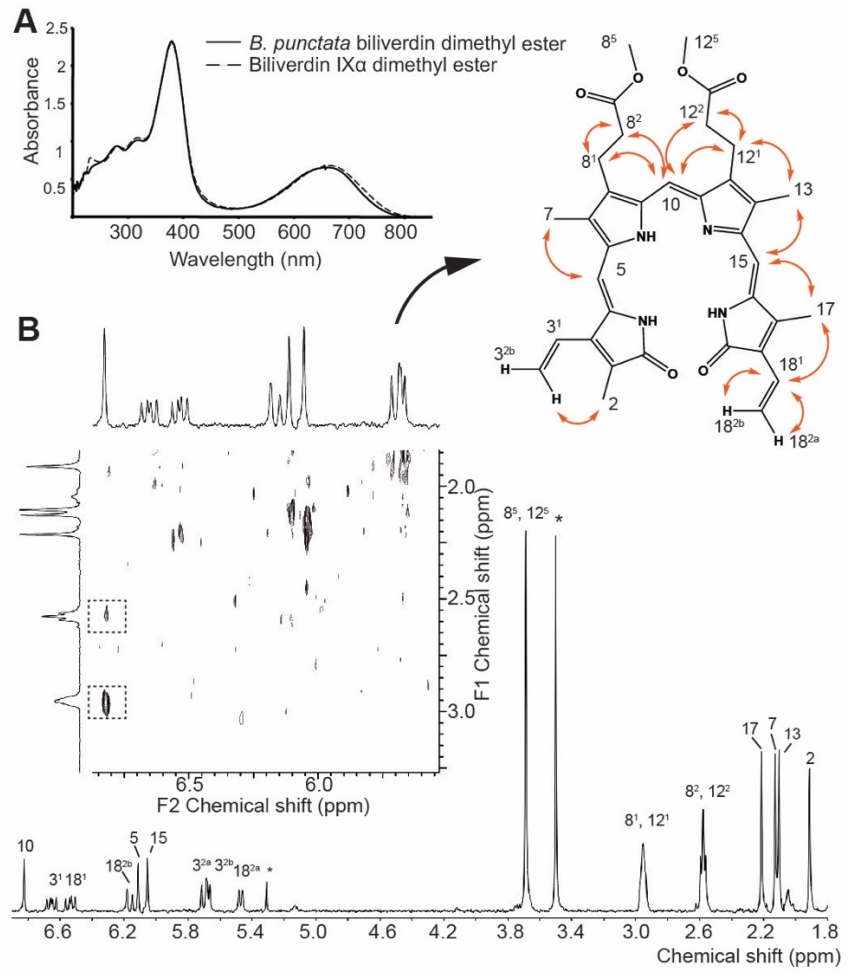

Fig. S6. Identification of biliverdin from BBS

The isolated pigment is biliverdin IX a. **(A)** UV-Vis spectra of derivatized BV from BBS and BVIXα standard, both after esterification as methyl esters. **(B)** 1D ^{1}H NMR and 2D NOESY NMR identified BV as IXα. Red arrows: NOE interactions. Framed in dotted boxes, the NOE cross-peaks between the central methine bridge and both methylenes from propionate lateral chains.

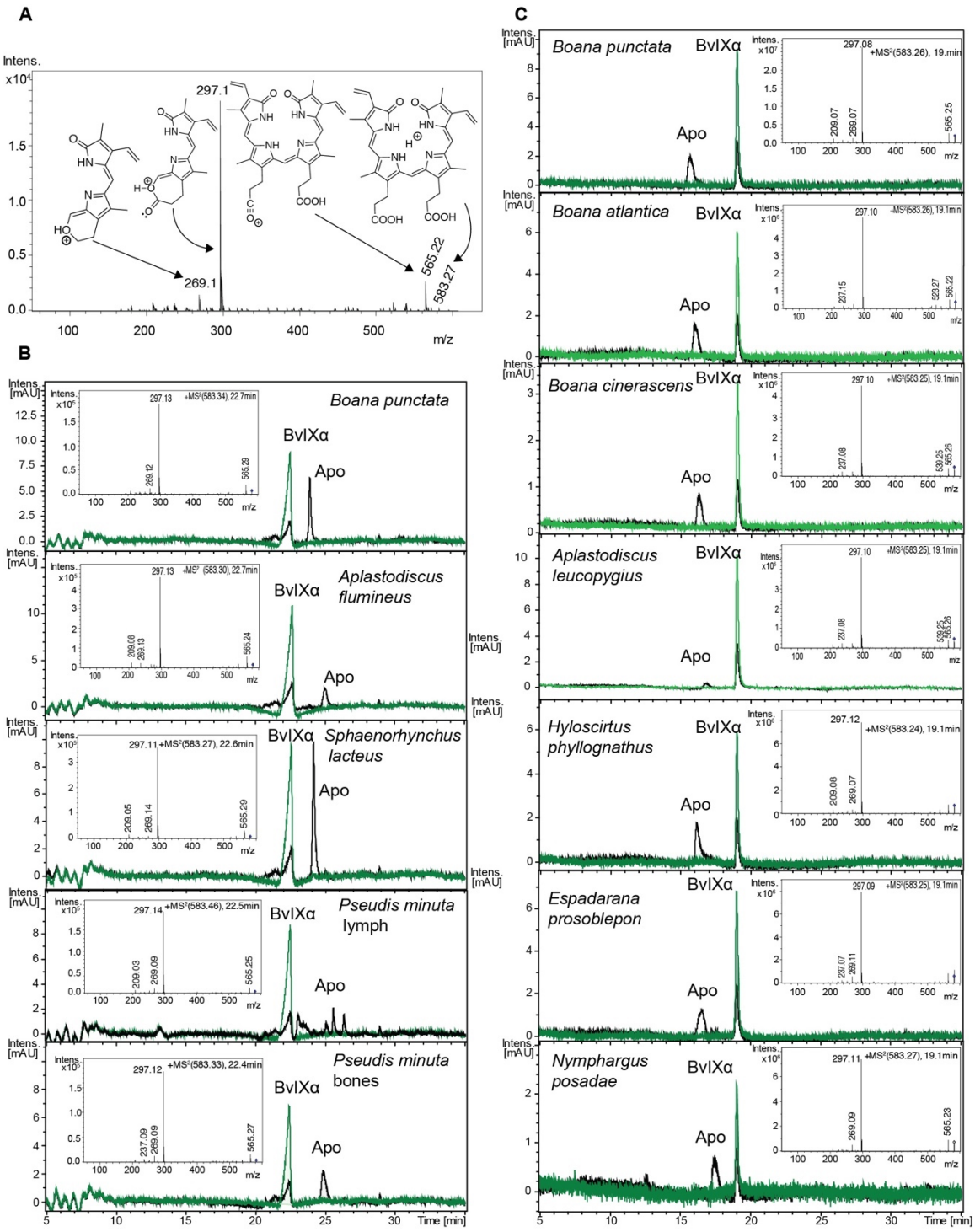

Fig. S7. HPLC-MS-DAD of BBSs from several frog species

(A) MSMS spectrum of biliverdin IXα from *Boana punctata* BBS. Fragmentation of the ions at 583.3 *m/z* gives the base peak at 297 *m/z*, consistent with a half-half fragmentation pattern of biliverdin (125), based on anquimeric assistance (102) to clive the molecule, followed by a CO

elimination affording a ion at *m/z* 269. **(B)**, **(C)** HPLC-DAD-MS of anuran BBSs from several frog species compared to *B. punctata* BBS, using two different gradients for the elution methods. Elution was monitored by DAD and absorbance at two wavelengths is shown: 280 nm (black) and 667 nm (green). For all of the species, retention time, and MSMS for the peak at 583.3 *m/z* are identical, and compatible with biliverdin IXα. Biliverdin is dissociated from the apoprotein (Apo) suggesting a non-covalent interaction as already described in *B. punctata*.

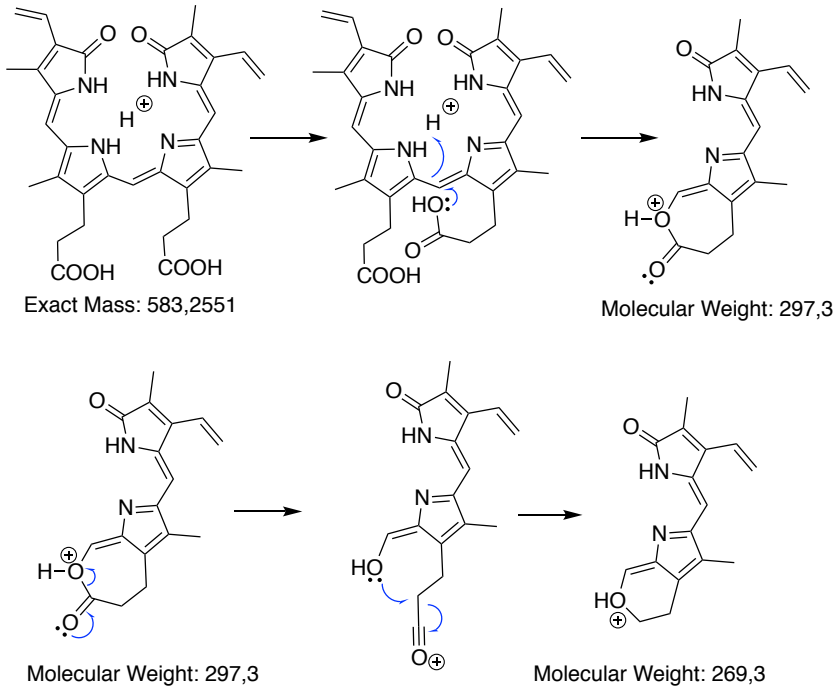

Fig. S8. Fragmentation pathway of biliverdin IXα as extracted from BBS. Interpretation of the fragmentation pattern observed in *SI Appendix,* Fig. S7*A*. Fragmentation of the ions at 583.3 *m/z* gives the base peak at 297 *m/z*, consistent with a half-half fragmentation pattern of biliverdin (125), based on anquimeric assistance (102) to clive the molecule, followed by a CO elimination affording a ion at *m/z* 269.

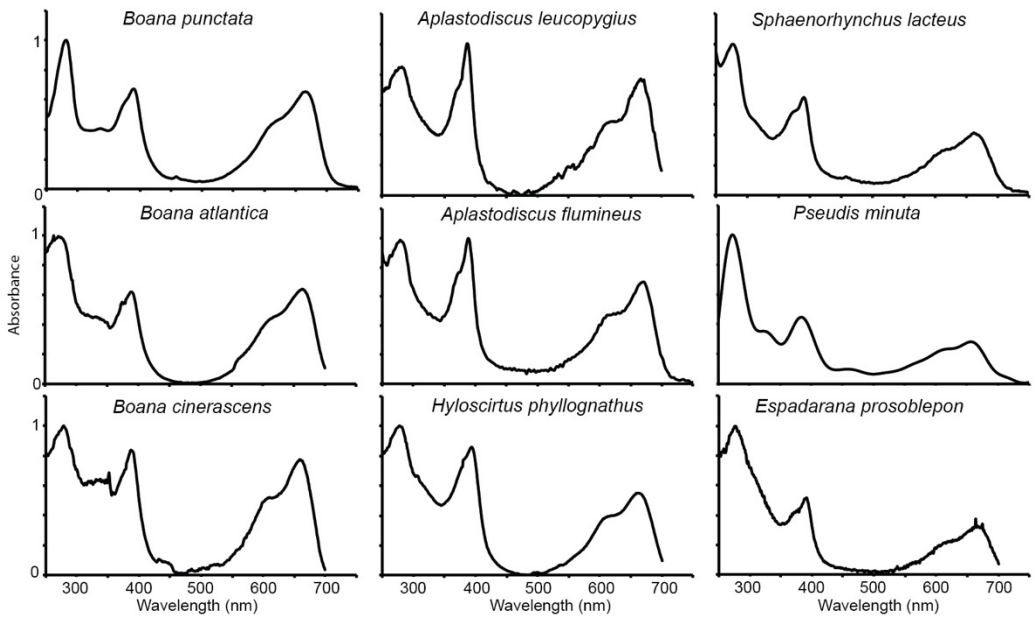

Fig. S9. UV-VIS spectra of BBSs from several anuran species.

Absorbance spectra of BBSs (phosphate buffer 0.01 M, pH 7) from different species show a common biliverdin type, with maximum absorbances at 390 nm (Soret band) and 667 nm (Q band). Ratio of absorbance Soret/Q ranges from 1 to 1.5. *Chimerella mariaelenae* and *Nymphargus posadae* could not be studied by this technique due to scarcity of the material.

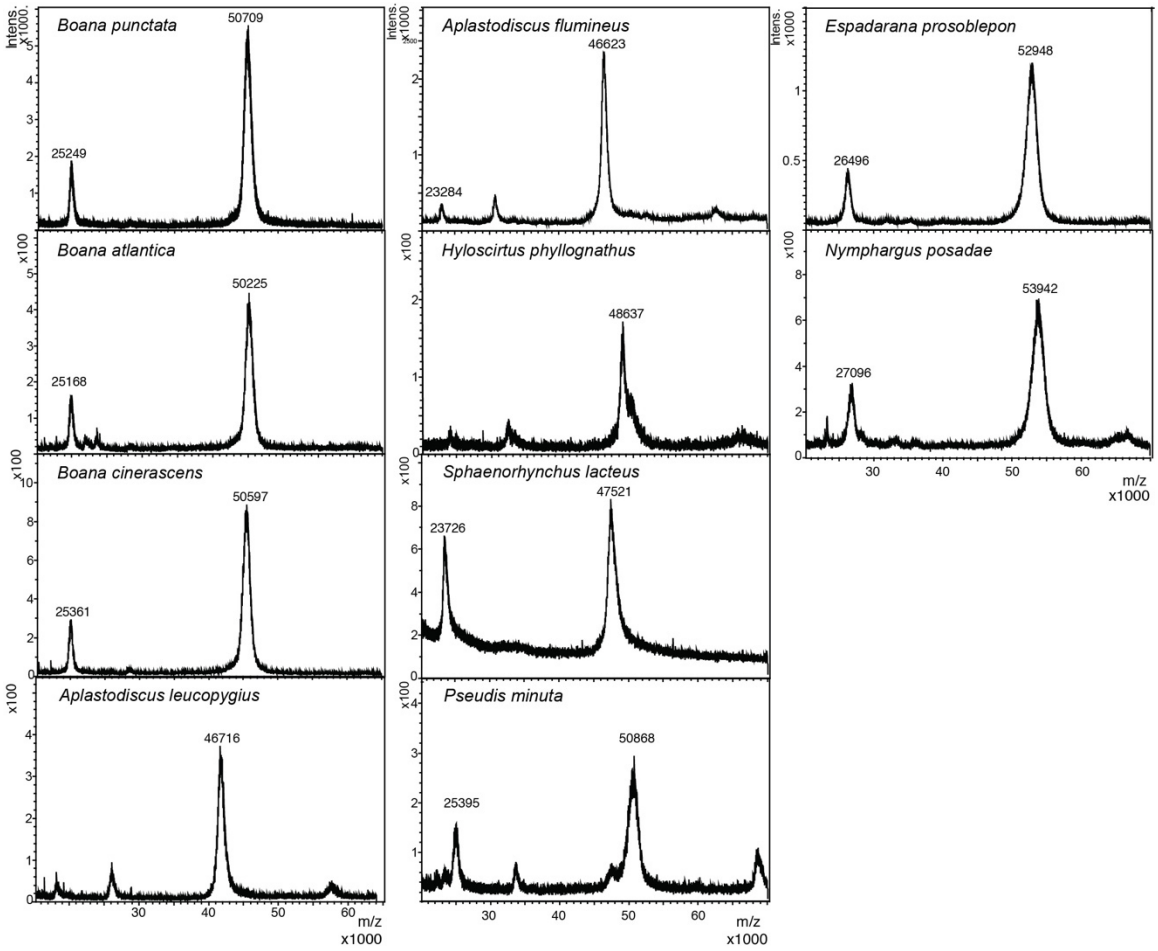

Fig. S10. MALDI-TOF of BBS from several frog species

Purified BBSs from chlorotic species were analyzed by MALDI-TOF. Each species has BBSs ranging from 46–54 KDa. Only *Chimerella mariaelenae* could not be studied by this technique due to scarcity of the material.

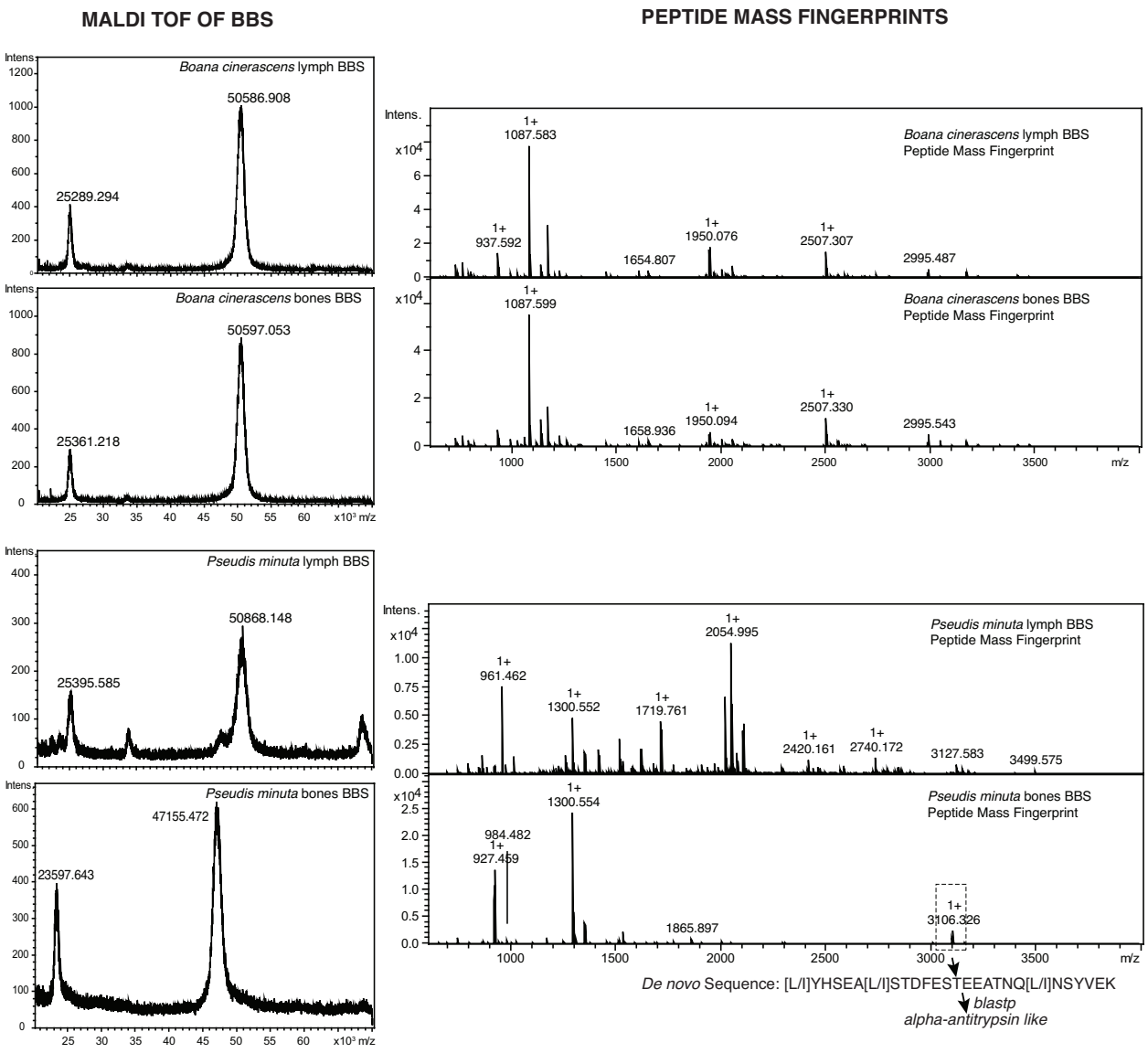

Fig. S11. BBSs from lymph and bones from two representative species, *Boana cinerascens* and *Pseudis minuta*. BBSs extracted from lymph and bones in *B. cinerascens* have the same molecular weight (50.6 KDa), and their peptide mass fingerprints show the same profile. The same situation is found in most of the studied species. In *Hyloscirtus phyllognathus* and *Pseudis minuta* instead, BBSs purified from lymph and bones have different molecular weight, and peptide mass fingerprints show different profiles (*P. minuta* in the figure). Interpretation of the MSMS from one of the ions (3106 m/z) revealed a sequence that blasted against a clade A serpin. However, neither the peptide mass fingerprint obtained from the bones BBS, nor the *de novo* for the peptide sequence match any of the assembled serpin contigs obtained with the

pipeline implemented in the current work (*SI Appendix*, Fig. S12), and it is unlikely that that protein is expressed in the liver.

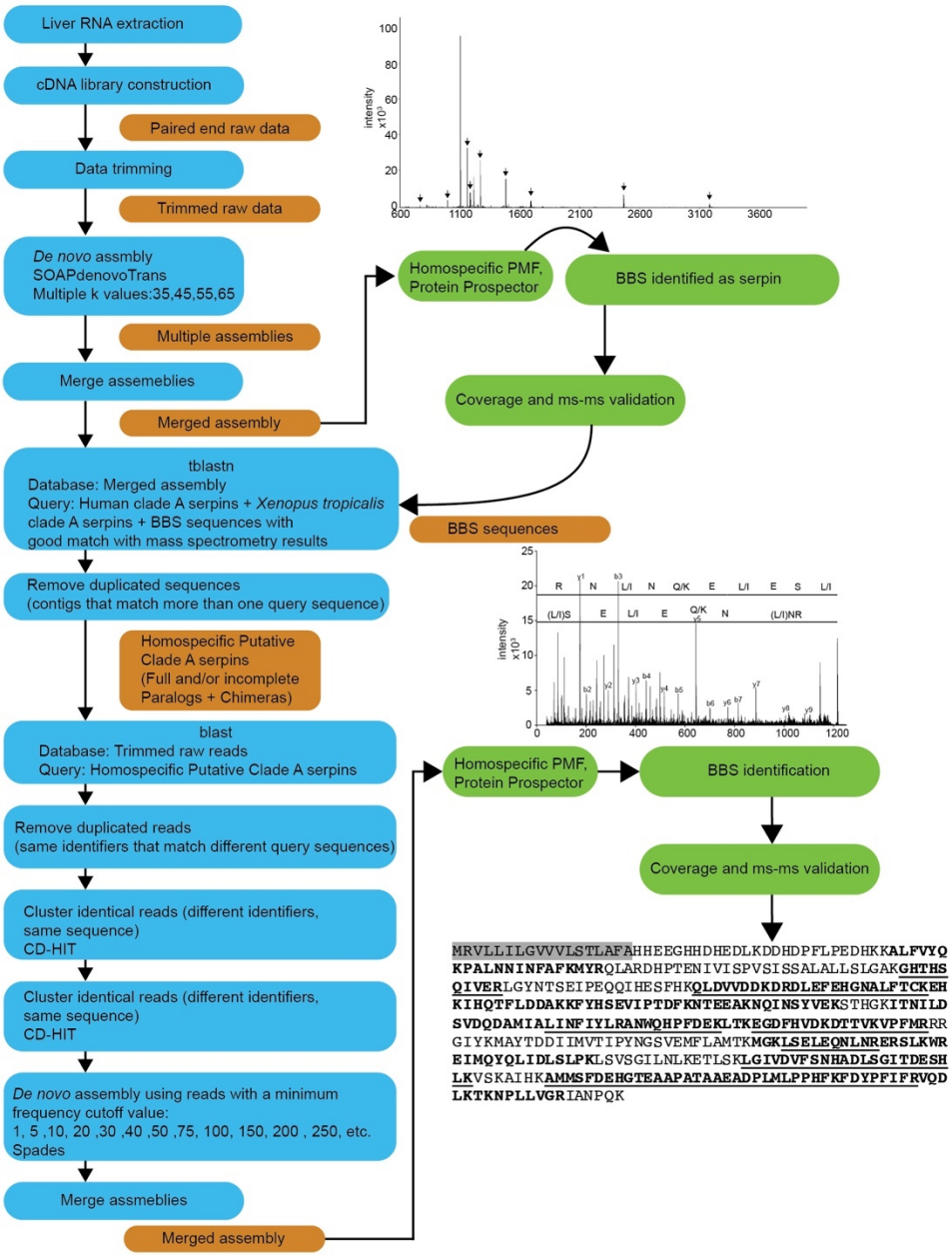

Fig. S12. Flowchart with the methods implemented to assemble BBS sequences from RNAseq data.

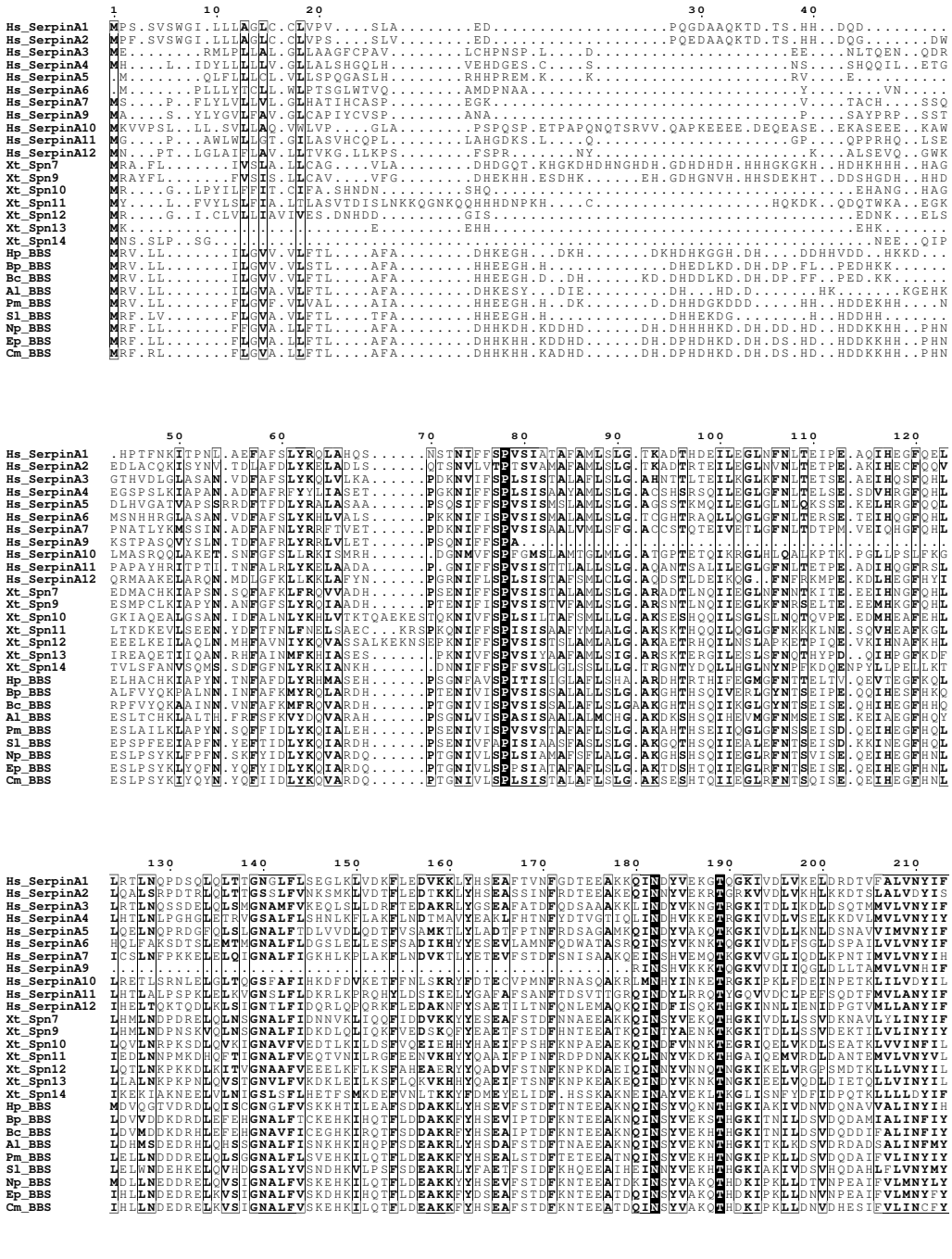
Hs_SerpinA1
Hs_SerpinA2
Hs_SerpinA3
Hs_SerpinA4
Hs_SerpinA5
Hs_SerpinA6
Hs_SerpinA7
Hs_SerpinA9
Hs_SerpinA10
Hs_SerpinA11
Hs_SerpinA12
Xt_Spn7
Xt_Spn9
Xt_Spn10
Xt_Spn11
Xt_Spn12
Xt_Spn13
Xt_Spn14
Hp_BBS
Bp_BBS
Bc_BBS
Al_BBS
Pm_BBS
Sl_BBS
Np_BBS
Ep_BBS
Cm_BBS

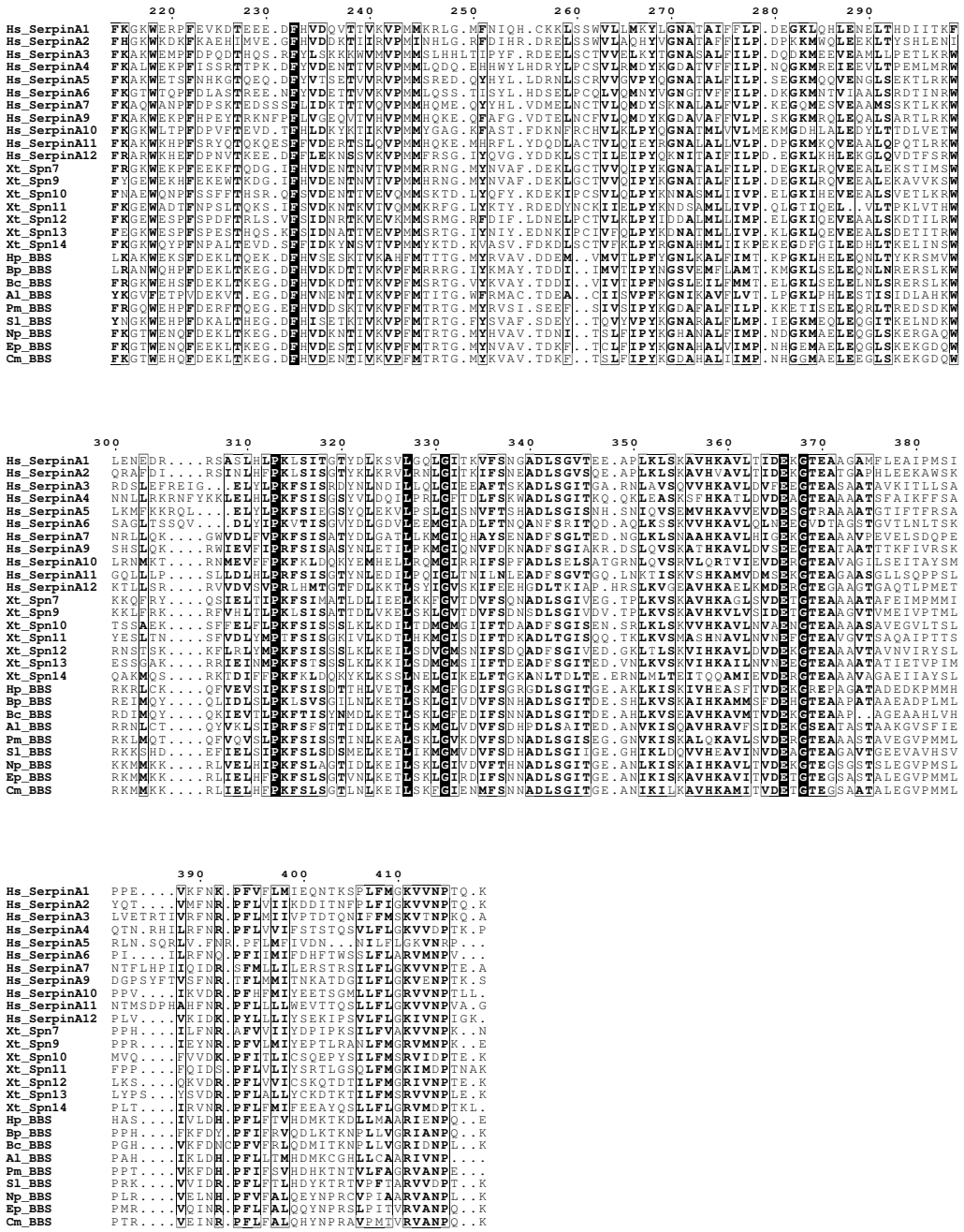

Fig. S13. Multiple alignment of serpins.

We used Clade A sequences from humans (Hs), *Xenopus tropicalis* (Xt), and BBS from *Hyloscirtus phyllognathus* (Hp), *Boana punctata* (Bp), *Boana cinerascens* (Bc), *Aplastodiscus leucopygius* (Al), *Pseudis minuta* (Pm), *Sphaenorhynchus lacteus* (Sl), *Nymphargus posadae* (Np), *Espadarana prosoblepon* (Ep) and *Chimerella mariaelenae* (Cm).

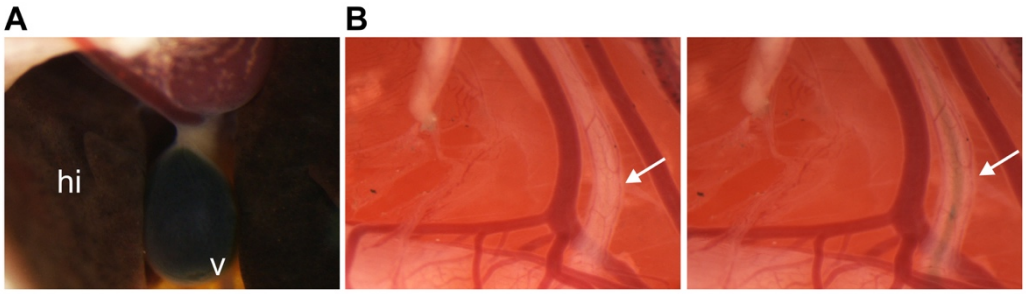

Fig. S14. Internal anatomy of *Pseudis minuta.* (A) Ventral view of liver (*hi*) and gall bladder (*v*) **(B)** Bile duct (arrow) links the gall bladder with the duodenum. After a slight compression of the gall bladder, bile can be seen along the duct and entering the duodenum (right). In none of the chlorotic species there are anatomical alterations compatible with bile duct obstructions. Pathological hyperbiliverdinemia was reported in humans with bile duct obstructions (*23*) as well as in toads in which bile ducts had been ligated (*13*) experimentally. Without obstructions, biliverdin excess is easily excreted (*12*, *13*).

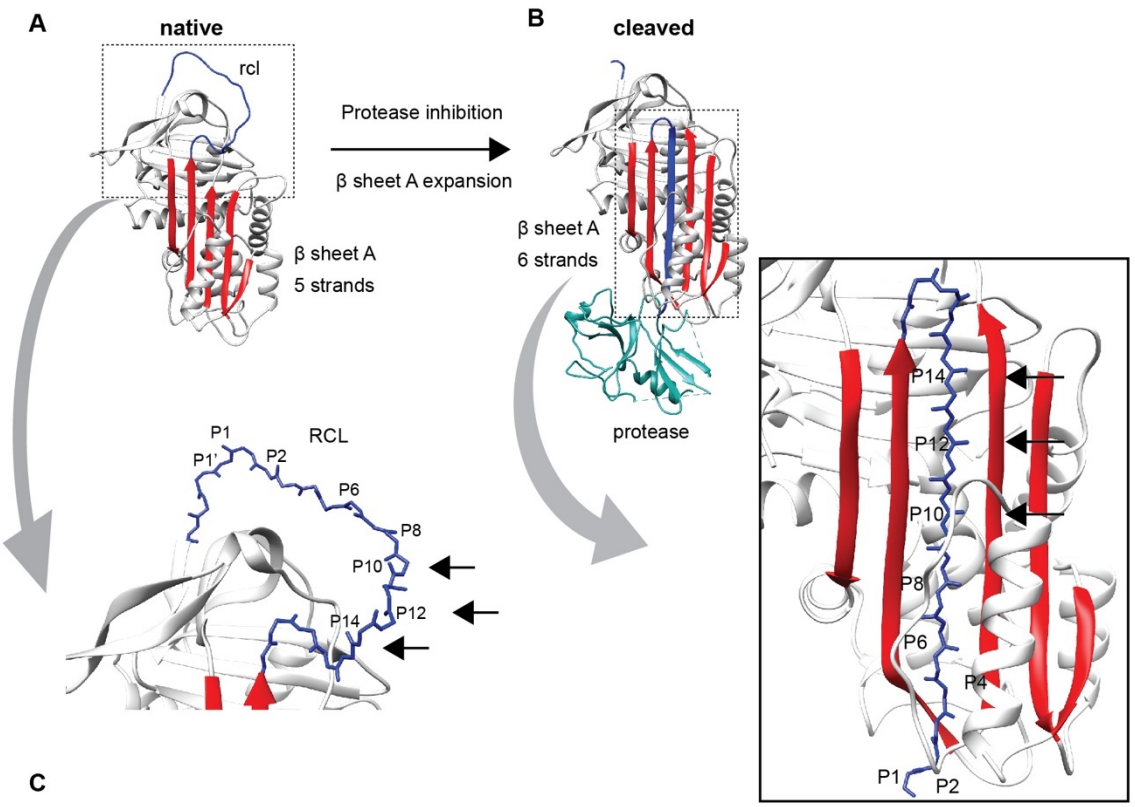

C

SERPIN*	P_{15}	P_{14}	P_{13}	P_{12}	P_{11}	P_{10}	P_9	P_8	P_7	P_6	P_5	P_4	P_3	P_2	P_1	P'_1	P'_2	P'_3	P'_4
Inhibitory serpins																			
SerpinA1 *α-1-antitrypsin*	G	T	E	A	A	G	A	M	F	L	E	A	I	P	M	S	I	P	P
SerpinA3 *α-chymotrypsin*	G	T	E	A	S	A	A	T	A	V	K	I	T	L	L	S	A	L	V
SerpinA4 *kallistatin*	G	T	E	A	A	A	A	T	S	F	A	I	K	F	F	S	A	Q	T
SerpinA5 *PCI*	G	T	R	A	A	A	A	T	G	T	I	F	T	F	R	S	A	R	L
SerpinA9 *centerin*	G	T	E	A	A	A	A	T	T	T	K	F	I	V	R	S	K	D	G
SerpinA10 *PZI*	G	T	E	A	V	A	G	I	L	S	E	I	T	A	Y	S	M	P	P
SerpinB1 *MNEI*	G	T	E	A	A	A	A	T	A	G	I	A	T	F	C	M	L	M	P
SerpinB2 *PAI-2*	G	T	E	A	A	A	G	T	G	G	V	M	T	G	R	T	G	H	G
SerpinC1 *Antithrombin*	G	S	E	A	A	A	S	T	A	V	V	I	A	G	R	S	L	N	P
SerpinD1 *heparin cofactor II*	G	T	Q	A	T	T	V	T	T	V	G	F	M	P	L	S	T	Q	V
SerpinE1 *PAI-1*	G	T	V	A	S	S	S	T	A	V	I	V	S	A	R	M	A	P	E
SerpinI1 *Neuroserpin*	G	S	E	A	A	A	V	S	G	M	I	A	I	S	R	M	A	V	L
Hyla simplex *HylaserpinS1***	G	T	E	A	A	G	S	T	A	I	E	I	S	P	T	M	I	L	P
Non-inhibitory serpins																			
SerpinA6 *CBG*	G	V	D	T	A	G	S	T	G	V	T	L	N	L	T	S	K	P	I
SerpinA7 *TBG*	G	T	E	A	V	A	V	P	E	V	E	L	S	D	Q	P	E	N	T
SerpinA8 *ATG*!	E	R	E	P	T	E	S	T	Q	Q	L	N	K	P	E	V	L	E	V
SerpinB5 *Maspin*	G	G	D	S	I	E	V	P	G	A	R	I	L	Q	H	K	D	E	L
SerpinF1 *PEDF*	G	A	G	T	T	P	S	P	G	L	Q	P	A	H	L	T	F	P	L
Biliverdin Binding Serpins																			
B. punctata *BBS*	G	T	E	A	A	P	A	T	A	A	E	A	D	P	L	M	L	P	P
B. cinerascens *BBS****	G	T	E	A	A	P	A	G			E	A	A	H	L	V	H	P	G
H. phyllognathus *BBS*	G	R	E	P	A	G	A	T	A	D	E	D	K	P	M	M	H	H	A

Fig. S15. Serpins inhibitory mechanisms and mutations in RCL.

(A) Serpins are normally serine proteases inhibitors with a conserved fold consisting of three β-sheets (A–C) and 8–9 α-helices (hA–hI). The reactive center loop (RCL, blue) is the region responsible for the interaction with the protease and forms an extended, exposed conformation above the body of the serpin scaffold (PDB: 1QLP). In α-antitrypsin, RCL comprises residues P17–P4'(126)and includes the scissile bond (P1–P1') that is cleaved by the target protease **(B)** RCL is crucial for the inhibitory mechanism: following proteolysis, the serpins undergo a large conformational change that involves an expansion of β-sheet A (red) from five to six strands, a transition that is known as the "stressed (S) to relaxed (R) transition". During this, the target protease (green) is translocated to the distal end of β-sheet A (PDB: 1EZX). Several regions are important modulating serpin conformational changes: the hinge (P15–P9 of the RCL), the breach (top of the A β-sheet, point of initial insertion of RCL)(127), and the shutter (in the center of β-sheet A, facilitates and accepts the hinge of the RCL after cleavage). In inhibitory serpins, RCL sequence composition and length is crucial for the β-sheet B expansion mechanisms. Chimera(128) was used for figures **(A)-(B). (C)** Multiple alignment of RCL sequences of diverse inhibitory and non-inhibitory serpins and three BBSs. In inhibitory serpins, P14 is normally T or S, and consists of the first side chain to become buried, playing a crucial role in the conformational change. Mutations in this position, especially from a non-charged to a charged residue, result in partial or complete loss of inhibitory function (25). Additionally, the region in the hinge P12–P9 has a consensus pattern that includes A or two other residues with short side-chains, such as G or S, which permit the efficient and rapid insertion of the RCL into β-sheet A. Proline insertions at positions P12 and P10 have been shown to impair the inhibitory mechanism in mutagenesis experiments and can be found in other non-inhibitory serpins that do not undergo conformational change(25, 46, 129). In some BBSs, these substitutions (highlighted in blue), are present in the RCL. BBSs show other deviations from the conserved serpins sequences and are shown in the Supporting Information. *Serpins nomenclature: Serpin[A–P]# includes the name Serpin, followed by the letter A-P denoting the clade and a numerical identifier. **Hylaserpin is an inhibitory serpin described in the skin secretions of *Hyla simplex* (122) *** In *Boana cinerascens* BBS, RCL sequence is shorter and two gaps were introduced at an arbitrary position to maintain the alignment of residues within the hinge region.

Table S1. Known occurrence of chlorosis in anurans.

Family	Genus	Species	Reference
Arthroleptidae	*Leptopelis*	*L. grandiceps*	(130)*
		L. karissimbensis	(131)
		L. uluguriensis	(130)*
Centrolenidae	*Celsiella*	*Cel. revocata*	(79)
		Cel. vozmedianoi	(79)
	Centrolene	*Cen. altitudinale*	(79)
		Cen. antioquiensis	(79)
		Cen. bacata	(79)
		Cen. ballux	(79)
		Cen. buckleyi	(79)
		Cen. charapita	(132)
		Cen. condor	(79)
		Cen. daidalea	(79)
		Cen. geckoidea	(79)
		Cen. gemmata	(79)
		Cen. heloderma	(79)
		Cen. hesperia	(79)
		Cen. huilensis	(79)
		Cen. hybrida	(79)
		Cen. lemniscata	(79)
		Cen. lynchi	(79)
		Cen. muelleri	(79)
		Cen. notosticta	(79)
		Cen. paezorum	(79)
		Cen. peristicta	(79)
		Cen. pipilata	(79)
		Cen. sabini	(133)
		Cen. sanchezi	(79)
		Cen. savagei	(79)
		Cen. scirtetes	(79)
		Cen. solitaria	(79)
		Cen. venezuelensis	(79)
	Chimerella	*Ch. corleone*	(79)
		Ch. mariaelenae	(79)
	Cochranella	*Co. erminea*	(79)
		Co. euknemos	(79)
		Co. granulosa	(79)
		Co. guayasamini	(132)
		Co. litoralis	(79)
		Co. mache	(79)
		Co. nola	(79)
		Co. phryxa	(79)
		Co. resplendens	(79)
	Espadarana	*E. andina*	(79)
		E. audax	(79)
		E. callistomma	(79)
		E. durrellorum	(79)
		E. prosoblepon	(79)
	Hyalinobatrachium	*H. anachoretus*	(132)
		H. aureoguttatum	(79)*
		H. bergeri	(79)*
		H. cappellei	(134)*
		H. carlesvilai	(132, 135)*
		H. chirripoi	(136)*
		H. colymbiphyllum	(136)*
		H. dianae	(137)*
		H. duranti	(79)*
		H. esmeralda	(132)*
		H. fleischmanni	(136)*; Taboada pers. obs.
		H. fragile	(79)*

	H. guairarepanense	?
	H. iaspidiense	(79)*
	H. ibama	(79)*
	H. kawense	(134)*
	H. mesai	(134)
	H. mondolfii	(134)*
	H. muiraquitan	(138)*
	H. munozorum	(135)*
	H. orientale	(79)*
	H. orocostale	(79)*
	H. pallidum	(79)*
	H. pellucidum	(79)*
	H. talamancae	(136)*
	H. tatayoi	(139)*
	H. taylori	(134)
	H. tricolor	?
	H. valerioi	(136)*
	H. vireovittatum	(136)*
	H. yaku	(140)8
Nymphargus	*N. anomalus*	(79), but see (141)
	N. armatus	(79)
	N. bejaranoi	(79)
	N. buenaventura	(79)
	N. cariticommatus	(79)
	N. caucanus	(141)
	N. chami	(79)
	N. chancas	(79)
	N. cochranae	(79)
	N. cristinae	(79)
	N. garciae	(79)
	N. grandisonae	(79)
	N. griffithsi	(79)
	N. ignotus	(79), but see (141)
	N. lasgralarias	(142)
	N. laurae	(79)
	N. luminosus	(79)
	N. luteopunctatus	(79)
	N. manduriacu	(79)
	N. mariae	(79)
	N. megacheirus	(79)
	N. mixomaculatus	(79)
	N. nephelophila	(79)
	N. ocellatus	(79)
	N. oreonympha	(79)
	N. phenax	(79)
	N. pluvialis	(79)
	N. posadae	(79)
	N. prasinus	(79)
	N. rosada	(79), but see (141)
	N. ruizi	(79)
	N. siren	(79)
	N. spilotus	(79)
	N. sucre	(79)
	N. truebae	(79)
	N. vicenteruedai	(79)
	N. wileyi	(79)
Rulyrana	*R. adiazeta*	(79)
	R. flavopunctata	(79)
	R. mcdiarmidi	(79)
	R. saxiscandens	(79)
	R. spiculata	(79)
	R. susatamai	(79)
Sachatamia	*S. albomaculata*	(79)
	S. electrops	(141)
	S. ilex	(79)
	S. orejuela	(79)
	S. punctulata	(79)

	Teratohyla	*T. adenocheira*	(79)
		T. amelie	(79)
		T. midas	(79)
		T. pulverata	(79)
		T. spinosa	(79)
	Vitreorana	*V. antisthenesi*	(79)
		V. baliomma	(143)
		V. castroviejoi	(79)
		V. eurygnatha	(79)
		V. franciscana	(144)
		V. gorzulae	(79)
		V. helenae	(79)
		V. parvula	(79)
		V. ritae	(79)
		V. uranoscopa	(79)
	Species of uncertain taxonomic position		
		"Centrolene" acanthidiocephalum	(79)
		"Centrolene" azulae	(79)
		"Centrolene" guanacarum	(79)
		"Centrolene" medemi	(79)
		"Centrolene" petrophilum	(79)
		"Centrolene" quindianum	(79)
		"Centrolene" robledoi	(79)
		"Cochranella" balionota	(79)
		"Cochranella" duidaeana	(79)
		"Cochranella" euhystrix	(79)
		"Cochranella" geijskesi	(79)
		"Cochranella" megista	(79)
		"Cochranella" ramirezi	(79)
		"Cochranella" riveroi	(79)
		"Cochranella" xanthocheridia	(79)
Craugastoridae	*Pristimantis*	*P. galdi*	Ron pers. comm.
Hemiphractidae	*Gastrotheca*	*G. albolineata*	(145)*
		G. andaquiensis	(146)
		G. argenteovirens	(146)
		G. ernestoi	(145)*
		G. fulvorufa	(145); Trevine, pers. comm.
		G. guentheri	(145)
		G. helenae	(145)
		G. longipes	(147)
		G. microdiscus	(148)*
		G. walkeri	(145)
		G. weinlandii	(145)
Hylidae	*Litoria*	*L. flavecens*	(149)
Pelodryadinae		*L. lutea*	(150, 151)
		L. thesaurensis	(150-152)
		L. pallidofemora	(87)
		L. nullicedens	(87)
	Ranoidea	*R. aruensis*	(153)
		R. dayi	(90)
Hylinae	*Myersiohyla*	*M. chamaeleo*	(154)
		M. liliae	(155)
	Aplastodiscus	*A. albofrenatus*	(156)

	A. albosignatus	(156)
	A. eugenioi	(157)
	A. leucopygius	(157)
	A. sibilatus	(157)
	A. ehrhardti	(157)
	A. musicus	(156)
	A. cochranae	(157)
	A. perviridis	(157)
	A. arildae	(157)
	A. flumineus	(157)
	A. ibirapitanga	(157)
	A. weygoldti	(157)
	A. cavicola	(157)
	A. lutzorum	(157)
Hyloscirtus	*H. albopunctulatus*	Ron & Read, 2018*
	H. alytolylax	(158); (159)*
	H. armatus	(160)
	H. callipeza	(161)*
	H. charazani	(162)
	H. colymba	(163)
	H. denticulentus	(158)
	H. jahni	(164)*
	H. mashpi	(159)*
	H. palmeri	(163)
	H. phyllognathus	(158)
	H. platydactylus	(164)*
	H. simmonsi	(161) *
	H. torrenticola	(165) *
	H. chlorosteus	(166)
Bokermannohyla	*B. martinsi*	(167)
	B. saxicola	(167)
Boana claresignata group	*B. claresignata*	(156)
Boana punctata group	*B. atlantica*	(168) *
	B. cinerascens	(169)
	B. punctata	(169)
	B. hobbsi	(170)*
Boana benitezi group	*B. nympha*	(160)
	B. ornatissimus	(169)
	B. sibleszi	(169)
Boana pellucens group	*B. rufitelus*	(163)
	B. pellucens	(171)
	B. rubracyla	Ron pers. obs.
Boana albopunctata group	*B. heilprini*	(5)
	B. raniceps[J]	Faivovich pers. obs.
	B. albopunctata[J]	(172)
	B. calcarata	(173)
	B. fasciata	(173)
	B. maculateralis	(173)
	B. alfaroi	(173)
	B. lanciformis[J]	Ron, pers. obs.
Boana pulchella group	*B. cambui*	(174)
	B. aguilari	Lehr, pers. comm
	B. alboniger	Baldo, pers. comm
	B. bandeirantes	Faivovich, pers. obs.
	B. bischoffi	(175)
	B. caipora	(176)
	B. callipleura	(177)
	B. cipoensis	Faivovich, pers. obs.
	B. curupi	(178, 179)
	B. ericae	(180)
	B. goiana	Pinheiro, pers. comm

	B. guentheri	(181)*
	B. joaquini	(182)
	B. latistriata	Faivovich, pers. obs.
	B. leptolineata	Pinheiro, pers. comm
	B. marginata	(183)
	B. marianitae	Taboada pers. obs.
	B. melanopleura	Lehr, pers. comm
	B. palaestes	(177)
	B. phaeopleura	Pinheiro, pers. comm
	B. poaju	(184)
	B. polytaenia	(175)
	B. riojana	(4)
	B. semiguttata	(179)
	B. stellae	Faivovich, pers. obs.
Boana semilineata group	*B. boans*	(5)
	B. wavrini	Suárez, pers. comm.
	B. semilineata	(175); Orrico, pers. comm.
Boana faber group	*B. crepitans*	(177)
	B. pugnax[J]	Rivera-Correa, pers. comm.
	B. lundii	Brunetti, pers. obs.
	B. faber[J]	Baldo pers. comm.
	B. albomarginata	(156)
	B. pardalis[J]	Pezutti, pers. comm.
	B. exastis	(185)
	B. rosenbergi	(163)
Scarthyla	*S. goinorum*	(186)*
	S. vigilans	(187)
Lysapsus	*L. limellum*	(4)
	L. laevis	(188)
	L. bolivianus	(186)*
	L. caraya	(189)*
Pseudis	*P. minuta*	(4)
	P. cardosoi	(189)*
	P. paradoxa	(188)
	P. platensis	(4)
	P. fusca	(189)*
	P. bolbodactyla	(189)*
	P. tocantins	(189)*
Dendropsophus	*D. branneri*	Orrico pers. comm
	D. cruzi	Orrico pers. comm
	D. juliani	Orrico pers. comm
	D. mathiasoni	Orrico pers. comm
	D. minusculus	Orrico pers. comm
	D. tintinnabulum	Orrico pers. comm
Sphaenorhynchus	*Sp. planicola*	(190)
	Sp. pauloalvini	(145)*
	Sp. botocudo	(191)*
	Sp. bromelicola	(192)
	Sp. carneus	(193)
	Sp. dorisae	(193)
	Sp. mirim	(191)*
	Sp. lacteus	(5)
	Sp. surdus	(145)*
	Sp. caramaschii	(194)*
	Sp. orophilus	(190)
	Sp. palustris	(145)*
	Sp. canga	(195)
	Sp. prasinus	(145)*
Scinax	*Sc. quinquefasciatus*	(171)
	Sc. cruentommus	Ron pers. comm.
	Sc. funereus	Ron pers. comm.
	Sc. elaeochroa	(196)

		Sc. caprarius	(196)
		Sc. boesemani	(248)
	Itapotihyla	*I. langsdorffii*	(197)
	Trachycephalus	*T. typhonius*	(4)
		T. atlas	(192)
		T. nigromaculatus	(198)
		T. jordani	Ron pers. comm.
		T. hadroceps	(199)*
		T. cunauaru	(200)
		T. resinifrictrix	Baeta pers. comm.
		T. macrotis	(201)*
		T. dibernardoi	(202)*
		T. macrotis	(201)
		T. helioi	Suárez, pers. comm.
	Osteopilus	*O. dominicensis*	(203)
		O. crucialis	(5)
		O. vastus	(5)
		O. wilderi	(204) (5)
		O. septentrionalis	(5)
	Osteocephalus	*O. buckleyi*	(205)
		O. cabrerai	(205)
		O. cannatellai	(206)
		O. castaneicola	(207)
		O. deridens	(208)
		O. festae	Ron et al., 2010
		O. fuscifacies	(208)
		O. helenae	(206)
		O. leoniae	(209)
		O. leprieurii[J]	(210)
		O. mutabor	(210)
		O. oophagus	(211)
		O. planiceps	(205)
		O. taurinus	(212)
		O. yasuni[J]	Ron, pers. obs.
	Phyllodytes	*P. luteolus*	(192)
		P. wuchereri	(145)*
		P. melanomystax	(213)
		P. kautskyi	(214)
		P. edelmoi	(145)*
		P. maculosus	(145)*
	Tepuihyla	*T. warreni*	Faivovich, pers. obs
		T. exophthalma	(215)
		T. tuberculosa	(201)
		T. shushupe	(201)
Hyperoliidae	*Alexteroon*	*A. jynx*	(216)*
		A. obstetricans	(216)*
	Hyperolius	*H. acutirostris*	(216)*
		H. acuticeps	(217) *
		H. adspersus	(217)*
		H. argus[P]	(218)*
		H. benguellensis[P]	(217, 219, 220)*
		H. bolifambae[P]	(221)*
		H. burguessi	(222)
		H. camerunensis[P]	(216)*
		H. castaneus[P]	(223) *
		H. chlorosteus	(224)
		H. dartevellei	(217)*
		H. dintelmanni[P]	(77)*
		H. discodactylus[P]	(225)
		H. drewesi	(226)*
		H. endjami[P]	(216)*

		H. friedmanni	(217)*
		H. frontalis	(227)*
		H. fusciventris[P]	(216)*
		H. guttulatus[P]	(216)*
		H. howelli	(217)*
		H. igbettensis	(217)*
		H. inyangae	(217)*
		H. jackie	(228)
		H. jacobseni	(217)*
		H. kohleri	(216)*
		H. kuligae[P]	(216)* (229)*
		H. lamottei	(217)
		H. langi	Calphotos ID: 0000 0000 0814 0955
		H. leucotaenius	(230)*
		H. lupiroensis	(217)
		H. microps	(217)
		H. mosaicus	(216)*
		H. nasicus	(217)
		H. nasutus	(217)
		H. nienokouensis	(227)*
		H. ocellatus[P]	(216)*
		H. pardalis[P]	(216)*
		H. parkeri	(220)*
		H. phantasticus[P]	Calphotos ID: 1111 1111 1111 7265, 1111 1111 1111 7268
		H. picturatus[P]	(231)
		H. poweri	(217)
		H. pseudargus	(218)*
		H. pusillus	(220)*
		H. riggenbachi[P]	(216)*
		H. rwandae	(217)
		H. spinigularis	(222)
		H. tanneri	(222)
		H. viridis	(217)
		H. wermuthi	(227)*
Limnodynastidae	*Philoria*	*P. frosti*	(90)
		P. sphagnicolus	(90)
Mantellidae	*Boophis luteus* group	*B. andohahela*	(232)*
		B. andreonei	(232)*
		B. anjanaharibeensis	(232)*
		B. elenae	(232)*
		B. enlaenderi	(232)*
		B. jaegeri	(232)*
		B. luteus	(232, 233)*
		B. sandrae	(234)*
		B. septentrionalis	(232)*
		B. tampoka	(234)*
	Boophis albipunctatus group	*B. albipunctatus*	(232)*
		B. ankaratra	(232)*
		B. boppa	(235)*
		B. haingana	(234)*
		B. luciae	(234)*
		B. miadana	(234)*
		B. schuboeae	(232)*
		B. sibilans	(232)*
	Boophis rappiodes group	*B. ankarafensis*	(236)*
		B. bottae	(232)*
		B. erythodactylus	(233) (232)*
		B. rappiodes	(232)
		B. tasymena	(232)
		B. viridis	(233) (232)*
	Boophis mandraka group	*B. mandraka*	(232, 233)*

		B. liami	(232)*
		B. sambirano	(232)*
		B. solomaso	(232)*
	Boophis tephraeomystax group	*B. pauliani*[P]	(233)
	Boophis majori group	*B. baetkei*	(237)*
		B. lilianae	(237)*
		B. ulftunni	(238)*
	Guibemantis	*G. liber*[P]	(232)*
		G. pulcher	(232)*
		G. tasifotsy	(239)*
	Mantidactylus	*M. argenteus*	(232)*
	Spinomantis	*S. massi*	(232)*
		S. peraccae	(240)
		S. phantasticus	(232)*
Myobatrachidae	*Paracrinia*	*P. haswelli*	(90)
	Taudactylus	*T. acutirostris*	(90)
Rhacophoridae	*Beddomixalus*	*B. bijui*[J]	(241)*
Rhacophorinae			
	Chiromantis	*C. samkosensis*	(242)
	Gracixalus	*G. gracilipes*	(243)
		G. supercornutus	(101)*
		G. quangi	(101)*
	Rhacophorus	*R. calcadensis*	(244)*
	Zhangixalus	*Z. prominanus*	(245)
		Z. achantharrhena	(245)
		Z. dulitensis	(246)
Ranidae	*Staurois*	*S. guttatus*	(97)*
		S. natator	(98)*

Chlorosis is explicitly mentioned in the literature cited either as green bones or green tissues. For some of the species -indicated with an asterisk (*)- chlorosis was inferred from pictures in the papers. [J]Chlorosis occurs in juveniles, [P]Chlorosis occurs in at least some color phases.

Table S2. RMN-^{1}H (CDCl3, 500 MHz) of derivatized biliverdin from *B. punctata.* Proton nomenclature follows *SI Appendix*, Fig S6.

	Isolated BV	
Proton	**Chemical shift (ppm)**	**Multiplicity**
H-10	6.83 (1H)	s
H-3^{1}	6.65 (1H)	dd (J: 18.0 y 11.6 Hz)
H-18^{1}	6.54 (1H)	dd (J: 17.6 y 11.8 Hz)
H-18^{2b}	6.16 (1H)	d (J_{trans}= 17.6 Hz)
H-5	6.11 (1H)	s
H-15	6.05 (1H)	s
H-3^{2a}	5.70	d (J_{trans}= 18.0 Hz)
H-3^{2b}	5.67	d (J_{cis}=11.6 Hz)
H-18^{2a}	5.47	d (J_{cis}= 11.8 Hz)
H-8^{5} and H-12^{5}	3.69	s
H-8^{1} and H-12^{1}	2.95	m
H-8^{2} and H-12^{2}	2.58	t (J=7.5 Hz)
H-17	2.22	s
H-13	2.13	s
H-7	2.11	s
H-2	1.91	s

Table S3. Summary information of chlorotic species' BBS. MS data for each peptide mass fingerprint experiment is presented in Supplementary Tables 4-12.

Species	Predicted MW (kDa)	Spectrometer	PMF coverage		Predicted N-Glycosylations sites		Sequence
			%	aa	# sites	position	
Boana punctata	48.85	MALDI TOF	62.4	249/399	2	N109 N269	MRVLLILGVVVLSTLAFAHHEEGHHDHEDLKDDHDPFLPEDHK K**ALFVYQKPALNNINFAFKMYR**QLARDHPTENIVISPVSISSA LALLSLGAK**GHTHSQIVER**LGYNTSEIPEQQIHESFHK**QLDVV** **DDKDRDLEFEHGNALFTCKEHKIHQTFLDDAKKFYHSEVIPTD** **FKNTEEAKNQINSYVEK**STHGK**ITNILDSVDQDAMIALINFIY** **LRANWQHPFDEKLTKEGDFHVDKDTTVKVPFMR**RRGIYKMAYT DDIIMVTIPYNGSVEMFLAMTK**MGKLSELEQNLNRERSLKWRE** **IMQYQLIDLSLPK**LSVSGILNLKETLSK**LGIVDVFSNHADLSG** **ITDESHLK**VSKAIHK**AMMSFDEHGTEAAPATAAEADPLMLPPH** **FKFDYPFIFRVQDLKTKNPLLVGR**IANPQK
		ORBITRAP[e]	100	399/399	2	N109 N269	MRVLLILGVVVLSTLAFA**HHEEGHHDHEDLKDDHDPFLPEDHK** **KALFVYQKPALNNINFAFKMYRQLARDHPTENIVISPVSISSA** **LALLSLGAKGHTHSQIVERLGYNTSEIPEQQIHESFHKQLDVV** **DDKDRDLEFEHGNALFTCKEHKIHQTFLDDAKKFYHSEVIPTD** **FKNTEEAKNQINSYVEKSTHGKITNILDSVDQDAMIALINFIY** **LRANWQHPFDEKLTKEGDFHVDKDTTVKVPFMRRRGIYKMAYT** **DDIIMVTIPYNGSVEMFLAMTKMGKLSELEQNLNRERSLKWR** **EIMQYQLIDLSLPKLSVSGILNLKETLSKLGIVDVFSNHADLS** **GITDESHLKVSKAIHKAMMSFDEHGTEAAPATAAEADPLMLPP** **HFKFDYPFIFRVQDLKTKNPLLVGRIANPQK**
Boana cinerascens	45.92	MALDI TOF	67.2	269/400	3	N112 N272 N293[a]	MRVLLILGVVVLFTLAFA**HHEEGHDDHKDDHDDLKDDHDPFFP** **EDKKRPFVYQKAAINNVNFAFKMFR**QVAR**DHPTGNIVISPVSI** **SSALAFLSL[G|A]AKGHTHSQIIK**GLGYNTSEISEQHIHEGF HHQLDVMDDKDR**HLEFEHGNAVFICEGHK**IRQTFSDDAK**RFYH** **SEAIPTDFK**NTEEAK**NQINSYVEKHTHGKITNILDSVDQDDIF** **ALINFIYFRGKWEHSFDEKLTK**EGDFHVDKDTTVK**VPFMSR**TG VYKVAYTDDIVIVTIPFNGSLEILFMMTELGK**LSELELNLSR**E RSLKWRDIMQYQK**IEVTLPKFTISYNMDLK**ETLSK**LGFEDIFS** **NNADLSGITDEAHLKVSEAVHKAVMTVDEKGTEAAPAGEAAHL** **VHPGHVKF[D|N]CPFVFRLQDMITKNPLLVGR**IDNPLK
Aplastodiscus leucopygius	43.97	MALDI TOF	63.9	250/391	1	N108	MRVLLILGVAVLFTLAFADHKESYDIEDHHDDHKKGEHKESLT CHK**LALTHFRFSFKVYDQVAR[A/D]HPSGNLVISPASISAAL** **ALMCHGAK**DKSHSQIHEVMGFNMSEISEK**EIAEGFHQYLDHMS** **DEDRHLQHSSGNALFISNK**HK**IHQPFSDEAKRLYHSDAFSTDF** **TNAEEAK**NQINSYVEKNTHGKITK**LKDSVDRDADSALINFMYY** **K**GVFETPVDEK**VTEGDFHVNENTIVKVPFMT[I/F]TGWFRMA** **CTDEACIISVPFK**GNIK**AVFLVTLPGKLPHLESTISIDLAHKW** **R**RNLCTQYVKLSIPR**FSFSTTIDLK**ETLSK**MGLVDVFS[D/N]** **HPDLSAITEDANVK**ISQAVHRAVFSIDEKGSEATASTAAK**GVS** **FIEPAHIKLDHPFLLTMHDMK**CGHLLCAARIVNP
Sphaenorhynchus lacteus	44.99	MALDI TOF	69.7	274/393	1	N103	MRFLVFLGVAVLFTLTFAHHEEGHHDHHEKDGHHDDHHEPSPF EEIAPFNYEFTIDLYKQIAR**DHPSENIVFAPISIAASFASLSL** **GAK**GQTHSQIIEALEFNTSEISDK**KINEGFHQLLELWNDEHKE** **LQVHDGSALYVSNDHKVLPSFSDEAK**RLYFAETFSIDFK**HQEE** **AIHEINNYVEK**HTHGKIAK**IVDSVHQDAHLFLVNYMYYNGKWE** **HPFDKALTHEGDFHISETK**TVK**VPFMTRTGFYSVAFSDEYTQV** **YVPYKGNARALFLMPIEGKMEQLEQGITK**ELNDKWRKK**SHDEF** **IELSIPKFSLSDSMELK**ETLIK**MGMVDVFSDHADLSGIIGEGH** **IKLDQVVHEAVINVDEAGTEAGAVTGEEVAVHSVPRKVVIDRP** **FLFTLHDYK**TRTVPFTARVVDPTK

Hyloscirtus phyllognathus	45.80	MALDI TOF	55.7	225/404	2	N114 N295[b]	MRVLLILGVVVLFTLAFADHKEGHDKHDKHDHKGGHDHDDHHV DDHKKDELHACHK**IAPYNTNFAFDLYRHMASEHPSGNFAVSPI** **TISIGLAFLSHAAR**DHTRTHIFEGMGFNTTELTVQEVTEGFK**Q** **LMDVQGTVDR**DLQISCGNGLFVSKKHTILEAFSDDAK**KLYHSE** **VFSTDFTNTEEAK**NQINSYVQKNTHGKIAK**IVDNVDQNAVVAL** **INYIHLK**AKWEKSFDEKLTQEKDFHVSESKTVK**AHFMTTTGMY** **R**VAVDDEMVMVTLPFYGNLKALFIMTKPGK**LHELEQNLTYKRS** **MVWRKRLCKQFVEVSIPKFSISDTTHLVETLSK**MGFGDIFSGR** GDLSGITGEAKLKISK**IVHEASFTVDEKGREPAGATADEDKPM** **MHHASIVLDHPFLFTVHDMK**TKDLLMAARIENPQ[I|E]
Pseudis minuta	45.30	MALDI TOF	62.3	250/401	2	N112 N48[c]	MRVLLFLGVFVLVALAIAHHEEGHHDKDDHHDGKDDDHHHD[D |H][E|K]**KKHHN[D|E]S[S|L]AILKLAPYNSQFFIDLYKQ** **IALEHPSENIVISPVSVSTAFAFLSLGAK**AHTHSEIIQGLGFN SSEISDQEIHEGFHQLLELLNDDDR**ELQLSGGNALFLSVEHKI** **LQTFLDEAKKFYHSEALSTDFTETEEATNQINSYVEK**HTNGKI PK**LLDSVDQDAIF[V|F]LINYIYFRGQW[E|Q]HPFDERFTQ** **EGEFHVDDSK**TVK**VPFMTR**TGMYR**VSISEEFSIVSIPYKGDAF** **ALFILPKKETISELEQR**LTREDSDK**WRKLMQTQFVQVSLPK**FS ISSTINLKEALSKLGVK**DVFSDNADLSGISEGGNVK**ISKALQK AVLSVDERGTEAAASTAVEGVPMMLPPTVK**FDHPFIFS[L|V]** **[Q|H]D[R|H]K**T[R|N][**S|T]VLFAGR**V[V|A]NP[Q|E]
Nymphargus posadae	46.54	MALDI TOF	54.5	223/409	3	N54 N123 N274[d]	MRFLLFFGVALLFTLAFADHHKDHKDDHDDHDHHHHKDDHDDH DHDDKK**HHPHNES**LPSYKLFPFNSKFYIDLYKQVARDQPTGNI VLSPLSIAMAFSFLALGAK**G[H/R]SHSQIIEGLR**FNTSVISE QEIHEGFHNLMDLLNEDDRELQVSIGNALFVSKEHK**ILQTFLD** **EAKKYYHSEVFSTDFK**NTEEATDKINSYVAKQTHDKIPK**LLDT** **VNPEAIFVLMNYLYFKGTWENQFDEKLTKEGDFHVDK**NTIVKV PFMTRTGMYHVAVTDNITSLFIPYK**GHANALFIMPNDGKMAE** **LEQGLSKER**GAQWKK**MMKKRLVELHIPKFSLAGTIDLK**EILSK **LGIVDVFTHNADLSGITGEANLK**ISK**AIHKAVLTVDEKGTEGS** **GSTSLEGVPMSLPLRVELNHPFVFALQEYNPR**CVPIAARVANP LK
Espadarana prosoblepon	46.89	MALDI TOF	57.9	237/409	2	N54 N119	MRFLLFLGVALLFTLAFADHHKHHKDDHDDHDPHDHKDDHDSH DHDDKKHHPHNESLPSYK**LYQFNYQFYIDLYK**QIAR**DQPTGNI** **VLSPPSIATAFAFLSLGAKTDSHTQIIEGLR**FNTSEISEQEIH EGFHNLIHLLNDEDRELK**VSIGNALFVSK**DHK**I[H|L]QTFLD** **EAKKFYDSEAFSTDFK**NTEEATDQINSYVAKQTHDKIPKLLDN VNPEAIFVLMNYFYFK**GTWENQFEEK**LTK**EGDFHVDESTIVKV** **PFMTR**TGMYNVAVTDK**FTCLFIPYKGNAHALVIMPNHGEMAEL** **EQGLSKEKGDQWRKMMKKRLIELHFPK**FSLSGTVNLKETLSK**L** **GIRDIFSNNADLSGITGEANIK**ISKAVHK**AVITVDETGTEGSA** **STALEGVPMMLPMR**V[E|Q]INRPFL[L|F][T|A][M|L]Q[H|Q]YNPR**SLPITVR**VANPQK
Chimerella mariaelenae	46.81	MALDI TOF	54.76%	224/409		N54 N119	MRFRLFLGVALLFTLAFADHHKHHKADHDDHDPHDHKDDHDSH DHDDKKHHPHNESLPSYK**IYQYNYQFIIDLYK**QVARDQPTGNI VLSPLSISTALAFLSLGAK**SESHTQIIEGLR**FNTSQISE[Q|K]EIH[E|I]GFHNL[I|M]HLLNDE[D|H]RELK**VSIGNALFV** **S[K|E]**[E|D]HK**ILQTFLD[E|K]AK**K**FY[H|Y]S[E|Q]AF** **STDFKNTEEATD[Q|E]INSYVAK**QTHDKIPKLLDNVDHESIF VLINCFYFK**GTWEHQFDEK**LTK**EGDFHVDENTIVKVPFMTRTG** **MYK**VAVTDK**FTSLFIPYKGDAHALIIMPNHGGMAELEEGLSKE** **KGDQWR**KMMKKR**LIELHFPK**FSLSGTLNLKEILSK**FGIENMFS** **NNADLSGITGEANIK**ILKAVHK**AMITVDETGTEGSAATALEGV** **PMMLPTRVEINRPFLFALQHYNPR**AVPMTVRVANPQK

Shaded in gray: signal peptide.
Bold: peptides that match the MS data
Bold and underlined: sequences verified by MSMS (Supplementary Tables 4-12).
Doble underline or **Double underline**: Sequons (N-glycosylation consensus sequences)
[aa|aa]: Between square brackets are alternative amino acids, most likely from different alleles of the same gene.
[a]N293 is not glycosylated: peptide was found in the PMF and confirmed with MSMS.
[b]Peptide encompassing the N295 residue was detected in MALDI TOF experiments so the non-glycosylated form exists.
[c] Non-glycosylated
[d] N54 may not be glycosylated (Peptide was detected in MALDI TOF experiments)
[e] With the data obtained using the Orbitrap Analyzer, we found the ion m/z 1116.2212, which corresponds to the $[Glycopeptide+4H]^{4+}$ with the sequence LGYNTSEIPEQQIHESFHK (Theoretical m/z 1116.2207). MSMS data revealed the following oxonium ions: 144.0652 [HexNac-

$C_2H_4O_2]^+$, 168.0653 [HexNac-$2H_2O]^+$, 186.0757 [HexNac-$H_2O]^+$, 204.0863 $[HexNac]^+$, 274.0915 [Neu5Ac − H2O]$^+$, 292.1020 $[Neu5Ac]^+$, 366.1390 $[Hex,HexNAc]^+$, 454.1534 $[Hex,Neu5Ac]^+$, 528.1902 [HexNac,Hex(2)]$^+$, 657.2270 [HexNac,Hex, Neu5Ac]$^+$. Also, we found the ions that correspond to the peptide+biantennary glycan [empirical m/z 1116,2207 (4+), theoretical m/z 1116.2212 (4+), Δ(ppm)=0.45], peptide+HexNac [empirical m/z 1230,5929 (2+), theoretical m/z 1230.5875 (2+), Δ(ppm)=4.39], peptide+ HexNac(2) [empirical m/z 1332.1239 (2+), 1332.1272 (2+), Δ(ppm)= -2.48], peptide+ HexNac(2),Hex [empirical m/z 1413.1562 (2+), theoretical m/z 1413.1536 (2+), Δ(ppm)=1.83].

Table S4. Peptide mass fingerprint of BBS from *Boana punctata.* Shaded in gray are the fragments whose MSMS spectra were used to confirm the sequences.

m/z	Match $(MH)^+$ Theoretical	Δ(ppm)	Modifications	Start	End	MC	Sequence	Notes
768.48	768.47	9.9		405	411	0	(K)NPLLVGR(I)	
997.62	997.62	0.561		403	411	1	(K)TKNPLLVGR(I)	
1051.69	**1051.63**	**57.0**		**210**	**217**		**(A)LINFYILR(A)**	
1094.48	1094.55	-65.4		181	189	0	(K)NQINSYVEK(S)	
1104.56	**1104.55**	**10.8**		**390**	**398**	**0**	**(K)FDYPFIFR(V)**	
1163.60	**1163.59**	**9.7**		**96**	**106**	**0**	**(K)GHTHSQIVER(L)**	
1187.62	1187.61	11.6		152	151	0	(K)IHQTFLDDAK(K)	
1202.60	1202.60	2.81		125	134	1	(K)QLDVVDDKDR(D)	
1215.64	**1215.63**	**3.09**		**266**	**275**	**0**	**(K)LSELEQNLNR(E)**	
1271.59	**1271.58**	**9.09**		**200**	**209**	**0**	**(R)ANWQHPFDEK(L)**	
1482.74	**1482.73**	**10**		**145**	**156**	**0**	**(K)FYHSEVIPTDFK(N)**	
1505.79	1505.84	-33.5		221	232	3	(K)DTTVKVPFMRRR(G)	
1690.90	1690.91	-2.24		283	296	0	(R)EIMQYQLIDLSLPK(L)	
1694.78	1694.78	-4.33	Cam->Prop	117	130	0	(R)DLEFEHGNALFTC(Cam)K(E)	
2098.14	2098.15	-4.37		27	44	0	(K)ALFVYQKPALNNINFAFK(M)	
2121.06	**2121.04**	**6.9**		**231**	**248**		**(K)EGDFHVDKDTTVKVPFMR(R)**	
2467.24	**2467.25**	**-3.24**		**312**	**334**	**0**	**(K)LGIVDVFSNHADLSGITDESHLK(V)**	
2878.4	**2878.33**	**24.3**	**Acryl(C)**	**125**	**148**		**(K)QLDVVDDKDRDLEFEHGNALFTCK(E)**	
3183.40	**3183.46**	**-18.2**		**342**	**371**	**0**	**(K)AMMSFDEHGTEAAPATAAEADPLMLPPHFK(F)**	

Table S5. Peptide mass fingerprint of BBS from *Boana cinerascens.* Shaded in gray are the fragments whose MSMS spectra were used to confirm the sequences.

m/z	Match (MH)$^+$ Theoretical	Δ(ppm)	Modifications	Start	End	MC	Sequence	Notes
688.44	688.38	95.7	1Dm	247	252	0	(K)VPFMSR(T)	
736.45	736.38	92.4		247	252	0	(K)VPFMSR(T)	
745.46	745.40	84.4	1Dm Cam	247	252	0	(K)VPFMSR(T)	
768.54	768.47	89		406	412	0	(K)NPLLVGR(I)	
793.47	793.40	82.8	Cam	247	252	0	(K)VPFMSR(T)	
825.56	825.49	74.9	Cam	406	412	0	(K)NPLLVGR(I)	
937.59	937.53	71.9		48	54	0	(K)RPFVYQK(A)	
994.61	994.55	58.8	Cam	48	54	0	(K)RPFVYQK(A)	
1065.68	1065.62	58.6		47	54	1	(K)KRPFVYQK(A)	
1077.52	1077.46	55.2		223	230	0	(K)WEHSFDEK(L)	
1077.52	1077.58	-52.8	Cam	99	107	0	(K)GHTHSQIIK(G)	
1086.58	**1086.62**	**64.2**	**Cam(C)**	**391**	**398**	**0**	**(K)FNC(Cam)PFVFR(L)**	**1**
1087.58	**1087.50**	**70.8**	**Cam(C)**	**391**	**398**	**0**	**(K)FDC(Cam)PFVFR(L)**	**1**
1143.60	**1143.54**	**62.0**	**Cam(C) Cam**	**391**	**398**	**0**	**(K)FNC(Cam)PFVFR(L)**	**1**
1144.61	**1144.52**	**74.8**	**Cam(C) Cam**	**391**	**398**	**0**	**(K)FDC(Cam)PFVFR(L)**	**1**
1173.72	**1173.65**	**60.3**		**287**	**296**	**0**	**(K)LSELELNLSR(E)**	
1183.66	1183.60	55.2	1Dm	318	327	0	(K)FTISYNMDLK(E)	
1208.71	1208.64	55.8		55	65	0	(K)AAINNVNFAFK(M)	
1230.74	1230.67	54.5	Cam(N-term)	287	296	0	(K)LSELELNLSR(E)	
1262.65	1262.58	53.1		221	230	1	(R)GKWEHSFDEK(L)	
1454.78	1454.70	56.2		166	177	0	(R)FYHSEAIPTDFK(N)	
1476.75	1476.71	25.1	Cam(N-term)	223	233	1	(K)WEHSFDEKLTK(E)	
1610.87	1610.80	43.3		165	177	1	(K)RFYHSEAIPTDFK(N)	
1642.93	1642.85	49.8		356	370	1	(K)VSEAVHKAVMTVDEK(G)	
1642.93	1642.85	46.6		55	68	1	(K)AAINNVNFAFKMFR(Q)	
1654.80	1654.83	-16.2		184	197	1	(K)NQINSYVEKHTHGK(I)	
1654.80	1654.93	-77.4	Cam(N-term)	399	412	1	(R)LQDMITKNPLLVGR(I)	
1658.92	1658.84	48.6	1Ox(M)	356	370	1	(K)VSEAVHKAVMTVDEK(G)	
1658.92	1658.85	45.4	1Ox(M)	55	68	1	(K)AAINNVNFAFKMFR(Q)	
1932.87	1932.93	-33.7	1Ox(M) Cam(C)	391	405	1	(K)FDC(Cam)PFVFRLQDMITK(N)	
1949.08	**1949.00**	**39.3**		**371**	**390**	**0**	**(K)GTEAAPAGEAAHLVHPGHVK(F)**	
2006.10	2006.02	41.1	Cam	371	390	0	(K)GTEAAPAGEAAHLVHPGHVK(F)	
2024.02	2023.94	38.3		138	154	0	(R)HLEFEHGNAVFIC(Cam)EGHK(I)	
2024.02	2023.94	38.3	Cam(C)	138	154	0	(R)HLEFEHGNAVFIC(Cam)EGHK(I)	
2028.12	2028.07	23.8	1Ox(M)	311	327	1	(K)IEVTLPKFTISYNMDLK(E)	
2038.04	2037.96	39.9	Cam->Prop	138	154	0	(R)HLEFEHGNAVFIC(Cam)EGHK(I)	
2506.30	**2506.21**	**34.8**		**333**	**355**	**0**	**(K)LGFEDIFSNNADLSGITDEAHLK(V)**	
2563.33	2563.23	38.9	Cam(N-term)	333	355	0	(K)LGFEDIFSNNADLSGITDEAHLK(V)	
2594.51	2594.42	36.1		73	98	0	(R)DHPTGNIVISPVSISSALAFLSLGAK(G)	2
2608.50	2608.43	26.9		73	98	0	(R)DHPTGNIVISPVSISSALAFLSLAAK(G)	2

2745.51	2745.41	34.7		198	220	0	(K)ITNILDSVDQDDIFALINFIYFR(G)
3421.53	3421.40	36.9		19	46	2	()HHEEGHDDHKDDHDDLKDDHDPFFPEDK(K)
3478.54	3478.42	36.9	Cam(N-term)	19	46	2	()HHEEGHDDHKDDHDDLKDDHDPFFPEDK(K)

(1) Peaks corresponding to the two different peptides are present. These belong to different isoforms of the BBS ether with D392 or N392 **(2)** Peaks corresponding to the two different peptides are present. These belong to different isoforms of the BBS ether with G96 or A96

Table S6. Peptide mass fingerprint of BBS from *Aplastodiscus leucopygius.* Shaded in gray are the fragments whose MSMS spectra were used to confirm the sequences.

m/z	Match $(MH)^+$ Theoretical	Δ(ppm)	Modifications	Start	End	MC	Sequence	Notes
810.48	910.45	27.1		347	353	0	(K)ISQAVHR(A)	
850.46	850.44	24.6		58	64	0	(K)VYDQVAR(A)	
857.52	857.50	27.1		47	53	0	(K)LALTHFR(F)	
1158.62	1158.60	10.6		309	318	0	(R)FSFSTTIDLK(E)	
1197.64	1197.66	-16.7		373	383	0	(K)GVSFIEPAHIK(L)	
1306.71	1306.69	12.3	Dm	232	248	0	(K)VPFMTITGWFR(M)	1
1327.70	1327.68	22.1		147	157	1	(K)IHQPFSDEAKR(L)	
1340.77	1340.68	68.3	Dm	232	248	0	(K)VPFMTFTGWFR(M)	1
1354.76	1354.70	49.5		232	248	0	(K)VPFMTITGWFR(M)	1
1359.73	1359.71	18.7		54	64	1	(R)FSFKVYDQVAR(A)	
1370.75	1370.69	39.1	1Ox(M)	232	248	0	(K)VPFMTITGWFR(M)	1
1388.77	1388.68	60.4		232	248	0	(K)VPFMTFTGWFR(M)	1
1404.75	1404.68	55.3	1Ox(M)	232	248	0	(K)VPFMTFTGWFR(M)	1
1411.81	1411.72	63.4	Cam	232	248	0	(K)VPFMTITGWFR(M)	1
1445.80	1445.70	64.9	Cam(N-term)	232	248	0	(K)VPFMTFTGWFR(M)	1
1550.78	1550.72	36.5		200	212	0	(R)DADSALINFMYYK(G)	
1597.79	1597.79	3.56		384	396	0	(K)LDHPFLLTMHDMK(C)	
1613.75	1613.78	-19.5	1Ox(M)	384	396	0	(K)LDHPFLLTMHDMK(C)	
1652.84	1652.85	18.0		130	144	0	(R)HLQHSSGNALFISNK(H)	
1673.93	1673.92	4.2		278	292		(K)LPHLESTISIDLAHK(W)	
1701.86	1701.84	9.26		223	237	0	(K)VTEGDFHVNENTIVK(V)	
1757.83	1757.89	22.4	1Ox(M)2Cam(C)	249	263	0	(R)MAC(Cam)TDEAC(Cam)IISVPFK(G)	
2016.07	2016.10	-16.1		278	294	1	(K)LPHLESTISIDLAHKWR(R)	
2045.90	2045.91	-2.03		158	175	0	(R)LYHSDAFSTDFTNAEEAK(N)	
2143.93	2143.93	-2.22	Dm	112	129	0	(K)EIAEGFHQYLDHMSDEDR(H)	
2191.96	2191.93	12.4		112	129	0	(K)EIAEGFHQYLDHMSDEDR(H)	
2202.04	2202.01	13.3		157	175	1	(K)RLYHSDAFSTDFTNAEEAK(N)	
2207.95	2207.93	10	1Ox	112	129	0	(K)EIAEGFHQYLDHMSDEDR(H)	
2249.00	2248.96	20.2	Cam	112	129	0	(K)EIAEGFHQYLDHMSDEDR(H)	
2364.18	2364.15	10.1		193	212	2	(K)LKDSVDRDADSALINFMYYK(G)	
2424.24	2424.20	14.8	Dm	324	346	0	(K)MGLVDVFSNHPDLSAITEDANVK(I)	2
2425.21	2425.19	7.14	Dm	324	346	0	(K)MGLVDVFSDHPDLSAITEDANVK(I)	2
2472.20	2472.21	-1.14		324	346	0	(K)MGLVDVFSNHPDLSAITEDANVK(I)	2
2473.21	2473.19	6.89		324	346	0	(K)MGLVDVFSDHPDLSAITEDANVK(I)	2
2489.20	2489.19	6.44	1Ox	324	346	0	(K)MGLVDVFSDHPDLSAITEDANVK(I)	2
2573.45	2573.33	45.6	Cam(C)	65	90	0	(R)AHPSGNLVISPASISAALALMC(Cam)HGAK(D)	3
2617.41	2617.32	33.4	Cam(C)	65	90	0	(R)DHPSGNLVISPASISAALALMC(Cam)HGAK(D)	3

2699.68	2699.55	49.9		268	292	1	(K)AVFLVTLPGKLPHLESTISIDLAHK(W)

(1) Peaks corresponding to the two different peptides are present. These belong to different isoforms of the BBS ether with I37 or F37. **(2)** The isotopic distribution of the peak at 2472-2473 is consistent with the overlapping of both peptides, either with D332 or N332. **(3)** Peaks corresponding to the two different peptides are present. These belong to different isoforms of the BBS ether with A65 or D65.

Table S7. Peptide mass fingerprint of BBS from *Sphaenorhynchus lacteus.* Shaded in gray are the fragments whose MSMS spectra were used to confirm the sequences.

m/z	Match $(MH)^+$ Theoretical	Δ(ppm)	Modifications	Start	End	MC	Sequence	Notes
702.36	702.39	-45.6	Dm	238	243	0	(K)VPFMTR(T)	
750.37	750.40	-38.8		238	243	0	(K)VPFMTR(T)	
759.39	759.41	-34.6	Cam Dm	238	243	0	(K)VPFMTR(T)	
791.42	791.44	-23.4		399	405	0	(R)TVPFTAR(V)	
807.40	807.42	-20.7	Cam	238	243	0	(K)VPFMTR(T)	
848.45	848.46	-15.7	Cam	399	405	0	(R)TVPFTAR(V)	
958.44	958.44	-2.9		214	220	0	(K)WEHPFDK(A)	
1015.46	1015.46	-6.24	Cam	214	220	0	(K)WEHPFDK(A)	
1070.62	**1070.62**	**0.0343**	**Dm**	**268**	**277**	**0**	**(R)ALFLMPIEGK(M)**	
1092.56	1092.56	5.76		146	155	0	(K)VLPSFSDEAK(R)	
1105.64	**1105.64**	**-0.4**		**364**	**372**	**0**	**(K)VVIDRPFLF(T)**	
1127.65	1127.65	5.69	Cam Dm	250	259	0	(R)ALFLMPIEGK(M)	
1149.59	1149.58	10.9	Cam	128	137	0	(K)VLPSFSDEAK(R)	
1165.60	1165.57	24.5	Cam Dm	291	300	0	(K)FSLSDSMELK(E)	
1233.73	1233.61	97.4	Cam	260	269	0	(K)MEQLEQGITK(E)	
1233.73	1273.73	-4.4		363	372	0	(R)KVVIDRPFLF(T)	
1414.72	1414.72	-3.76		279	290	0	(K)SHDEFIELSIPK(F)	
1471.73	1471.74	-7.74	Cam	279	290	0	(K)SHDEFIELSIPK(F)	
1584.75	**1584.77**	**-10.1**		**203**	**216**	**0**	**(K)ALTHEGDFHISETK(T)**	
1641.77	1641.79	-8.67	Cam	203	216	0	(K)ALTHEGDFHISETK(T)	
1852.86	1852.88	-10.4		151	165	0	(K)HQEEAIHEINNYVEK(H)	
1863.00	**1863.02**	**-9.86**		**364**	**378**	**0**	**(K)VVIDRPFLFTLHDYK(T)**	
1909.89	1909.90	-9.64	Cam	151	165	0	(K)HQEEAIHEINNYVEK(H)	
1920.03	**1920.04**	**-5.19**	**Cam**	**364**	**378**	**0**	**(K)VVIDRPFLFTLHDYK(T)**	
1968.93	1968.94	-7.81	Cam	111	127	0	(K)ELQVHDGSALYVSNDHK(V)	
1991.09	1991.11	-9.45		363	378	1	(R)KVVIDRPFLFTLHDYK(T)	
2048.12	2048.13	-6.46	Cam	363	378	1	(R)KVVIDRPFLFTLHDYK(T)	
2122.01	2122.04	-11.6		94	110	0	(K)INEGFHQLLELWNDEHK(E)	
2179.02	2179.06	-17.1	Cam	94	110	0	(K)INEGFHQLLELWNDEHK(E)	
2250.10	2250.13	-15.5		93	110	1	(K)KINEGFHQLLELWNDEHK(E)	
2332.13	2332.16	-11.3	2Dm	306	328	0	(K)MGMVDVFSDHADLSGIIGEGHIK(L)	
2364.07	2364.11	-15.8		226	245	0	(R)TGFYSVAFSDEYTQVYVPYK(G)	
2380.13	2380.16	-13.2	Dm	306	328	0	(K)MGMVDVFSDHADLSGIIGEGHIK(L)	
2389.14	2389.18	-15.2	Cam 2Dm	306	328	0	(K)MGMVDVFSDHADLSGIIGEGHIK(L)	
2421.09	2421.13	-15.8	Cam	226	245	0	(R)TGFYSVAFSDEYTQVYVPYK(G)	
2437.17	2437.18	-5.63	Cam Dm	306	328	0	(K)MGMVDVFSDHADLSGIIGEGHIK(L)	
2642.34	2642.27	26.4	Ox(M)	174	195	0	(K)IVDSVHQDAHLFLVNYMYYNGK(W)	
2642.34	2642.38	-15.8		46	71	0	(R)DHPSENIVFAPISIAASFASLSLGAK(G)	
2642.34	2642.40	-21.4	Ox(M) Dm	246	269	2	(K)GNARALFLMPIEGKMEQLEQGITK(E)	
3497.62	**3497.75**	**-37**		**329**	**362**	**0**	**(K)LDQVVHEAVINVDEAGTEAGAVTGEEVAVHSVPR(K)**	

3554.64	3554.77	-36.6	Cam	329	362	0	(K)LDQVVHEAVINVDEAGTEAGAVTGEEVAVHSVPR(K)

Table S8. Peptide mass fingerprint of BBS from *Hyloscirtus phyllognathus.* Shaded in gray are the fragments whose MSMS spectra were used to confirm the sequences.

m/z	Match $(MH)^+$ Theoretical	ΔPPM	Modifications	Start	End	MC	Sequence	Notes
1038.51	1038.50	4.78	Dm	335	344	0	(K)MGFGDIFSGR(G)	
1068.47	1068.50	-28.9		225	232	1	(K)WEKSFDEK(L)	
1086.52	**1086.50**	**13.5**		**335**	**344**	**0**	**(K)MGFGDIFSGR(G)**	
1102.51	1102.50	9.87	Ox(M)	335	344	0	(K)MGFGDIFSGR(G)	
1143.55	**1143.53**	**24.9**	**Cam**	**335**	**344**	**0**	**(K)MGFGDIFSGR(G)**	
1260.61	1260.59	17.2	1Gln->pyro-Glu Ox(M)	119	129	0	(K)QLMDVQGTVDR(D)	
1261.63	1261.62	7.4		119	129	0	(K)QLMDVQGTVDR(D)	
1267.60	1267.59	8.89	Dm	249	259	0	(K)AHFMTTTGMYR(V)	
1267.60	1267.63	-25		223	232	2	(K)AKWEKSFDEK(L)	
1315.61	**1315.59**	**10.1**		**249**	**259**	**0**	**(K)AHFMTTTGMYR(V)**	
1331.63	1331.59	32.2	Ox(M)	249	259	0	(K)AHFMTTTGMYR(V)	
1346.67	1346.65			155	166		(K)HTILEAFSDDAK(K)	
1372.62	1372.61	4.53	Cam	249	259	0	(K)AHFMTTTGMYR(V)	
1374.67	1374.69	-12.3		361	372	0	(K)IVHEASFTVDEK(G)	
1543.88	1543.82	24.1		289	300		(K)LHELEQNLTYKR(S)	
1677.87	1677.87	-2.33		302	316	0	(K)FSISDTTHLVETLSK(M)	
1704.87	**1704.84**	**18.3**		**57**	**70**	**0**	**(K)IAPYNTNFAFDLYR(H)**	
1761.90	**1761.86**	**25.4**	**Cam**	**57**	**70**	**0**	**(K)IAPYNTNFAFDLYR(H)**	
2093.08	2093.06	9.21	Dm	260	278	0	(R)VAVDDEMVMVTLPFYGNLK(A)	
2117.99	2117.97	9.06		168	185	0	(K)LYHSEVFSTDFTNTEEAK(N)	
2141.06	2141.07	-0.522		260	278	0	(R)VAVDDEMVMVTLPFYGNLK(A)	
2246.10	2246.06	17.5		167	185	1	(K)KLYHSEVFSTDFTNTEEAK(N)	
2251.27	**2251.24**	**9.71**		**203**	**222**	**0**	**(K)IVDNVDQNAVVALINYIHLK(A)**	
3118.63	**3118.59**	**12.7**		**89**	**118**	**0**	**(R)HMASEHPSGNFAVSPITISIGLAFLSHAAR(D)**	
3900.92	**3900.86**	**15.4**		**373**	**407**	**1**	**(K)GREPAGATADEDKPMMHHASIVLDHPFLFTVHDMK(T)**	

Table S9. Peptide mass fingerprint of BBS from *Pseudis minuta.* Shaded in gray are the fragments whose MSMS spectra were used to confirm the sequences.

m/z	Match $(MH)^+$ Theoretical	Δ(ppm)	Modifications	Start	End	MC	Sequence	Notes
702.34	702.39	-69.7	Dm	229	234	0	(K)VPFMTR(T)	
749.39	749.43	-54		390	396	0	(R)SVLFAGR(V)	
750.35	750.40	-62.1		229	234	0	(K)VPFMTR(T)	
800.33	800.37	-44.1		207	212	0	(K)HPFDER(F)	
807.38	807.42	-43.2	Cam(N-term)	229	234	0	(K)VPFMTR(T)	
857.36	857.39	-39.4	Cam(N-term)	207	212	0	(K)HPFDER(F)	
978.53	978.54	-7.52		388	396	0	(K)TNTVLFAGR(V)	
1177.63	1177.65	-10.6		137	146	0	(K)ILQTFLDEAK(K)	
1191.66	1191.68	-14.55		255	265	0	(K)GDAFALFILPK(K)	
1218.67	1218.66	6.84	Cam(N-term)	27	36	0	(K)HHNESLAILK(L)	
1232.64	1232.65	-3.32		266	275	1	(K)KETISELEQR(L)	
1300.56	1300.57	-7.69		203	212	0	(R)GQWEHPFDER(F)	
1357.58	**1357.59**	**-9.51**	**Cam(N-term)**	**203**	**212**	**0**	**(R)GQWEHPFDER(F)**	
1470.82	1470.83	-6.19	Dm	287	299	0	(K)LMQTQFVQVSLPK(F)	
1521.72	**1521.75**	**-18.6**		**375**	**386**	**0**	**(K)FDHPFIFSLQDR(K)**	
1538.67	**1538.68**	**-3.98**		**213**	**225**	**0**	**(R)FTQEGEFHVDDSK(T)**	**1**
1578.73	1578.77	-20.7	Cam(N-term)	375	386	0	(K)FDHPFIFSLQDR(K)	
1595.69	1595.70	-1.84	Cam(N-term)	213	225	0	(R)FTQEGEFHVDDSK(T)	
1625.76	**1625.79**	**-16.7**		**375**	**387**	**0**	**(K)FDHPFIFSVHDHK(T)**	**1**
1682.78	1682.81	-19.3	Cam(N-term)	375	387	0	(K)FDHPFIFSVHDHK(T)	
1697.88	1697.90	-12.1		240	254	0	(R)VSISEEFSIVSIPYK(G)	
1718.85	**1718.87**	**-12.6**		**37**	**50**	**0**	**(K)LAPYNSQFFIDLYK(Q)**	
1841.94	1841.98	-16.7		120	136	0	(R)ELQLSGGNALFLSVEHK(I)	
1923.88	1923.89	-6.78		319	337	0	(K)DVFSDNADLSGISEGGNVK(I)	
1940.99	1941.11	-58.5	Dm	284	299	2	(K)WRKLMQTQFVQVSLPK(F)	
1988.99	1989.11	-59.6		284	299	2	(K)WRKLMQTQFVQVSLPK(F)	
2045.95	2046.13	-91.1	Cam	284	299	2	(K)WRKLMQTQFVQVSLPK(F)	
2417.21	2417.27	-25.7		183	202	0	(K)LLDSVDQDAIFVLINYIYFR(G)	2
2465.23	2465.28	-17		183	202	0	(K)LLDSVDQDAIFFLINYIYFR(G)	2
2849.20	2849.45	-90.4		310	337	2	(K)EALSKLGVKDVFSDNADLSGISEGGNVK(I)	
3125.56	3125.69	-39.9		51	80	0	(K)QIALEHPSENIVISPVSVSTAFAFLSLGAK(A)	
3128.59	3128.70	-34.1		120	147	2	(R)ELQLSGGNALFLSVEHKILQTFLDEAKK(F)	
3153.31	3153.42	-34.4		148	174	0	(K)FYHSEALSTDFTETEEATNQINSYVEK(H)	

(1) Peaks corresponding to the two different peptides are present. These belong to different isoforms of the BBS ether with L383, Q384, R386 or V383, H384, H386. **(2)** Both ions are present: V194-F194

Table S10. Peptide mass fingerprint of BBS from *Nymphargus posadae.* Shaded in gray are the fragments whose MSMS spectra were used to confirm the sequences.

m/z	Match $(MH)^+$ Theoretical	ΔPPM	Modifications	Start	End	MC	Sequence	Notes
946.45	946.43	27.6		223	230	0	(K)EGDFHVDK(N)	
1057.53	1057.55	-23.7	Dm	276	285	0	(K)MAELEQGLSK(E)	
1064.59	1064.60	-11.9		307	316	0	(K)FSLAGTIDLK(E)	
1104.67	1104.69	-12.8		298	306	1	(K)RLVELHIPK(F)	
1139.60	**1139.62**	**-16**		**90**	**99**	**0**	**(R)SHSQIIEGLR(F)**	
1177.61	1177.65	-26.7		144	153	0	(K)ILQTFLDEAK(K)	
1196.61	1196.64	-25	Cam(Nterm)	90	99	0	(R)SHSQIIEGLR(F)	
1253.52	**1253.54**	**-21**		**210**	**219**	**0**	**(K)GTWENQFDEK(L)**	
1288.71	1288.65	42.2		220	230	1	(K)LTKEGDFHVDK(N)	
1310.53	1310.56	-23.4	Cam(N-term)	210	219	0	(K)GTWENQFDEK(L)	
1333.67	**1333.70**	**-22.9**		**88**	**99**	**0**	**(K)GHSHSQIIEGLR(F)**	
1345.73	1345.67	38.1	Cam(N-term)	220	230	1	(K)LTKEGDFHVDK(N)	
1436.70	**1436.73**	**-19.6**	**Dm**	**262**	**275**	**0**	**(K)GHANALFIMPNDGK(M)**	
1445.78	1445.69	60.8		32	43	0	(K)HHPHNESLPSYK(L)	
1463.77	1463.72	37	Cam(N-term)	276	287	1	(K)MAELEQGLSKER(G)	
1484.70	1484.73	-21.2		262	275	0	(K)GHANALFIMPNDGK(M)	
1493.73	1493.75	-13.1	Cam(N-term)DM	262	275	0	(K)GHANALFIMPNDGK(M)	
1522.65	**1522.68**	**-22.9**		**155**	**166**	**0**	**(K)YYHSEVFSTDFK(N)**	
1541.72	1541.75	-21.4	Cam(N-term)	262	275	0	(K)GHANALFIMPNDGK(M)	
1579.67	1579.71	-23	Cam(N-term)	155	166	0	(K)YYHSEVFSTDFK(N)	
1638.82	1638.95	-82.1	1Ox(M)	294	306	3	(K)MMKKRLVELHIPK(F)	
1650.74	1650.78	-24.1		154	166	1	(K)KYYHSEVFSTDFK(N)	
1707.74	1707.80	-35.9	Cam(N-term)	154	166	1	(K)KYYHSEVFSTDFK(N)	
1851.86	1851.97	-59.6	Cam(N-term)	44	57	1	(K)LFPFNSKFYIDLYK(Q)	
1926.93	1926.98	-22.1	Dm	360	379	0	(K)GTEGSGSTSLEGVPMSLPLR(V)	
1974.93	1974.98	-25.5		360	379	0	(K)GTEGSGSTSLEGVPMSLPLR(V)	
1983.94	1984.00	-30.5	Cam(N-term)	360	379	0	(K)GTEGSGSTSLEGVPMSLPLR(V)	
1990.92	1990.98	-26.8	1Ox(M)	360	379	0	(K)GTEGSGSTSLEGVPMSLPLR(V)	
2031.94	2032.00	-29.1	Cam(N-term)	360	379	0	(K)GTEGSGSTSLEGVPMSLPLR(V)	
2073.02	**2073.06**	**-18**		**380**	**396**	**0**	**(R)VELNHPFVFALQEYNPR(C)**	
2130.08	**2130.08**	**-0.188**	Cam(N-term)	**380**	**396**	**0**	**(R)VELNHPFVFALQEYNPR(C)**	
2384.17	2384.25	-33.5		322	344	0	(K)LGIVDVFTHNADLSGITGEANLK(I)	
2403.24	2403.26	-9.1		208	227		(K)LLDTVNPEAIFVLMNYLYFK(G)	
2441.21	2441.27	-25	Cam(N-term)	322	344	0	(K)LGIVDVFTHNADLSGITGEANLK(I)	
3295.48	3295.72	-71.4	1Ox(M)	348	379	2	(K)AIHKAVLTVDEKGTEGSGSTSLEGVPMSLPLR(V)	

Table S11. Peptide mass fingerprint of BBS from *Espadarana prosoblepon.* Shaded in gray are the fragments whose MSMS spectra were used to confirm the sequences.

m/z	Match $(MH)^+$ Theoretical	Δ(ppm)	Modifications	Start	End	MC	Sequence	Notes
661.31	661.31	0.181		288	292	0	(K)GDQWR(K)	
750.40	750.40	-0.0772		236	241	0	(K)VPFMTR(T)	
750.40	750.41	-19.5	Cam(N-term)	294	298	2	(K)MMKKR(L)	
785.49	785.49	-3.27		397	403	0	(R)SLPITVR(V)	
807.42	807.42	-1.08	Cam(N-term)	236	241	0	(K)VPFMTR(T)	
918.44	918.44	-6.76		286	292	1	(K)EKGDQWR(K)	
975.45	975.46	-14.3	Cam(N-term)	286	292	1	(K)EKGDQWR(K)	
996.57	996.59	-13.1		299	306	0	(R)LIELHFPK(F)	
1134.62	1134.65	-26		130	140	0	(K)VSIGNALFVSK(D)	
1152.67	1152.69	-17.7		298	306	1	(K)RLIELHFPK(F)	
1191.64	1191.67	-26.8	Cam(N-term)	130	140	0	(K)VSIGNALFVSK(D)	
1201.60	1201.62	-17.6		144	154	0	(K)IHQTFLDEAK(K)	
1202.60	1202.63	-26.6	Cam->Prop	253	261	0	(K)FTC(Cam)LFIPYK(G)	
1267.53	**1267.56**	**-21**		**210**	**219**	**0**	**(K)GTWENQFEEK(L)**	
1324.55	1324.58	-22.9	Cam(N-term)	210	219	0	(K)GTWENQFEEK(L)	
1369.69	**1369.71**	**-14**		**88**	**99**	**0**	**(K)TDSHTQIIEGLR(F)**	
1426.70	1426.73	-18.6	Cam(N-term)	88	99	0	(K)TDSHTQIIEGLR(F)	
1456.59	**1456.63**	**-24.1**		**155**	**166**	**0**	**(K)FYDSEAFSTDFK(N)**	
1493.78	1493.74	30.5	Cam(N-term)	286	296	3	(K)EKGDQWRKMMK(K)	
1584.67	1584.72	-30.2		154	166	1	(K)KFYDSEAFSTDFK(N)	
1917.87	1917.94	-35.2		44	57	0	(K)LYQFNYQFYIDLYK(Q)	
1978.92	**1978.97**	**-27.1**		**326**	**344**	**0**	**(R)DIFSNNADLSGITGEANIK(I)**	
2104.10	**2104.15**	**-20.4**		**380**	**396**	**0**	**(R)VQINRPFLFALQQYNPR(S)**	
2161.14	2161.17	-12.4	Cam(N-term)	380	396	0	(R)VQINRPFLFALQQYNPR(S)	
2207.00	2207.08	-34.9		223	241	1	(K)EGDFHVDESTIVKVPFMTR(T)	
2418.11	2418.26	-61.7		322	344	1	(K)LGIRDIFSNNADLSGITGEANIK(I)	
2498.20	2498.25	-17.6	Dm	262	285	0	(K)GNAHALVIMPNHGEMAELEQGLSK(E)	
2546.18	2546.25	-28.1		262	285	0	(K)GNAHALVIMPNHGEMAELEQGLSK(E)	
2555.22	2555.27	-16.6	Cam(N-term)	262	285	0	(K)GNAHALVIMPNHGEMAELEQGLSK(E)	
2603.20	2603.27	-25.5	Cam(N-term)	262	285	0	(K)GNAHALVIMPNHGEMAELEQGLSK(E)	
2615.32	2615.41	-34.4		62	87	0	(R)DQPTGNIVLSPPSIATAFAFLSLGAK(T)	
2815.34	2815.39	-17	Dm	352	379	0	(K)AVITVDETGTEGSASTALEGVPMMLPMR(V)	
2863.34	2863.39	-15.6		352	379	0	(K)AVITVDETGTEGSASTALEGVPMMLPMR(V)	
2879.33	2879.38	-17.4	Ox(M)	352	379	0	(K)AVITVDETGTEGSASTALEGVPMMLPMR(V)	

Table S12. Peptide mass fingerprint of BBS from *Chimerella mariaelenae.* Shaded in gray are the fragments whose MSMS spectra were used to confirm the sequences.

m/z	Match $(MH)^+$ Theoretical	Δ(ppm)	Modifications	Start	End	MC	Sequence	Notes
661.31	661.31	12.6		306	310	0	(K)GDQWR(K)	
918.45	918.44	3.8		304	310	1	(K)EKGDQWR(K)	
996.58	996.59	-2.96		317	324	0	(R)LIELHFPK(F)	
1053.61	1053.61	-2.15	Cam	317	324	0	(R)LIELHFPK(F)	
1115.54	1115.61	-63.7		271	279	0	(K)FTSLFIPYK(G)	
1134.63	1134.65	-16.5		148	158	0	(K)VSIGNALFVSK(E)	
1152.69	1152.69	1.2		316	324	1	(K)RLIELHFPK(F)	
1172.57	1172.64	-58.1	Cam	271	279	0	(K)FTSLFIPYK(G)	
1177.64	1177.65	-8.09		162	171	0	(K)ILQTFLDEAK(K)	
1191.62	1191.67	-45.4	Cam	148	158	0	(K)VSIGNALFVSK(E)	
1234.66	1234.66	0.757	2Dm	254	264	1	(K)VPFMTRTGMYK(V)	
1234.66	1234.67	-7.26	Cam	162	171	0	(K)ILQTFLDEAK(K)	
1276.55	1276.56	-4.75		228	237	0	(K)GTWEHQFDEK(L)	
1333.57	1333.58	-5.78	Cam	228	237	0	(K)GTWEHQFDEK(L)	
1369.70	**1369.71**	**-5.32**		**106**	**117**	**0**	**(K)SESHTQIIEGLR(F)**	
1426.71	1426.73	-10.1	Cam	106	117	0	(K)SESHTQIIEGLR(F)	
1478.66	1478.66	1.74		173	184	0	(K)FYHSEAFSTDFK(N)	
1502.75	1502.71	28.2		241	253	0	(K)EGDFHVDENTIVK(V)	
1535.68	1535.68	1.41	Cam	173	184	0	(K)FYHSEAFSTDFK(N)	
1559.78	1559.73	32.5	Cam	241	253	0	(K)EGDFHVDENTIVK(V)	
1682.78	1682.79	-6.37		185	199	0	(K)NTEEATDQINSYVAK(Q)	
1883.94	1883.96	-11.8		62	75	0	(K)IYQYNYQFIIDLYK(Q)	
1940.90	1940.98	-43.3	Cam	62	75	0	(K)IYQYNYQFIIDLYK(Q)	
2114.11	**2114.13**	**-7.16**		**398**	**414**	**0**	**(R)VEINRPFLFALQHYNPR(A)**	
2171.13	2171.15	-9.58	Cam	398	414	0	(R)VEINRPFLFALQHYNPR(A)	
2442.16	2442.16	-1.86		340	362	0	(K)FGIENMFSNNADLSGITGEANIK(I)	
2490.18	2490.21	-11.3		280	303	0	(K)GDAHALIIMPNHGGMAELEEGLSK(E)	
2708.22	2708.36	-52.6	Cam 2Dm	280	305	1	(K)GDAHALIIMPNHGGMAELEEGLSKEK(G)	
2747.14	2747.35	-76.9		280	305	1	(K)GDAHALIIMPNHGGMAELEEGLSKEK(G)	
2849.35	2849.37	-8.31		370	397	0	(K)AMITVDETGTEGSAATALEGVPMMLPTR(V)	

Table S13. Identity matrix between human clade A serpins, *Xenopus tropicalis* clade A serpins, and BBSs. Multiple alignment of serpins revealed that compared to all the human clade A serpins, BBSs have maximum identity to α1-AT (38.8–47.1 %) even though no inhibitory activity is expected (*SI Appendix*, Fig. S15). Comparison between different BBSs shows that within hylids sequence identities are around 50%, ranging between 46.4% and 76% between the closely related species *Boana punctata* and *B. cinerascens*. Within centrolenids, sequence identity between species of different genera range between 79.2% and 85.5%, which is consistent with the common origin of chlorosis in the family.

			BBS									*Xenopus tropicalis* serpins							Humans Clade A Serpins										
			Hylids						Centrolenids																				
			B. punctata	*B. cinerascens*	*H. phyllognathus*	*A. leucopygius*	*P. minuta*	*S. lacteus*	*N. posadae*	*E. prosoblepon*	*C. mariaelenae*	X. tr_Spn7	X. tr_Spn9	X. tr_Spn10	X. tr_Spn11	X. tr_Spn12	X. tr_Spn13	X. tr_Spn14	SerpinA1	SerpinA2	SerpinA3	SerpinA4	SerpinA5	SerpinA6	SerpinA7	SerpinA9	SerpinA10	SerpinA11	SerpinA12
BBS	Hylids	*B. punctata*	100.0																									
		B. cinerascens	76.0	100.0																								
		H. phyllognathus	51.4	52.7	100.0																							
		A. leucopygius	51.0	52.3	52.3	100.0																						
		P. minuta	58.1	57.5	52.9	52.9	100.0																					
		S. lacteus	46.4	48.1	47.3	49.3	55.1	100.0																				
	Centrolenids	*N. posadae*	53.3	54.9	49.7	49.6	61.1	53.3	100.0																			
		E. prosoblepon	53.6	54.6	49.5	49.0	61.6	56.0	81.1	100.0																		
		C. mariaelenae	54.6	55.5	49.5	48.2	61.1	53.8	79.2	88.5	100.0																	
X. tropicalis Serpins		X. tr_Spn7	48.9	50.5	46.4	44.6	54.5	45.1	49.7	51.6	52.2	100.0																
		X. tr_Spn9	44.8	45.1	41.8	38.8	51.2	42.6	47.8	49.7	49.5	70.1	100.0															
		X. tr_Spn10	35.5	35.0	31.7	29.2	39.2	36.1	39.3	38.8	40.2	40.8	41.0	100.0														
		X. tr_Spn11	35.2	33.6	33.1	30.6	37.0	34.7	36.1	35.2	34.4	38.6	39.4	46.6	100.0													
		X. tr_Spn12	36.9	37.7	33.9	33.1	41.1	39.9	38.5	38.5	39.9	43.2	39.7	53.3	44.2	100.0												
		X. tr_Spn13	37.4	37.2	35.8	31.7	39.7	39.1	38.3	39.6	40.2	44.0	41.3	56.8	43.5	56.5	100.0											
		X. tr_Spn14	30.9	30.3	26.5	22.9	32.1	32.2	31.1	32.0	31.1	34.5	33.4	31.4	32.0	32.5	31.0	100.0										
Humans Clade A Serpins		SerpinA1	45.4	45.1	39.6	38.8	47.1	40.2	45.9	46.2	44.0	54.1	49.2	39.0	37.9	40.7	42.4	35.0	100.0									
		SerpinA2	36.1	35.5	34.7	30.9	38.9	35.5	37.7	39.6	38.0	43.5	39.4	33.9	32.8	36.0	35.9	31.4	59.3	100.0								
		SerpinA3	35.2	38.3	35.8	32.0	41.6	37.4	38.5	39.3	39.9	45.9	42.1	44.0	37.2	42.9	43.2	34.1	46.6	40.7	100.0							
		SerpinA4	35.5	35.2	36.1	30.6	40.0	37.2	39.1	38.3	39.6	45.9	44.0	41.3	39.1	42.7	40.5	31.4	45.8	40.9	47.2	100.0						
		SerpinA5	35.5	36.1	35.8	32.5	39.2	38.3	39.6	39.3	39.3	48.5	44.7	38.4	37.6	39.5	39.5	34.3	46.3	40.1	49.6	47.1	100.0					
		SerpinA6	35.8	36.3	34.4	32.5	39.2	32.8	37.7	35.5	34.2	43.9	41.4	39.2	36.5	39.8	38.4	31.9	43.6	39.2	48.8	45.5	42.5	100.0				
		SerpinA7	34.4	33.9	34.4	32.5	38.4	35.0	36.9	37.2	36.1	45.4	43.5	39.0	37.7	41.2	40.2	33.9	43.1	37.1	44.9	45.2	39.8	42.8	100.0			
		SerpinA9	32.1	32.1	33.2	28.8	36.5	33.9	33.2	33.2	33.9	43.1	38.0	38.7	35.4	39.8	40.5	33.2	40.5	37.6	46.4	48.9	47.4	42.7	50.7	100.0		
		SerpinA10	29.5	30.6	27.9	27.5	33.7	30.9	30.9	32.5	29.2	33.2	32.3	28.1	29.5	31.9	30.7	49.1	33.1	30.9	32.4	28.6	32.2	27.5	31.6	31.8	100.0	
		SerpinA11	34.4	31.7	32.0	29.8	37.0	31.7	34.7	37.7	38.3	42.7	41.6	36.2	32.3	39.1	37.0	29.8	45.0	39.8	43.4	46.1	43.3	40.6	44.2	45.6	26.5	100.0
		SerpinA12	37.2	36.1	33.1	34.2	38.1	31.4	37.4	38.0	37.7	40.6	42.2	33.2	37.9	33.5	34.3	32.4	41.7	31.6	36.8	34.3	39.2	34.3	37.3	32.8	30.8	36.2

Table S14. Quantification of BBSs abundances from chlorotic species and diverse Clade A serpins from *Xenopus tropicalis* (a non-chlorotic species), for two different alignment thresholds (60 or 80 bp).

Species	FPKM 80 alignment	FPKM 60 alignment
Aplastodiscus leucopygius	49,616.78	51,570.79
Boana cinerascens	53,013.59	53,945.13
Chimerella mariaelenae	37,119.08	37,530.07
Espadarana prosoblepon	46,825.08	47,195.34
Hyloscirtus phyllognathus	80,015.82	80,015.82
Nymphargus posadae	10,390.58	10,492.69
Pseudis minuta	11,051.49	11,325.35
Boana punctata	22,745.15	23,965.87
Sphaenorhynchus lacteus	100,046.30	104,455.82
Xp_spn7	102.32	4234.91
Xp_spn8	0.16	602.92
Xp_spn9	16.92	1252.81
Xp_spn10	3.72	274.55
Xp_spn11	0.00	1.43
Xp_spn12	2.48	55.10
Xp_spn13	1.61	364.30
Xp_spn14	5.07	118.30

Table S15. Quantification of Heme oxygenase 1 (HMOX1) from chlorotic and non-chlorotic species. The enzyme is responsible for the α biliverdin isomer formation. Expression of the HMOX-1 gene in chlorotic livers is normal compared to other non-chlorotic amphibians, which makes unlikely that increased hemolytic rates are responsible for biliverdin accumulation.

Species	Experiment code	FPKM 80 alignment	FPKM 60 alignment
Aplastodiscus leucopygius		8.94	9.10
Boana cinerascens		17.27	17.62
Chimererlla mariaelenae		18.43	19.24
Espadarana prosoblepon		150.11	153.25
Hyloscirtus phyllognathus		257.46	261.63
Nymphargus posadae		26.34	27.25
Pseudis minuta		26.89	28.51
Boana punctata		65.70	71.53
Sphaenorhynchus lacteus		2.21	2.26
Uperoleia mahonyi	SRR3901719	3.60	3.91
Ranoidea australis	SRR3901720	6.06	6.47
Litoria rubella	SRR3901722	5.62	5.98
Austrochaperina robusta	SRR3901723	8.61	9.29
Oreobates cruralis	SRR5507181	2.80	2.90
Xenopus tropicalis	SRR579561	1.82	104.38

SI References

51. I. Letunic, P. Bork, Interactive Tree Of Life (iTOL) v4: recent updates and new developments. *Nucleic Acids Res.* **47**, W256–W259 (2019).

52. J. Robert, J. Gantress, N. Cohen, G. D. Maniero, Xenopus as an experimental model for studying evolution of hsp--immune system interactions. *Methods* **32**, 42–53 (2004).

53. C. N. Pace, F. Vajdos, L. Fee, G. Grimsley, T. Gray, How to measure and predict the molar absorption coefficient of a protein. *Protein Sci.* **4**, 2411–2423 (1995).

54. D. Kessner, M. Chambers, R. Burke, D. Agus, P. Mallick, ProteoWizard: open source software for rapid proteomics tools development. *Bioinformatics* **24**, 2534–2536 (2008).

55. S. Tanaka *et al.*, Mass++: A Visualization and Analysis Tool for Mass Spectrometry. *J. Proteome Res.* **13**, 3846-3853 (2014).

56. O. Yeku, M. A. Frohman, "Rapid amplification of cDNA ends (RACE)" in *RNA: Methods in Molecular Biology (Methods and Protocols)*, H. Nielsen, Ed. (Humana Press, 2011), vol. 703, pp. 107–122

57. Y. G. Liu, N. Mitsukawa, T. Oosumi, R. F. Whittier, Efficient isolation and mapping of Arabidopsis thaliana T-DNA insert junctions by thermal asymmetric interlaced PCR. *Plant J.* **8**, 457–463 (1995).

58. Y. G. Liu, R. F. Whittier, Thermal asymmetric interlaced PCR: automatable amplification and sequencing of insert end fragments from P1 and YAC clones for chromosome walking. *Genomics* **25**, 674–681 (1995).

59. H. Barsnes, S. O. Mikalsen, I. Eidhammer, MassSorter: a tool for administrating and analyzing data from mass spectrometry experiments on proteins with known amino acid sequences. *BMC Bioinformatics* **7**, 42 (2006).

60. S. Moretti *et al.*, The M-Coffee web server: a meta-method for computing multiple sequence alignments by combining alternative alignment methods. *Nucleic Acids Res.* **35**, W645–W648, (2007).

61. I. M. Wallace, O. O'Sullivan, D. G. Higgins, C. Notredame, M-Coffee: combining multiple sequence alignment methods with T-Coffee. *Nucleic Acids Res.* **34**, 1692–1699, (2006).

62. F. Armougom *et al.*, Expresso: automatic incorporation of structural information in multiple sequence alignments using 3D-Coffee. *Nucleic Acids Res.* **34**, W604-608 (2006)

63. K. Okonechnikov, O. Golosova, M. Fursov, the UGENE team, Unipro UGENE: a unified bioinformatics toolkit. *Bioinformatics* **28**, 1166–1167 (2012).

64. X. Robert, P. Gouet, Deciphering key features in protein structures with the new ENDscript server. *Nucleic Acids Res.* **42**, W320–W324 (2014).

65. K. B. Chandler, P. Pompach, R. Goldman, N. Edwards, Exploring site-specific N-glycosylation microheterogeneity of haptoglobin using glycopeptide CID tandem mass spectra and glycan database search. *J. Proteome Res.* **12**, 3652–3666 (2013).

66. A. Savitzky, M. J. Golay, Smoothing and differentiation of data by simplified least squares procedures. *Anal. Chem.* **36**, 1627–1639 (1964).

67. N. Sreerama, R. W. Woody, Estimation of protein secondary structure from circular dichroism spectra: comparison of CONTIN, SELCON, and CDSSTR methods with an expanded reference set. *Anal. Biochem.* **287**, 252–260 (2000).

68. A. M Bolger, M. Lohse, B. Usadel, Trimmomatic: a flexible trimmer for Illumina sequence data. *Bioinformatics* **30**, 2114–2120 (2014).

69. Y. Xie *et al.*, SOAPdenovo-Trans: de novo transcriptome assembly with short RNA-Seq reads. *Bioinformatics* **30**, 1660-1666 (2014)

70. L. Fu, B. Niu, Z. Zhu, S. Wu, W. Li, CD-HIT: accelerated for clustering the next-generation sequencing data. *Bioinformatics* **28**, 3150–3152 (2012).

71. X. Huang, A. Madan, CAP3: A DNA sequence assembly program. *Genome Res.* **9**, 868–877 (1999).

72. X. J. Min, G. Butler, R. Storms, A. Tsang, A. OrfPredictor: predicting protein-coding regions in EST-derived sequences. *Nucleic Acids Res.* **33**, W677–W680 (2005).

73. R. Edwards, J. A. Edwards, fastq-pair: efficient synchronization of paired-end fastq files. *BioRxiv*, 552885 (2019).

74. A. Bankevich *et al.*, SPAdes: a new genome assembly algorithm and its applications to single-cell sequencing. *J. Comput. Biol.* **19**, 455-477 (2012)

75. A. E. Brunetti, G. N. Hermida, J. Faivovich, New insights into sexually dimorphic skin glands of anurans: the structure and ultrastructure of the mental and lateral glands in Hypsiboas punctatus (Amphibia: Anura: Hylidae). *J. Morphol.* **273**, 1257–1271, (2012).

76. D. Frost, Amphibian Species of the World: an Online Reference. Version 6.0 (October 1). Electronic Database accessible at

http://research.amnh.org/herpetology/amphibia/index.html. American Museum of Natural History, New York, USA.

77. D. M. Portik *et al.*, Sexual Dichromatism Drives Diversification within a Major Radiation of African Amphibians. *Syst. Biol.* syz023 (2019)

78. D. F. Cisneros-Heredia, R. W. Mcdiarmid, Revision of the characters of Centrolenidae (Amphibia: Anura: Athesphatanura), with comments on its taxonomy and the description of new taxa of glassfrogs. *Zootaxa* **1572**, 1–82 (2007).

79. J. M. Guayasamin *et al.*, Phylogenetic systematics of Glassfrogs (Amphibia: Centrolenidae) and their sister taxon *Allophryne ruthveni*. *Zootaxa* **2100**, 1–97 (2009).

80. P. A. Silverstone, A revision of the poison-arrow frogs of the genus *Phyllobates* Bibron in Sagra (Family Dendrobatidae). *Natural History* **27**, 1–53 (1976).

81. S. Castroviejo-Fisher *et al.*, Phylogenetic systematics of egg-brooding frogs (Anura: Hemiphractidae) and the evolution of direct development. *Zootaxa* **4004**, 1–75 (2015).

82. J. Faivovich *et al*., On the Monophyly and Relationships of Several Genera of Hylini (Anura: Hylidae: Hylinae), with Comments on Recent Taxonomic Changes in Hylids. *South Am. J. Herpetol.* **13**, 1–32 (2018).

83. J. Faivovich *et al.*, Systematic review of the frog family Hylidae, with special reference to Hylinae: phylogenetic analysis and taxonomic revision. *Bull. Am. Mus. Nat. Hist.* **294**, 1–240 (2005).

84. W. E. Duellman, A. B. Marion, S. B. Hedges, Phylogenetics, classification, and biogeography of the treefrogs (Amphibia: Anura: Arboranae). *Zootaxa* **4104**, 1–109 (2016).

85. F. J. M. Rojas-Runjaic, E. E. Infante-Rivero, P. E. Salerno, F. L. Meza-Joya, A new species of Hyloscirtus (Anura, Hylidae) from the Colombian and Venezuelan slopes of Sierra de Perijá, and the phylogenetic position of Hyloscirtus jahni (Rivero, 1961). *Zootaxa* **4382**, 121−146 (2018).

86. P. D. P. Pinheiro *et al.*, A new genus of Cophomantini, with comments on the taxonomic status of *Boana liliae* (Anura: Hylidae). *Zool. J. Linn. Soc.* **185,** 226–245 (2019).

87. F. Kraus, Taxonomy of *Litoria graminea* (Anura: Hylidae), with descriptions of two closely related new species. *Zootaxa* **4457**, 264–284 (2018).

88. R. C. Bell, R. C. Drewes, K. R. Zamudio, Reed frog diversification in the Gulf of Guinea: Overseas dispersal, the progression rule, and in situ speciation. *Evolution* **69**, 904–915 (2015).

89. D. R. Frost *et al.*, The amphibian tree of life. *Bull. Am. Mus. Nat. Hist.* **2006**, 1–291 (2006).

90. M. J. Tyler, The occurrence of bone pigmentation in Australian frogs. *Search* **1**, 75 (1970).

91. R. Knowles, M. Mahony, J. Armstrong, S. C. Donnellan, Systematics of sphagnum frogs of the genus *Philoria* in eastern Australia, with the description of two new species. *Rec. Aust. Mus.* **56**, 57–74 (2004).

92. R. A. Pyron, Temperate extinction in squamate reptiles and the roots of latitudinal diversity gradients. *Glob. Ecol. Biogeogr.* **23**, 1126–1134 (2014).

93. C. R. Hutter, S. M. Lambert, Z. F. Andriampenomanana, F. Glaw, M. Vences, Molecular phylogeny and diversification of Malagasy bright-eyed tree frogs (Mantellidae: Boophis). *Mol. Phylogenet. Evol.* **127**, 568–578, (2018).

94. M. C. Bletz *et al.*, Stumbling upon a New Frog Species of *Guibemantis* (Anura: Mantellidae) on Top of the Marojejy Massif in Northern Madagascar. *Copeia* **106**, 255–263, 259 (2018).

95. K. C. Wollenberg, D. R. Vieites, F. Glaw, M. Vences, Speciation in little: the role of range and body size in the diversification of Malagasy mantellid frogs. *BMC evolutionary biology* **11**, 217 (2011).

96. R. A. Pyron, J. J. Wiens, A large-scale phylogeny of Amphibia including over 2800 species, and a revised classification of extant frogs, salamanders, and caecilians. *Mol. Phylogenenetics Evol.* **61**, 543–583 (2011).

97. A. Haas *et al.*, An updated checklist of the amphibian diversity of Maliau Basin Conservation Area, Sabah, Malaysia. *Evol. Syst.* **2**, 89–114 (2018).

98. U. Arifin *et al.*, Phylogenetic relationships within the genus Staurois (Anura, Ranidae) based on 16S rRNA sequences. *Zootaxa* **2744**, 39–52 (2011).

99. C. K. Onn, R. K. Abraham, J. L. Grismer, L. L. Grismer, Elevational size variation and two new species of torrent frogs from Peninsular Malaysia (Anura: Ranidae: Amolops Cope). *Zootaxa* **4434**, 250–264 (2018).

100. D. Jiang, K. Jiang, J. Ren, J. Wu, J. Li, Resurrection of the genus *Leptomantis*, with description of a new genus to the family Rhacophoridae (Amphibia: Anura). *Asian Herpetol. Res.* **10**, 1–12 (2019).

101. J. J. Rowley, Q. Dau, T. T. Nguyen, T. T. Cao, S. Nguyen, A new species of *Gracixalus* (Anura: Rhacophoridae) with a hyperextended vocal repertoire from Vietnam. *Zootaxa* **3125**, 22–38 (2011).

102. D. P. Demarque, A. E. Crotti, R. Vessecchi, J. L. Lopes, N. P Lopes, Fragmentation reactions using electrospray ionization mass spectrometry: an important tool for the structural elucidation and characterization of synthetic and natural products. *Nat. Prod. Rep.* **33**, 432–455 (2016).

103. P. P. de Abreu Manso, L. de Brito-Gitirana, M. Pelajo-Machado, Localization of hematopoietic cells in the bullfrog (*Lithobates catesbeianus*). *Cell Tissue Res.* **337**, 301–312, (2009).

104. G. M. Maniatis, V. M. Ingram, Erythropoiesis during amphibian metamorphosis: I. Site of Maturation of Erythrocytes in *Rana catesbeiana*. *J. Cell Biol.* **49**, 372–379, (1971).

105. N. L. Barbosa-Morais *et al.*, The evolutionary landscape of alternative splicing in vertebrate species. *Science* **338**, 1587–1593 (2012).

106. R. Lester, R. Schmid, Bile pigment excretion in amphibia. *Nature* **190**, 452 (1961).

107. K. D. Cole, Bile Pigment Metabolism During Anuran Metamorphosis. (Texas Tech University, Lubbock, Texas, US) (1981)

108. M. R. Redshaw, B. K. Follet, G. J. Lawes, Biliverdin: A component of yolk proteins in *Xenopus laevis*. *Int. J. Biochem.* **2**, 80–84 (1971).

109. G. V. Marinetti, J. T. Bagnara, Characterization of blue and yellow pigments in eggs of the Mexican leaf frog. *Biochemistry* **22**, 5651–5655 (1983).

110. A. Sorokin, E. Steigerwald, Evidence for parental care in *Feihyla kajau* (Anura: Rhacophoridae). *Phyllomedusa* **17**, 127–130 (2018).

111. M. D. Kusrini, M. I. Lubis, B. Darmawan, L. N. Rahman, Morphological and ecological observations on *Chiromantis vittiger* (Anura: Rhacophoridae) in mount Halimun - Salak National Park, Indonesia. *Treubia* **44,** 47–66 (2018).

112. P. A. Schwalm, J. A. McNulty, The morphology of dermal chromatophores in the infrared-reflecting glass-frog *Centrolenella fleischmanni*. *J. Morphol.* **163**, 37–44 (1980).

113. J. T. Bagnara, P. J. Fernandez, R. Fujii, On the blue coloration of vertebrates. *Pigment Cell Res* **20**, 14–26 (2007).

114. J. Hill *et al.*, Recurrent convergent evolution at amino acid residue 261 in fish rhodopsin. *Proceedings of the National Academy of Sciences* **116**, 18473–18478 (2019).

115. Y. Zhen, M. L. Aardema, E. M. Medina, M. Schumer, P. Andolfatto, Parallel molecular evolution in an herbivore community. *Science* **337**, 1634–1637 (2012).

116. S. Dobler, S. Dalla, V. Wagschal, A. A. Agrawal, Community-wide convergent evolution in insect adaptation to toxic cardenolides by substitutions in the Na, K-ATPase. *Proceedings of the National Academy of Sciences* **109**, 13040–13045 (2012).

117. C. Rey *et al.*, Detecting adaptive convergent amino acid evolution. *Philosophical Transactions of the Royal Society B* **374**, 20180234 (2019).

118. H. E. Hoekstra, R. J. Hirschmann, R. A. Bundey, P. A. Insel, J. P. Crossland, A single amino acid mutation contributes to adaptive beach mouse color pattern. *Science* **313**, 101–104 (2006).

119. G. Vashchenko *et al.*, Identification of avian corticosteroid-binding globulin (SerpinA6) reveals the molecular basis of evolutionary adaptations in SerpinA6 structure and function as a steroid-binding protein. *J. Biol. Chem.* **291**, 11300–11312 (2016).

120. C. Heit *et al.*, Update of the human and mouse SERPIN gene superfamily. *Hum Genomics* **7**, 22 (2013).

121. L. J. Holland *et al.*, A major estrogen-regulated protein secreted from the liver of Xenopus laevis is a member of the serpin superfamily. Nucleotide sequence of cDNA and hormonal induction of mRNA. *Journal of Biological Chemistry* **267**, 7053–7059 (1992).

122. J. Wu *et al.*, Proteomic analysis of skin defensive factors of tree frog Hyla simplex. *J. Proteome Res.* **10**, 4230–4240 (2011).

123. P. A. Schwalm, J. A. McNulty, The morphology of dermal chromatophores in the infrared-reflecting glass-frog Centrolenella fleischmanni. *J Morphol* **163**, 37–44 (1980).

124. D. Kolarich *et al.*, Biochemical, molecular characterization, and glycoproteomic analyses of alpha(1)-proteinase inhibitor products used for replacement therapy. *Transfusion* **46**, 1959–1977 (2006).

125. Y. Zhu, D. Nikolic, R. B. Van Breemen, R. B. Silverman, Mechanism of inactivation of inducible nitric oxide synthase by amidines. Irreversible enzyme inactivation without inactivator modification. *J. Am. Chem. Soc.* **127**, 858–868, (2005).

126. T. Schechter, On the size of the acitive site in proteases. I. Papain. *Biochem. Biophys. Res. Commun.* **27**, 157–162 (1967).

127. Whisstock, J. C., Skinner, R., Carrell, R. W. & Lesk, A. M. Conformational changes in serpins: I. The native and cleaved conformations of α1-antitrypsin. *J. Mol. Biol.* **295**, 651–665 (2000).

128. E. F. Pettersen *et al.*, UCSF Chimera—a visualization system for exploratory research and analysis. *J. Comput. Chem.* **25**, 1605–1612 (2004)

129. M. Al-Ayyoubi, P. G. Gettins, K. Volz, Crystal Structure of Human Maspin, a Serpin with Antitumor Properties. *J. Biol. Chem.* **279**, 55540–55544 (2004).

130. V. Gvoždík, F. Tillack, M. Menegon, S. P. Loader, The status of *Leptopelis barbouri* Ahl, 1929 and eleven other nomina of the current tree-frog genus *Leptopelis* (Arthroleptidae) described from East Africa, with a redescription of *Leptopelis grandiceps* Ahl, 1929. *Zootaxa* **3793**, 165–187 (2014).

131. C. E. Roelke, E. Greenbaum, C. Kusamba, M. M. Aristote, E. N. Smith, Systematics and Conservation Status of Two Distinct Albertine Rift Treefrogs, *Leptopelis karissitnbensis* and *Leptopelis kivuensis* (Anura: Arthroleptidae). *J. Herpetol.* **45**, 343–351 (2011).

132. E. Twomey, J. Delia, S. Castroviejo-Fisher, A review of Northern Peruvian glassfrogs (Centrolenidae), with the description of four new remarkable species. *Zootaxa* **3851**, 1–87 (2014).

133. A. Catenazzi, R. Von May, E. Lehr, G. Gagliardi-Urrutia, J. M. Guayasamin, A new, high-elevation glassfrog (Anura: Centrolenidae) from Manu National Park, southern Peru. *Zootaxa* **3388**, 56–68 (2012).

134. S. Castroviejo-Fisher, C. Vila, J. Ayarzagueena, M. Blanc, R. Ernst, Species diversity of *Hyalinobatrachium* glassfrogs (Amphibia: Centrolenidae) from the Guiana Shield, with the description of two new species. *Zootaxa* **3132**, 1–55 (2011).

135. S. Castroviejo-Fisher, J. Moravec, J. Aparicio, M. Guerrero-Reinhard, G. Calderon, DNA taxonomy reveals two new species records of *Hyalinobatrachium* (Anura: Centrolenidae) for Bolivia. *Zootaxa* **2798**, 64–68 (2011).

136. B. Kubicki, *Glass frogs of Costa Rica*. (INBio, Santo Domingo de Heredia, Santo Domingo, Costa Rica, 2007).

137. Kubicki, B., Salazar, S. & Puschendorf, R. A new species of glassfrog, genus Hyalinobatrachium (Anura: Centrolenidae), from the Caribbean foothills of Costa Rica. *Zootaxa* **3920**, 69–84 (2015).

138. E. A. de Oliveira, E. J. Hernández-Ruz, New species of glassfrog, genus *Hyalinobatrachium* (Anura: Centrolenidae), for the Brazilian Amazon revealed by mitochondrial DNA and morphology. *Int. J. Res. Stud. Biosci.* **5**, 1–12 (2017).

139. S. Castroviejo-Fisher, J. Ayarzaguena, C. Vila, A new species of *Hyalinobatrachium* (Centrolenidae: Anura) from Serrania de Perijá, Venezuela. *Zootaxa*, 51–62 (2007).

140. J. M. Guayasamin *et al.*, A marvelous new glassfrog (Centrolenidae, *Hyalinobatrachium*) from Amazonian Ecuador. *ZooKeys*, 1 (2017).

141. Rada, M., Ospina-Sarria, J. J. & Guayasamin, J. M. A Taxonomic Review of Tan-Brown Glassfrogs (Anura: Centrolenidae), with the Description of a New Species from Southwestern Colombia. *South Am. J. Herpetol.* **12**, 136–156, 121 (2017).

142. C. R. Hutter, J. M. Guayasamin, A new cryptic species of glassfrog (Centrolenidae: *Nymphargus*) from Reserva Las Gralarias, Ecuador. *Zootaxa* **3257**, 1–21 (2012).

143. R. Pontes, U. Caramaschi, J. P. Pombal Jr, A remarkable new glass frog (Centrolenidae: *Vitreorana*) from the northeast Atlantic forest, Brazil. *Herpetologica* **70**, 298–308 (2014).

144. D. J. Santana, A. B. Barros, R. Pontes, R. N. Feio, A new species of Glassfrog genus *Vitreorana* (Anura, Centrolenidae) from the Cerrado Domain, southeastern Brazil. *Herpetologica* **71**, 289–298 (2015).

145. C. F. B. Haddad, L. F. Toledo, C. P. A. Prado, D. Loebmann, J. L. Gasparini, I. Sazima, Guia dos anfíbios da Mata Atlântica: diversidade e biologia. (Anolis Books, São Paulo, Brazil, 2013).

146. W. E. Duellman, L. Trueb, Marsupial frogs: *Gastrotheca* and allied genera. (JHU Press, Baltimore, MD, 2015).

147. O. Rojas Padilla, E. J. Ríos Alva, G. Gagliardi Urrutia, First records of *Gastrotheca longipes* (Boulenger, 1882), *Cochranella resplendens* (Lynch and Duellman, 1973) and *Teratohyla midas* (Lynch and Duellman, 1973) for the Allpahuayo-Mishana National Reserve, Peru, with comments on their distribution in the Amazon basin. *Herpetol. Notes* **12**, 461–472 (2019).

148. J. P. Monteiro, T. H. Condez, L. R. Malagoli, E. C. De Nardin, C. F. B. Haddad, The marsupial frog *Gastrotheca microdiscus* (Anura: Hemiphractidae) in South Brazil:

distribution, natural history, advertisement call and molecular genetics. *Salamandra* **55**, 48–53 (2019).

149. F. Kraus, A. Allison, Two New Treefrogs from Normanby Island, Papua New Guinea. *J. Herpetol.* **38**, 197–207 (2004).

150. M. J. Tyler, Papuan hylid frogs of the genus *Hyla*. *Zoöl. Verh.* **96**, 1–203 (1968).

151. J. Menzies, *The frogs of New Guinea and the Solomon Islands*. (Pensoft Publishers, Sofia, Bulgaria, 2006).

152. G. A. Boulenger, On the Reptiles and Batrachians of the Solomon Islands. *Trans. Zool. Soc. Lond.* **12**, 3562 (1886).

153. R. Günther, S. Richards, A new species of the *Litoria gracilenta* group from Irian Jaya (Anura: Hylidae). *Herpetozoa* **13**, 27–43 (2000).

154. J. Faivovich, R. W. Mcdiarmid, C. W. Myers, Two new species of *Myersiohyla* (Anura: Hylidae) from Cerro de la Neblina, Venezuela, with comments on other species of the genus. *Am. Mus. novit.* **2013**, 1–63 (2013).

155. P. Kok, A new species of *Hypsiboas* (Amphibia: Anura: Hylidae) from Kaieteur National Park, eastern edge of the Pakaraima Mountains, Guyana. *Bull. -Inst. R. Sci. Nat. Bel., Biol.* **76**, 191–200 (2006).

156. B. Lutz, Anfíbios Anuros da coleção Adolpho Lutz: III-Hyla claresignata Lutz & B. Lutz, 1939. *Mem. Inst. Oswaldo Cruz* **46**, 747–757 (1948).

157. B. V. M. Berneck, C. F. B. Haddad, M. L. Lyra, C. A. G. Cruz, J. Faivovich, The Green Clade grows: A phylogenetic analysis of Aplastodiscus (Anura; Hylidae). *Mol. Phylogenet. Evol.* **97**, 213–223 (2016).

158. W. E. Duellman, A review of the Neotropical frogs of the Hyla bogotensis group. *Occas. Pap. Mus. Nat. Hist. Univ. of Kansas* **11**, 1–31 (1972).

159. J. M. Guayasamin *et al.* , Molecular phylogeny of stream treefrogs (Hylidae: *Hyloscirtus bogotensis* Group), with a new species from the Andes of Ecuador. *Neotropical Biodiversity* **1**, 2–21 (2015).

160. J. Faivovich, J. Moravec, D. F. Cisneros-Heredia, J. Köhler, A new species of the *Hypsiboas benitezi* group from the western Amazon basin (Amphibia: Anura: Hylidae). *Herpetologica* **62**, 96–108 (2006).

161. W. E. Duellman, New species of hylid frogs from the Andes of Colombia and Venezuela. *Occas. Pap. Mus. Nat. Hist. Univ. Kansas* **131**, 1–12 (1989).

162. S. Lötters, S. Reichle, J. Faivovich, R. H. Bain, The stream-dwelling tadpole of *Hyloscirtus charazani* (Anura: Hylidae) from Andean Bolivia. *Stud. Neotrop. Environ.* **40**, 181–185 (2005).

163. W. E. Duellman, The hylid frogs of Middle America. *Monogr. Mus. Nat. Hist., Univ. Kansas* **1–2**, 1–753 (1970).

164. E. La Marca, Systematics and ecological observations on the Neotropical frogs *Hyla jahni* and *Hyla platydactyla*. *J. Herpetol.* **19**, 227–237 (1985).

165. W. E. Duellman, R. Altig, New species of tree frogs (family Hylidae) from the Andes of Colombia and Ecuador. *Herpetologica* **34**, 177–185 (1978).

166. R. P. Reynolds, M. S. Foster, Four new species of frogs and one new species of snake from the Chapare region of Bolivia, with notes on other species. *Herpetol. Monogr.* **6**, 83–104 (1992).

167. W. C. A. Bokermann, Dos nuevas especies de *Hyla* de Minas Gerais y notas sobre *Hyla alvarengai* bok (Amphibia, Salientia, Hylidae). *Neotropica* **10**, 67–76 (1964).

168. U. Caramaschi, A. Velosa, Nova espécie de *Hyla* Laurenti, 1768 do leste brasileiro (Amphibia, Anura, Hylidae). *Bol. Mus. Nac., Nova Sér., Zool.* (1996).

169. M. S. Hoogmoed, Resurrection of *Hyla ornatissima* Noble (Amphibia, Hylidae) and remarks on related species of green tree frogs from the Guiana area: notes on the herpetofauna of Surinam VI. *Zoöl. Verh.* **172**, 1–46 (1979).

170. W. Pyburn, The voice and relationships of the treefrog *Hyla hobbsi* (Anura: Hylidae). *Proc. Biol. Soc. Wash.* **91**, 123–131 (1978).

171. W. E. Duellman, The identities of some Ecuadorian hylid frogs. *Herpetologica* **27**, 212–227 (1971).

172. F. Maffei, F. Ubaid, J. Jim, *Anfíbios da Fazenda Rio Claro, Lençóis Paulista, SP, Brasil*. (Canal 6, Bauru, SP, Brazil, 2011).

173. M. A. Caminer, S. R. Ron, Systematics of treefrogs of the *Hypsiboas calcaratus* and *Hypsiboas fasciatus* species complex (Anura, Hylidae) with the description of four new species. *Zookeys* **370**, 1 (2014).

174. P. D. P. Pinheiro *et al.*, A New Species of the *Hypsiboas pulchellus* Group from the Serra da Mantiqueira, Southeastern Brazil (Amphibia: Anura: Hylidae). *Herpetologica* **72**, 256–270 (2016).

175. B. Lutz, A. Lutz, *Brazilian species of Hyla*. (University of Texas Press, 1973).

176. A. P. Antunes, J. Faivovich, C. F. B. Haddad, A new species of *Hypsiboas* from the Atlantic forest of Southeastern Brazil (Amphibia: Anura: Hylidae). *Copeia* **2008**, 179–190 (2008).

177. W. E. Duellman, I. de la Riva, E. R. Wild, Frogs of the *Hyla arntata* and *Hyla pulchella* Groups in the Andes of South America, with Definitions and Analyses of Phylogenetic Relationships of Andean Groups of *Hyla*. *Sci. Pap. Nat. Hist. Mus. Univ. Kansas* **3**, 1–41 (1997).

178. J. Faivovich, La larva de *Hyla semiguttata* A. Lutz, 1925 (Anura: hylidae). *Cuad. Herpetol.* **9,** 61–67 (1996).

179. P. C. A. Garcia, J. Faivovich, C. F. B. Haddad, Redescription of *Hypsiboas semiguttatus*, with the description of a new species of the Hypsiboas pulchellus group. *Copeia* **2007**, 933–949 (2007).

180. P. C. A. Garcia, C. F. B. Haddad, Vocalizations and comments on the relationships of *Hypsiboas ericae* (Amphibia, Hylidae). *Iheringia, Sér. Zool.* **98**, 161–166 (2008).

181. A. Kwet, R. Lingnau, M. Di-Bernardo, *Pró-Mata: Anfíbios da Serra Gaúcha, sul do Brasil – Amphibien der Serra Gaúcha, Südbrasilien – Amphibians of the Serra Gaúcha, South of Brazil.* (Brasilien-Zentrum der Universität Tübingen, 2010).

182. P. C. A. Garcia, G. Vinciprova, C. F. B. Haddad, The taxonomic status of the *Hyla pulchella* joaquini B. Lutz, 1968 (Anura, Hylidae, Hylinae). *Herpetologica* **59**, 350–363 (2003).

183. P. C. A. Garcia, G. Vinciprova, C. F. B. Haddad, Vocalização, girino, distribuição geográfica e novos comentários sobre *Hyla marginata* Boulenger, 1887 (Anura, Hylidae, Hylinae). *Bol. Mus. Nac., Nova Sér., Zool.* **460**, 1–19 (2001).

184. P. C. A. Garcia, O. L. Peixoto,C. F. B. Haddad, C. F. A new species of *Hypsiboas* (Anura: Hylidae) from the Atlantic Forest of Santa Catarina, Southern Brazil, with comments on its conservation status. *South Am. J. Herpetol.* **3**, 27–36 (2008).

185. U. Caramaschi, M. T. Rodrigues, A new large treefrog species, genus *Hyla Laurenti*, 1768, from southern Bahia, Brazil (Amphibia, Anura, Hylidae). *Arq. Mus. Nac.* **61**, 255–260 (2003).

186. I. de la Riva, J. Köhler, S. Lötters, S. Reichle, Ten years of research on Bolivian amphibians: updated checklist, distribution, taxonomic problems, literature and iconography. *Rev. Esp. Herpetol.* **14**, 19–164 (2000).

187. C. L. Barrio-Amoros, A. Díaz, J. J. Mueses-Cisneros, E. Infante, A. Chacon, *Hyla vigilans* Solano, 1971, a second species for the genus *Scarthyla*, redescription and distribution in Venezuela and Colombia. *Zootaxa* **1349**, 1–18 (2006).

188. H. W. Parker, The frogs, lizards, and snakes of British Guiana. *Proc. Zool. Soc. Lond.* **105**, 505–530 (1935)

189. A. A. Garda, D. J. Santana, V. D. A. São-Pedro, Taxonomic characterization of Paradoxical frogs (Anura, Hylidae, Pseudae): geographic distribution, external morphology, and morphometry. *Zootaxa* **2666**, 1–28 (2010).

190. A. Lutz, B. Lutz, On *Hyla aurantiaca* Daudin and Sphoenorhynchus Tschudi and on two allied Hylae from south-eastern Brasil. *An. Acad. Bras. Ciênc.* **10**, 175–194 (1938).

191. U. Caramaschi, A. Almeida, J. L. Gasparini, Description of two new species of *Sphaenorhynchus* (Anura, Hylidae) from the state of Espírito Santo, Southeastern Brazil. *Zootaxa* **2115**, 34–46 (2009).

192. W. C. A. Bokermann, Una nueva especie de *Trachycephalus* de Bahia, Brasil (Amphibia, Hylidae). *Neotropica* **12**, 120–124 (1966).

193. C. J. Goin, Status of the prog genus *Sphoenohyla* with a synopsis of the species. *Caldasia* **8**, 11–31 (1957).

194. L. F. Toledo, P. C. A. Garcia, R. Lingnau, C. F. B. Haddad, A new species of *Sphaenorhynchus* (Anura; Hylidae) from Brazil. *Zootaxa* **1658**, 57–68 (2007).

195. K. Araujo-Vieira, A. Tacioli, J. Faivovich, V. G. D. Orrico, T. Grant, T. The tadpole of *Sphaenorhynchus* caramaschii, with comments on larval morphology of *Sphaenorhynchus* (Anura: Hylidae). *Zootaxa* **3904**, 270–282 (2015).

196. A. R. Acosta-Galvis, Una nueva rana de huesos verdes del género *Scinax* (Anura: Hylidae) asociada a los bosques subandinos de la cuenca del río Magdalena, Colombia. *Biota colombiana* **19**, 131–159 (2018).

197. B. Lutz, Anfíbios anuros do distrito federal. *Mem. Inst. Oswaldo Cruz* **52**, 155–197 (1954).

198. D. M. Cochran, Frogs of southeastern Brazil. *Bull. U. S. Natl. Mus.* **206**, 1–423(1955).

199. J. Lescure, C. Marty, *Atlas des amphibiens de Guyane*. (Les publications scientifiques du Muséum National d'Histoire Naturelle, 2000).

200. M. Gordo *et al.*, A New Species of Milk Frog of the Genus *Trachycephalus* Tschudi (Anura, Hylidae) from the Amazonian Rainforest. *Herpetologica* **69**, 466–479 (2013).

201. S. R. Ron, P. J. Venegas, H. M. Ortega-Andrade, G. Gagliardi-Urrutia, P. E. Salerno, Systematics of *Ecnomiohyla tuberculosa* with the description of a new species and comments on the taxonomy of *Trachycephalus typhonius* (Anura, Hylidae). *Zookeys* **630**, 115–154 (2016).

202. A. Kwet, M. Sole, A new species of *Trachycephalus* (Anura: Hylidae) from the Atlantic Rain Forest in southern Brazil. *Zootaxa* **1947**, 53–67 (2008).

203. W. G. Lynn, Some Amphibians from Haiti and a New Subspecies of *Eleutherodactylus schmidti*. *Herpetologica* **14**, 153–157 (1958).

204. E. R. Dunn, The frogs of Jamaica. *Proc. Boston Soc. Nat. Hist.* **38**, 11–130 (1926).

205. K. H. Jungfer, The taxonomic status of some spiny-backed treefrogs, genus *Osteocephalus* (Amphibia: Anura: Hylidae). *Zootaxa* **2407**, 28–50 (2010).

206. S. R. Ron *et al.*, Systematics of the *Osteocephalus buckleyi* species complex (Anura, Hylidae) from Ecuador and Peru. *Zookeys* **229**, 1–52 (2012).

207. J. Moravec *et al.*, A new species of *Osteocephalus* (Anura: Hylidae) from Amazonian Bolivia: first evidence of tree frog breeding in fruit capsules of the Brazilian nut tree. *Zootaxa* **2215**, 37–54 (2009).

208. K. H. Jungfer, S. R. Ron, R. Seipp, A. Almendáriz, Two new species of hylid frogs, genus *Osteocephalus*, from Amazonian Ecuador. *Amphibia-Reptilia* **21**, 327–340 (2000).

209. K. H. Jungfer, E. A. Lehr, New Species of *Osteocephalus* with Bicoloured Iris from Pozuzo (Peru: Departamento de Pasco)(Amphibia: Anura: Hylidae). *Zool. Abh.* **51**, 321–329 (2001).

210. K. H. Jungfer, W. Hödl, A new species of *Osteocephalus* from Ecuador and a redescription of *O. leprieurii* (Duméril & Bibron, 1841)(Anura: Hylidae). *Amphibia-Reptilia* **23**, 21–46 (2002).

211. K. H. Jungfer, L. C. Schiesari, Description of a central Amazonian and Guianan tree frog, genus *Osteocephalus* (Anura, Hylidae), with oophagous tadpoles. *Alytes* **13**, 1–13 (1995).

212. M. A. Donnelly, C. W. Myers, Herpetological results of the 1990 Venezuelan expedition to the summit of Cerro Guaiquinima, with new tepui reptiles. *Am. Mus. Novit.* **3017**, 54 pp (1991).

213. U. Caramaschi, H. R. da Silva, M. C. de Britto-Pereira, A new species of *Phyllodytes* (Anura, Hylidae) from southern Bahia, Brazil. *Copeia* **1992**, 187–191 (1992).

214. O. L. Peixoto, C. A. G. Cruz, Descrição de duas espécies novas do gênero *Phyllodytes* Wagler (Amphibia, Anura, Hylidae). *Rev. Bras. Biol.* **48**, 265–272 (1988).

215. E. N. Smith, B. P. Noonan, A new species of *Osteocephalus* (Anura: Hylidae) from Guyana. *Rev. Biol. Tropical* **49**, 347–357 (2001).

216. J. -L. Amiet, *Les Rainettes du Cameroun:(Amphibiens Anoures)* (La Nef des Livres, Saint-Nazaire, France, 2012)

217. A. Channing *et al.*, Taxonomy of the super-cryptic *Hyperolius nasutus* group of long reed frogs of Africa (Anura: Hyperoliidae), with descriptions of six new species. *Zootaxa* **3620**, 301–350 (2013).

218. E. B. Harper, G. J. Measey, D. A. Patrick, M. Menegon, J. R. Vonesh, I. Swilla, *Field guide to the amphibians of the Eastern Arc Mountains and Coastal Forests of Tanzania and Kenya* (Camerapix Publishers International, Nairobi, Kenya, 2010).

219. L. Du Preez, *A complete guide to the frogs of southern Africa* (Penguin Random House, South Africa, 2015).

220. L. Du Preez, V. Carruthers, A Complete Guide to the Frogs of Southern Africa (Struik Nature, Cape Town, South Africa, 2009).

221. D. Portik *et al.*, A survey of amphibians and reptiles in the foothills of Mount Kupe, Cameroon. *Amphib. Reptile Conserv.* **10**, 37–67 (2016).

222. S. P. Loader, L. P. Lawson, D. M. Portik, M. Menegon, Three new species of spiny throated reed frogs (Anura: Hyperoliidae) from evergreen forests of Tanzania. *BMC Res. Notes* **8**, 167 (2015).

223. E. Greenbaum, U. Sinsch, E. Lehr, F. Valdez, C. Kusamba, Phylogeography of the reed frog Hyperolius castaneus (Anura: Hyperoliidae) from the Albertine Rift of Central Africa: Implications for taxonomy, biogeography and conservation. *Zootaxa* **3731**, 473–494 (2013).

224. E. G. Boulenger, On two new tree-frogs from Sierra Leone, recently living in the Society's Gardens. *Proc. Zool. Soc. London* **1915**, 243 (1915)

225. H. C. Liedtke *et al*., One or two species? On the case of Hyperolius discodactylus Ahl, 1931 and H. alticola Ahl, 1931 (Anura: Hyperoliidae). *Zootaxa* **3768**, 253–290 (2014).

226. R. C. Bell, A New Species of *Hyperolius* (Amphibia: Hyperoliidae) from Príncipe Island, Democratic Republic of São Tomé and Príncipe. *Herpetologica* **72**, 343–351 (2016).

227. A. Schiøtz, *Treefrogs of Africa* (Chimaira, Frankfurt, 1999).

228. J. M. Dehling, An African glass frog: A new *Hyperolius* species (Anura: Hyperoliidae) from Nyungwe national park, southern Rwanda. *Zootaxa* **3391**, 52–64 (2012).

229. M. Dewynter, T. Frétey, Liste taxonomique commentée et catalogue illustré des Amphibiens du Gabon. *Les cahiers de la fondation Biotope* **27**, 2–84 (2019).

230. E. Greenbaum, C. Kusamba, Conservation implications following the rediscovery of four frog species from the Itombwe Natural Reserve, eastern Democratic Republic of the Congo. *Herpetol. Rev.* **43**, 253–259 (2012).

231. M. -O. Rödel, J. Glos, Herpetological surveys in two proposed protected areas in Liberia, West Africa. *Zoosystematics Evol.* **95**, 15 (2019).

232. F. Glaw, M. Vences, *A field guide to the amphibians and reptiles of Madagascar* (Vences & Glaw Verlags GbR, Köln, Germany, ed. 3, 2007)

233. R. Blommers-Schlösser, Biosystematics of the malagasy frogs. II. The genus *Boophis* (Rhacophoridae). *Bijdragen tot de Dierkunde* **49**, 261–312 (1979).

234. F. Glaw, J. Köhler, I. de la Riva, D. R. Vieites, M. Vences, Integrative taxonomy of Malagasy treefrogs: combination of molecular genetics, bioacoustics and comparative morphology reveals twelve additional species of *Boophis*. *Zootaxa* **2383**, 1–82 (2010).

235. C. R. Hutter, S. M. Lambert, K. A. Cobb, Z. F. Andriampenomanana, M. Vences, A new species of bright-eyed treefrog (Mantellidae) from Madagascar, with comments on call evolution and patterns of syntopy in the *Boophis ankaratra* complex. *Zootaxa* **4034**, 531–555 (2015).

236. S. G. Penny *et al.,* A new species of the Boophis rappiodes group (Anura, Mantellidae) from the Sahamalaza Peninsula, northwest Madagascar, with acoustic monitoring of its nocturnal calling activity. *ZooKeys* **435**, 111–132 (2014).

237. J. Köhler, F. Glaw, M. Vences, Two additional treefrogs of the Boophis ulftunni species group (Anura: Mantellidae) discovered in rainforests of northern and south-eastern Madagascar. *Zootaxa* **1814**, 37–48 (2008).

238. K. Wollenberg, F. Andreone, F. Glaw, M. Vences, Pretty in pink: a new treefrog species of the genus *Boophis* from north-eastern Madagascar. *Zootaxa* **1684**, 58–68 (2008).

239. R. M. Lehtinen, F. Glaw, F. Andreone, M. Pabijan, M. Vences, A new species of putatively pond breeding frog of the genus *Guibemantis* from southeastern Madagascar. *Copeia* **2012**, 648–662 (2012).

240. F. Andreone, F. Glaw, M. Vences, D. Vallan, A new *Mantidactylus* from south-eastern Madagascar, with a review of *Mantidactylus peraccae* (Ranidae: Mantellinae). *Herpetological Journal* **8**, 149–160 (1998).

241. R. K. Abraham, R. A. Pyron, B. Ansil, A. Zachariah, A. Zachariah, Two novel genera and one new species of treefrog (Anura: Rhacophoridae) highlight cryptic diversity in the Western Ghats of India. *Zootaxa* **3640**, 177–189 (2013).

242. L. Lee Grismer, N. Thy, T. Chav, J. Holden, A new species of *Chiromantis* Peters 1854 (Anura: Rhacophoridae) from Phnom Samkos in the northwestern Cardamom Mountains, Cambodia. *Herpetologica* **63,** 392–400 (2007).

243. R. H. Bain, N. Q. Truong, Herpetofaunal diversity of Ha Giang Province in northeastern Vietnam, with descriptions of two new species. *Am. Mus. Novit.* **2004**, 1–42 (2004).

244. S. Biju *et al*., Taxonomic review of the tree frog genus *Rhacophorus* from the Western Ghats, India (Anura: Rhacophoridae), with description of ontogenetic colour changes and reproductive behaviour. *Zootaxa* **3636**, 257–289 (2013).

245. M. B. Harvey, A. J. Pemberton, E. N. Smith, New and poorly known parachuting frogs (Rhacophoridae: *Rhacophorus*) from Sumatra and Java. *Herpetol. Monogr.* **16**, 46–92 (2002).

246. R. F. Inger, R. B. Stuebing, *A field guide to the frogs of Borneo* (Natural History Publications, Kota Kinabalu, Borneo, 1997)

247. B. L. Blotto, M.L. Lyra, M.C.S. Cardoso, M.T. Rodrigues, I. Ribeiro Dias, E. Marciano-Jr., F. Dal Vechio, V.G.D. Orrico, R. A. Brandão, C. L. Assis, A. S. F Lantyer-Silva, M. G. Rutherford, G. Gagliardi-Urrutia, M. Solé, D. Baldo, I. Nunes, R. Cajade, A. Torres, T. Grant, K.-H. Jungfer, H.R. Silva, C. F. B. Haddad, J. Faivovich. The phylogeny of the Casque-headed Treefrogs (Anura: Hylinae: Lophyohylini). *Cladistics*, in press. DOI 10.1111/cla.12409 (2020).

248. C. J. Cole, C. R. Towsend, R. P. Reynolds, R. D. MacCulloch, A. Lathrop. Amphibians and reptiles of Guyana, South America: illustrated keys, annotated accounts, and a biogeographic synopsis. *Proc. Biol Soc. Washington* 125, 317–620 (2013)